Investigation of Application of Porous Material to Turbocharged Gasoline Engine

過給ガソリンエンジンへの多孔質材料の応用に関する研究

2020 年 8 月

千葉大学大学院工学研究科

人工システム科学専攻　機械系コース

董　東升

（千葉大学審査学位論文）

Investigation of Application of Porous Material to Turbocharged Gasoline Engine
過給ガソリンエンジンへの多孔質材料の応用に関する研究

2020 年 8 月

千葉大学大学院工学研究科

人工システム科学専攻　機械系コース

董　東升

ABSTRACT

Turbocharging techniques have been demonstrated to improve engine performance. However, due to the poor responsiveness of the turbocharged engine and the constantly strict regulations on fuel economy and emission, the application of a porous material to 4-cylinder turbocharged gasoline engine was studied to further improve the turbocharged gasoline engine performance. Porous materials, which have large surface areas, have been used for heat storage and cooling. However, porous Si-SiC material, as heat storage medium to be applied to a turbocharged gasoline engine has not been investigated extensively. In this study, porous Si-SiC material was used in the upstream of the turbine as heat storage medium and a model was thereby developed for further study. Substrate surface area and substrate volume of Si-SiC were calculated for structure model calibration. Following these calculations and test results, the pressure loss and thermal model were validated. The added porous Si-SiC material before the turbine could affect the exhaust gas pressure and temperature. In order to study the effect of porous Si-SiC material as heat storage medium on the fuel consumption for a turbocharged gasoline engine, steady and transient engine conditions were considered. A one-dimensional flow dynamic model of the porous heat storage material was established and comprehensively validated by experimental data. Then, this model was applied to predict the performance of the engine with heat storage medium under various conditions, including steady operation condition at targeted torque and transient operation conditions following the worldwide harmonized light vehicles test cycles (WLTC).

Due to its own characteristic of combustion cycle in the cylinder, the 4-cylinder turbocharged gasoline engine has indelible cyclic variation during intake and exhaust, which results in pulsation of exhaust pressure and temperature, leading to inconstant turbine operation and turbine efficiency. With porous Si-SiC material added before the turbine, the turbine inlet pressure and temperature pulsations were reduced, meanwhile, the exhaust gas energy was reused through the exhaust gas energy storage and reuse by the porous Si-SiC material. Results show that the weaken exhaust gas pulsation by porous Si-SiC leads to better turbine performance. The possibility of improving the transient response was investigated in which and less response time was required for the engine to reach the target torque at transient conditions compared to normal engine due to the improved turbine efficiency and small exhaust temperature variation by the porous Si-SiC material.

Exhaust gas energy recovery systems have shown great potential in improving internal combustion engine's fuel consumption. The use of porous Si-SiC material as heat storage medium to reduce the fuel consumption of the engine has not been investigated. As a result, under steady operation conditions, using heat storage medium, a fuel consumption reduction of about 1.1% was obtained due to increased turbine efficiency and reduced pumping loss. Moreover, the simulation under WLTC driving cycles

achieved fuel consumption saving up to 6.6% at medium vehicle speed due to the reuse of recovered exhaust gas energy in the heat storage medium. Thus, to use of the porous Si-SiC material as a kind of heat storage medium can be deemed as a prominent way to improve the turbine efficiency and engine performance of turbocharged gasoline engines.

The variable geometry turbocharger (VGT) is effective to improve the engine performance and reduce the fuel consumption. VGT has been widely used in diesel engines, however, due to the higher exhaust temperature of gasoline engine, it still has challenge for gasoline engine application. The high temperature of exhaust gas could damage the components of the complex variable structure in VGT, which may become to be useless after long-term use. To improve the durability of VGT, researchers have been considering enhancing the high-temperature stability and durability by new components of the variable structure or advanced material for VGT production. In this study, a kind of porous material was installed before the turbine to study the effects on fuel consumption and turbine inlet temperature in a 4-cylinder turbocharged gasoline engine. As a result, using porous material, under steady condition of medium load at 3200 RPM, a fuel economy improvement about 1% was obtain due to the higher turbine efficiency and less pump loss, and a 33℃ reduction of the turbine inlet temperature occurred due to the extra heat loss by adding porous material. In addition, under high load of 4000 RPM, due to the decreased turbine inlet temperature by using of porous material, the stoichiometric combustion range of the engine was expanded, and peak torque could be increased with 25 ℃ lower than the temperature limit. Thus, porous Si-SiC material could improve the fuel economy, the high temperature durability, and peak torque of the VGT engines.

TABLE OF CONTENTS

NOMENCLATURE

A/F	air-fuel ratio
A_0	sectional area of HSM（m^2）
a	sound velocity
α	the thermal diffusivity (m^2/s)
BSFC	brake specific fuel consumption
BMEP	brake mean effective pressure
C	gas velocity (m/s)
c	dynamic viscosity (kg/m-s)
c_p	specific heat capacity (J/Kg· K)
CI	compression ignition
CT	computed tomography
EGR	exhaust gas recirculation
GDI	gasoline direct injection
h	specific enthalpy (J/kg)
HEV	hybrid electrical vehicles
HCCI	homogeneous charge compression ignition
HSM	heat storage material
I	the moment of inertia of the shaft
K	permeability of porous medium (m^2)
k_c	the corrected thermal conductivity （W/m-K）
k_m	the measured conductivity（W/m-K）
k_p	pressure loss coefficient
L	characteristic length scale (m)
M	mass (kg)
$\dot{m}$	mass flow rate (kg/s)
NA	natural aspirated engine
n	cylinder number (-)
PFI	port fuel injection
PN	particle emission
PM	particulate matter
P_s	static pressure
P_t	total pressure
P_1	compressor inlet pressure

P_2	compressor outlet pressure
P_3	turbine inlet pressure
P_4	turbine outlet pressure
∇P	pressure drop between HSM (kPa)
P_{in}	pressure before HSM (kPa)
P_{out}	pressure after HSM (kPa)
ρ	bulk density（-）
ρ_0	substrate density (kg/m^3)
RDE	real driving emission
Rg	gas constant
SEM	scanning electron microscope
SI	spark ignition
Si-SiC	Si and SiC infiltrated porous material
SOC	battery state of charge
T	torque
T_d	dynamic temperature
Ts	static temperature
T_t	total temperature
T_0	reference temperature (K)
T_1	compressor inlet temperature
T_2	compressor outlet temperature
T_3	turbine inlet temperature
T_4	turbine outlet temperature
Δt	time step
u	internal energy
$\tilde{\mu}$	effectivity dynamic viscosity (kg/m-s)
V	volume (m^3)
V_d	void volume fraction（%）
V_0	substrate volume (m^3)
v	velocity(m/s)
WLTC	worldwide harmonized light vehicles test cycles
WLTP	worldwide harmonized light vehicles test procedure
w	rotation speed
ω	angular frequency (Hz)

Chapter 1 Introduction

1.1 Background and Motivation

In recent years, due to the urgent need for environmental protection and energy conservation, countries around the world have continuously issued stringent regulations on vehicle emission and fuel consumption. Europe, Japan, China and the United States continue to introduce strict automotive exhaust emissions regulations and CO_2 emission limits [1]. In China, new emission standards (China VI – Emcission Standard) for light-duty vehicles were announced, and all new vehicles should meet it at the start of 2020 [2]. Under Worldwide Harmonized Light Vehicle Test Procedure (WLTP), CO, THC, NOx and PM should be reduced by 50%, 50%, 40%, and 33%, respectively, compared to China VI – Emission Standard. It announced that National VIa Emission Standard is equivalent to European VI Standard, and National VIb has higher requirements than European VI Standard, becoming one of the most stringent automotive exhaust emission standards in the world. These have brought new challenges and requirements to the development of engine technologies, especially for emissions reducing and economy improvement. The future global CO_2 emission regulations and fuel consumption for passenger vehicles are summarized in Figure 1-1 [3]. The proposed target of CO_2 emission values of EU will decrease quickly and will reach 67 g/km in 2030. This means that EU plans to shrink CO_2 emission by about 30% by 2030 compared to the CO_2 emission value in 2020. It requires a reduction in the fuel consumption of the engine. Thus, engine advanced techniques are urgent need for continuous innovation and application in engines.

Recently, electrical vehicles and hybrid electrical vehicles, development is another motivation to promote the advanced engine technologies research and application. However, the total lifecycle economic cost and environmental impact analysis are always the Focus of argument. Figure 1-2 shows the electric cars development conditions around the world in the past 5 years (2013-2018) [4]. These include some characteristics: electric vehicles have grown rapidly, reaching 5 million units in 2018, an increase of 63% over the previous year. The electric vehicles in China are mainly concentrated in big cities, where the environmental protection is even more urgent [5]. However, due to the drawbacks of battery, such as battery capacity, life issues, after recycling, cost, the partial-electric vehicles are becoming popular in these days, such hybrid electrical vehicles [6]. Figure1-3 shows the schematic diagram of a hybrid electric car [7]. Beside the engine, battery and electric motor were also introduced and combined in the same vehicle.

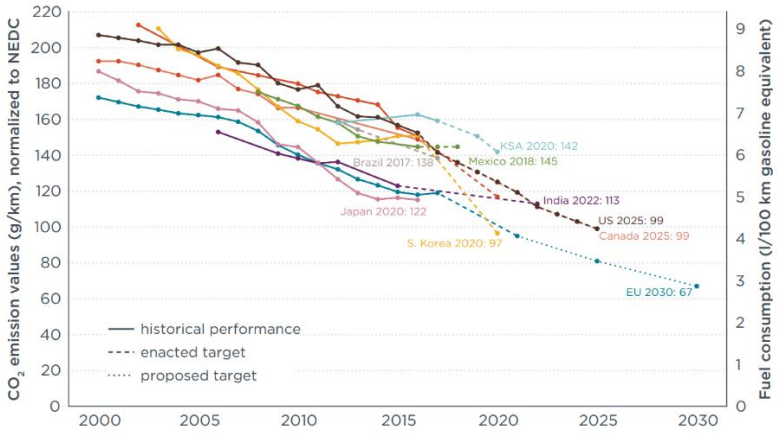

Figure 1-1. Global CO_2 emission and fuel consumption regulations for passenger vehicles [3]

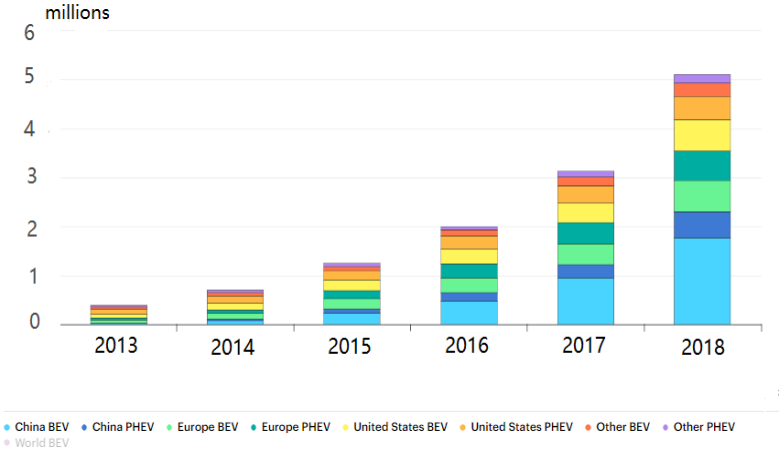

Figure 1-2. Electric car deployment in selected countries, 2013-2018 [4]

Real driving emission (RDE) testing showed a higher particle emission (PN) of hybrid electrical vehicles (HEVs) both port fuel injection (PFI) and gasoline direct injection (GDI) compared to engine-only vehicle [7]. The battery state of charge (SOC) has large effects on fuel consumption and emission based on the on on-board diagnostics (OBD) interface test [8-10]. For low SOC level such as 40%-50%, higher fuel consumption, CO_2 and lower NO_x, CO were obtained. However, high battery SOC level, such as between 70 and 80%, the previous reviewed parameters were reduced totally.

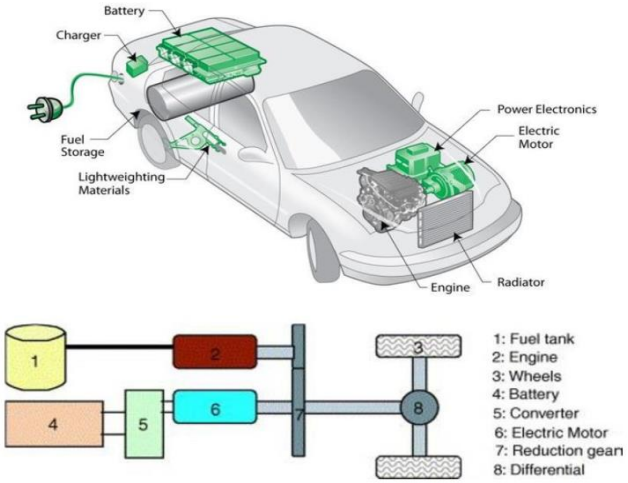

Figure 1-3. Schematic Diagram of a Hybrid Electric Car [7]

As a result, the stringent environmental protection and vehicle emission reduction regulations are promoting the continuous innovation and development of the automotive and engine technologies. Electric vehicles as an alternative to conventional vehicles may be a good selection of alleviating fuel shortages to meet the need of sustainable development of vehicle. However, due to the drawbacks of electric vehicles, the battery and fuel cell techniques are still on the way of development. Further technology breakthroughs of battery and fuel cell is the main challenge of wide application of electric vehicles. Thus, the internal combustion engines are still accepted to remain as a major part of modern vehicle market in the foreseeable future. All these indicate that continuous investigation of advanced internal combustion engine techniques to improve the fuel efficiency and reduce the emission are meaningful and important.

1.2 Advanced Techniques of Engines

More and more advanced technologies have been continuously developed and applied in internal combustion engines, such as new way of burning (homogeneous charge compression ignition, lean burn), new types of injection (port injection, direct injection, dual-injection, new kind of injector etc.), alternative fuels, and engine downsizing , variable valve timing, exhaust gas recirculation (EGR) and turbocharging [11-16].

As a kind of low temperature combustion concept, homogeneous charge compression ignition (HCCI) could decrease the combustion temperature due to well mixed vaporized fuel with the air in the cylinder and slower combustion resulting from longer chemical reactions. This low combustion temperature could suppress soot and NO_x formation, thereby reducing exhaust emission, as shown in Figure1-4. [11,12]. However, HCCI has its challenges such as difficulty in combustion phasing control and high load operating problem, which makes it difficult to successfully apply to commercial use. In order to

improve the usage of HCCI in gasoline engine applications, MORIYOSHI has developed Blow Down Super Charging (BDSC) system as shown in Figure 1-5, which experimentally demonstrated that it could expand the operating ranges of HCCI [13].Lean burn is another efficient method to improve the engine fuel economy and reduce the exhaust emission. [14] However, the low burn velocity of lean burn leads to large cycle variability which should be avoided in engines. Pre-chamber is an effective method to extent the lean burn limit by reducing the combustion duration [15,16]. A repetitive pulse discharges was used in the ignition system to improve the ignition quality in a spark ignition (SI) engine [17]. Experimental results found that the flammability of the mixture was improved by reducing the combustion duration and cycle variation.

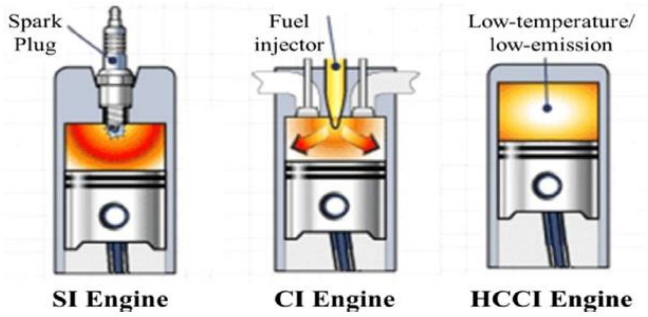

Figure1-4. Schematic diagram of HCCI [12]

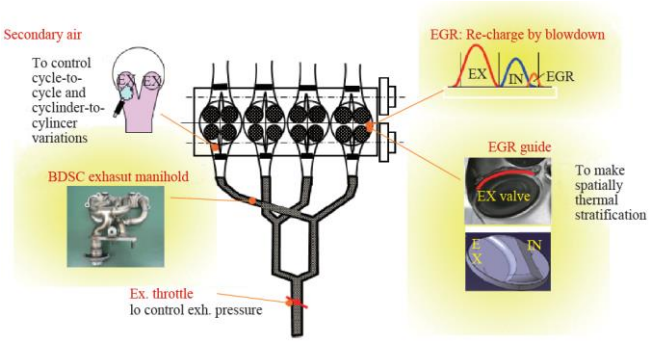

Figure 1-5. Schematic of BDSC system [6]

New types of injectors and injection methods have been developed to improve the engine performance. By these methods, gasoline direct injection (GDI) has been proved to improve the thermal efficiency and reduce the emissions (HC and NOx) as shown in Figure 1-6 [18,19]. However, GDI engines also have challenges of knock and particulate matter (PM) [20]. Thus, new technologies were developed for better application of GDI engines. Multi-hole injectors were designed for using in direct-injection gasoline engines [12]. A V-type intersecting hole nozzle was designed and studied using X-ray and three-fluid method [22,23]. Results showed that non-cavitating internal flow improved the discharge coefficients of V-type intersecting hole nozzles. Spray guided parts were designed and used to improve the stratified strategy in GDI engines [14,24].

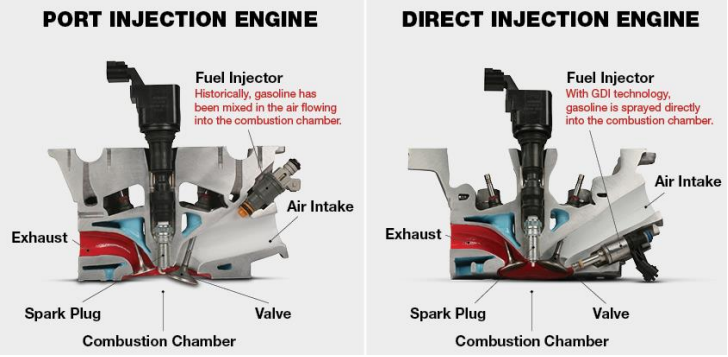

Figure1-6. Port Injection Engines versus Direct Injection Engines [19]

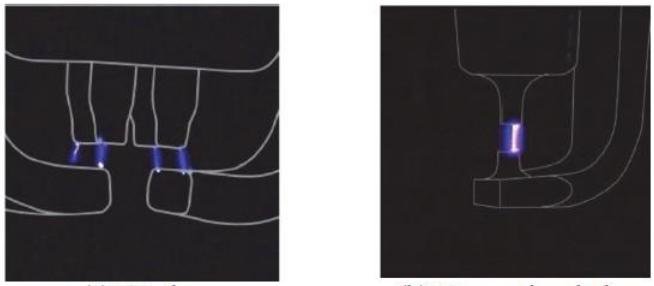

Figure 1-7. Difference of discharge channel characteristics of FE and conventional spark plug [26]

New types of spark plug have been developed to improve combustion. Low temperature plasma maybe a promising ignition technology for ignition engines. A new low temperature plasma was designed with high-frequency voltage (15 kHz) [25]. This expanded the auto-ignition region and improved the lean air-fuel (A/F) ratio limit in HCCI combustion. In Figure 1-7, Moriyoshi used visualization method to study the low temperature plasma ignition, in which found the characteristic of better wear resistance, lower energy release and combustion enhancement of low temperature plasma compared to normal ignition spark plug [26]. Low temperature plasma technique has been paid attention to and studied based on reaction mechanism of gas mixtures [27].

Due to the crises of environmental degradation and lack of fossil fuels, alternative fuels were also studied and applied in internal combustion engines [28]. Figure 1-8 shows the primary energy sources, including fossil and regenerative energy, such as biomass, solar and wind. A part of them can be produced by absorbing CO_2 from the environment [29]. Alternative fuels are environmentally friendly to help ease the oil shortage and allow CO_2 to reach balance in the atmosphere. In addition, it is also beneficial to improve the engine efficiency and reduce the exhaust emissions. Gong [30] has applied the methanol to port-injection and direct-injection engines. It proved that it was effective to extend the lean-burn range and improve the high indicated mean effective pressure (IMEP) by using methanol added with hydrogen. Due to higher low heating value, faster combustion speed, lower knock occurrence properties of methanol, it is beneficial to increase the compression ratio and engine efficiency [31].

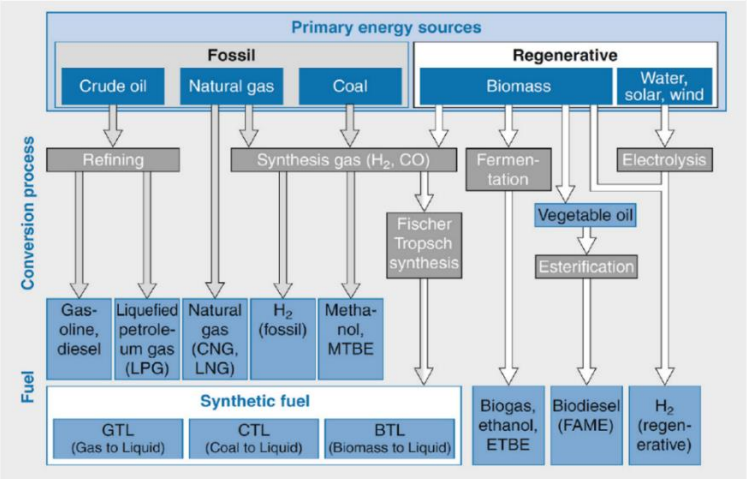

Figure 1-8. Manufacturing paths of fossil and regenerative fuels [29]

Downsizing was introduced to decrease the engine capacity for decades, as shown in Figure 1-9, such as turbocharged engines [32]. This allows reducing engine size and weight greatly both gasoline engines and diesel engines. Due to turbocharging system utilization, Engine downsizing did not deteriorate the performance of the engine, and loss the engine power. Engine downsizing technique has become a kind of widely accepted technology for engine fuel consumption improvement and CO_2 emissions reduction, especially turbocharged engines [33]. The reduction in greenhouse CO_2 resulting from downsizing engines is an effective method to meet the stringent emission regulations of global vehicles compared to large size engines [34]. Thus, turbocharging techniques are widely applied to engines of spark ignition (SI) and compression ignition (CI). Under stoichiometric combustion of turbocharged gasoline engines, the engine output power is based on the air supplied by intake system. With a turbocharged system, the intake pressure is boosted to higher than atmospheric pressure, thereby increase intake air density and the air mass flow rate. Under stoichiometric operation condition, more air means more fuel injection in the cylinder to increase the engine power directly for a given engine displacement [35]. As a usual, the engine output power is proportion to the mount of air, and for naturally aspirated (NA) engines, it depends on the engine displacement. Turbocharging allows reducing the required engine displacement for required engine power by boost the intake pressure compared to conventional naturally aspirated engines [36]. In addition, turbocharging techniques could expand the engine utilization region with different turbine sizes. This greatly enhances the versatility of the engine. For example, A 1.5-litre turbocharged engine may provide the same power of 2.0-liter, 2.5-liter and 3.0-liter NA engines [37]. As a result, turbocharged techniques downsize the engine, and these small size engines achieve less heat and mechanical loss which benefits the engine fuel consumption improvement [38].For the same power requirements, gasoline engine downsizing technology leads to about 20%-60% engine size reduction and 8%-10% brake specific fuel consumption (BSFC) decreasing in throttling losses [39]. Grant Lumsden [40] designed a 1.2 L turbocharged engine to replace a 2.4 L NA engine which obtained higher torque, simultaneously 25%- 30% on-road fuel consumption benefits.

Engine cam timing controls the air intake and exhaust. To optimize the breathing of the engine, intake and exhaust phase angle of cams should be changed based on different engine speed, thereby Variable Valve Timing (VVT) designed and introduced. At high engine speed, the durations of engine intake and exhaust are decrease, they become not enough to meet the gas exchange of the engine cylinder, namely the exhaust scavenging and intake air breathing. Thus, intake valve earlier opening and exhaust valves later closing leading to overlap were applied to improve the gas exchange condition of the engine. Meanwhile, the engine could change to be the best valve timing at different engine speed. Figure 1- 9 shows different types of VVT [41]. In addition, VVT can wide the engine performance under different engine conditions. Honda's Variable Valve Timing and Valve Lift Electronic Control System (VTEC) was developed to improve the volumetric efficiency, resulting in lower fuel consumption [42]. Toyota's VVT-iW (Variable Valve Timing – intelligent wide) was able to change the valve timing smoothly based on the target engine operation conditions [43]. The previous reviewed VVT are based on cam and mechanical design. To develop electric assist VVT, namely camless variable valve actuation (VVA), electronic control of VVT was developed. This is beneficial to reduce the engine cold-start emissions and the cost of electrical drive systems [44]. In addition, the electronic control of VVT could improve the performance of HCCI with better fuel efficiency. Mitsubishi developed Valve Timing Electronic Control system, and the phase angle of cam timing was shown in Figure 11, varying with engine load [45].

Figure1- 9. Engine downsizing [32]

In addition, VVT was used widely in engine to change the residual gas in the cylinder, thereby changing the initial unburned gas temperature and combustion temperature in the cylinder. This works as EGR method to improve the fuel efficiency and reduce the emission of the engine. EGR reused and introduced the exhaust gas by external EGR system to the intake pipe and inner EGR with overlap. This is an effective method to reduce the pump loss, NOx emission, and increase the engine efficiency in engines. With EGR, the throttle loss at part load range could be reduced by wider opening throttle angle. The CO_2 in the exhaust gas is introduced into the cylinder to mix fresh air, which reduces the combustion temperature,

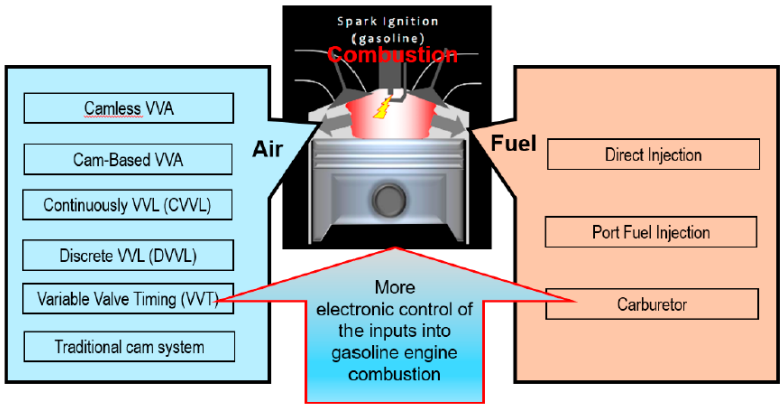

Figure 10. Different types of variable cam timing [44]

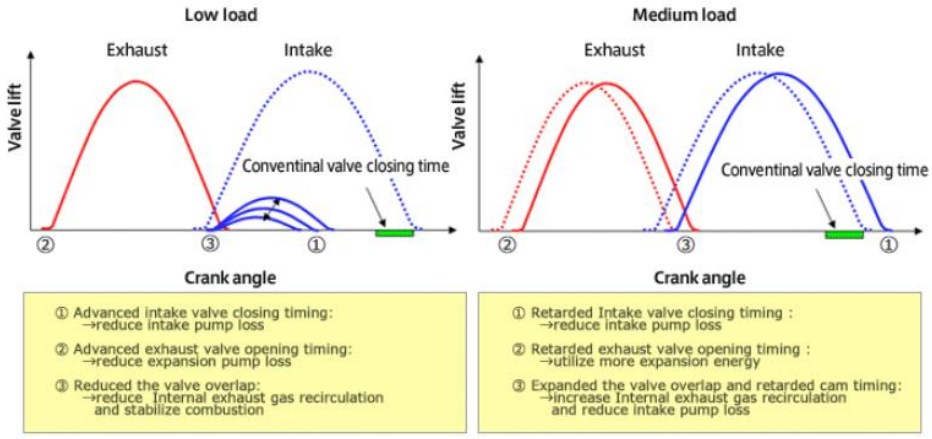

Figure 1-11. Valve Timing Electronic Control of Mitsubish [45]

improves the knock resistance, and advances the ignition timing, thereby improving the engine economy. This has been widely used in gasoline engines and diesel engines. Figure 1-12 shows the 4 types of EGR application in engines [46]. EGR is always combined with EGR Cooler to decrease the temperature of exhaust gas. Low pressure loop EGR and high-pressure loop EGR are basic applied EGR circuits in engines, as shown in Figure 1- 11. With cooled EGR system, the combustion was proved to more retard, and the burn durations are longer [47]. As a result, with EGR, the increased specific heat ratio and decreased heat loss allow reducing the engine fuel consumption. In addition, EGR is also effective to combine with natural gas SI engines and hydrogen fueled SI Engine. With EGR, experimental study showed that the combustion characteristics were affected by natural gas-hydrogen blends. The combustion duration and flame development duration increase with increased EGR rate, however, theses decreased with the increased H_2 in the blends [48-50]. When Butanol fueled engine combined with EGR, the knock was suppressed, and the fuel economy was improved in butanol/ethanol−gasoline engine [51]. However, the increased combustion variation is the main EGR application problem in engines. Thus, to expand the high EGR rate limit is the topic of future trends of EGR application research.

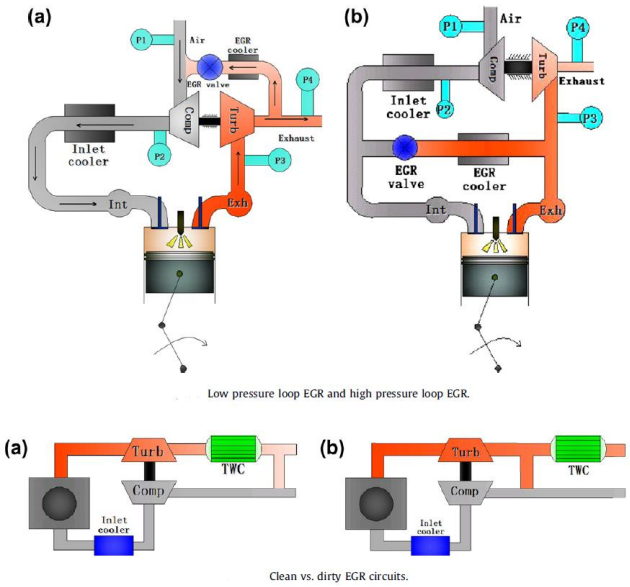

Figure 1-12. EGR circuits [46]

1.3 Fundamentals and Types of Boost Technologies

Boost is a technology to increase the intake pressure, intake air density, then, more fuel injection entering the cylinder, resulting high engine output power. Boost technologies has been used in many types of machines, and for engine application, both SI engine and diesel engine are useful. After decades of development, different types of boost tools have been designed and applied in internal combustion engines (ICE), which will be discussed in the following section.

1.3.1 Mechanical Supercharging

Mechanical supercharging was firstly used in diesel engine, and probably one of the earliest devices to increase the intake pressure for ICE [52]. The traditional mechanical supercharger was connected to the engine's crankshaft directly by a belt, which used part of the engine output power to allow the supercharger working. As usual, due to the difference of gas transfer, there are always 2 main types of supercharger, positive-displacement compressors and centrifugal compressors.

The positive-displacement supercharger has been always utilized in passenger vehicles, such as Screw and Roots types [53], in which Lysholm supercharger was been developed for automotive use [54-57]. Figure 1-13 shows a kind of Lysholm supercharger, linked to the engine supercharger by a belt. By this means, the supercharger obtained belt-driven from the engine crankshaft. High-pressure, high-efficiency available characteristics led to good response at low engine speed. In addition, the high-speed characteristic made it possible to achieve a smaller installed size than supercharger of Roots type. In a

Miller cycle engine, by using Lysholm supercharger, reduced fuel consumption, higher boost pressure and quicker response obtained in Shiver's research [57].

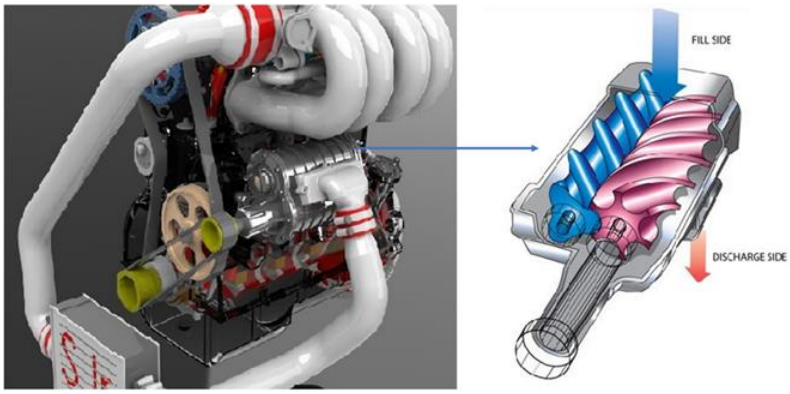

Figure 1-13. Lysholm supercharger [55-56]

In general, centrifugal compressors is always with higher efficiency, reduced size and weight compared to the positive-displacement compressor. Figure 1-14 shows a kind of centrifugal compressor combined supercharger [58]. However, it is along with more inevitable mechanical loss, resulting from external gear or other parts to drive the centrifugal compressors efficiently. The used centrifugal-type supercharger system was driven via a Torotrak continuously variable transmission (CVT). Furthermore, the system is also combined with a conditional turbocharger as shown in Figure 1-15. Due to the variable ratio between the crankshaft and the supercharger, by this means, the used system was able to help the engine to achieve better transient response at both load and part load. In addition, the fuel consumption of this type of engine was also reduced by about 1%, resulting from reduced transmission losses and increased novel compressor isentropic efficiency. Another type of centrifugal supercharger is SuperGen variable-speed centrifugal supercharger [59]. For its variable drive ratio, and similar characteristic like an electrical-driven compressor, the full-load and transient performance of engine was improved. However, at low engine speed, the air supply is not enough and sufficient for targeted torque of 400 Nm at 1000 rpm with conventional positive-displacement supercharger, and this was improved by 26.5% by using SuperGen device.

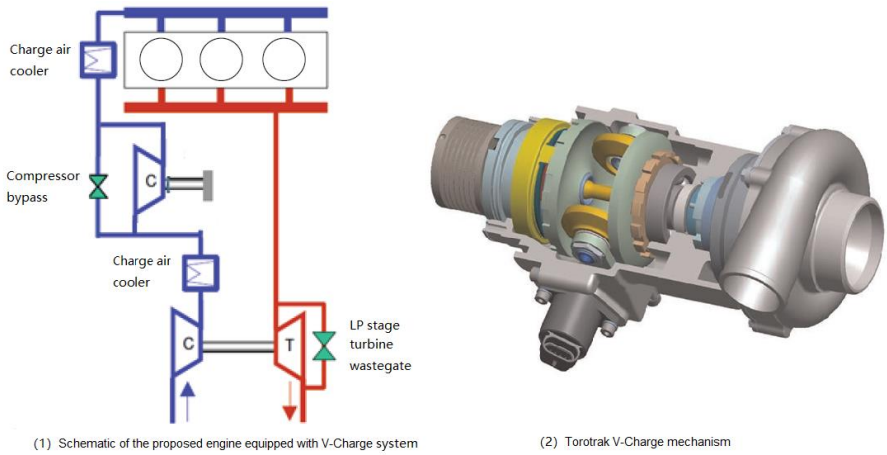

Figure 1-14. Centrifugal supercharger of Torotrak V-Charge mechanism [58]

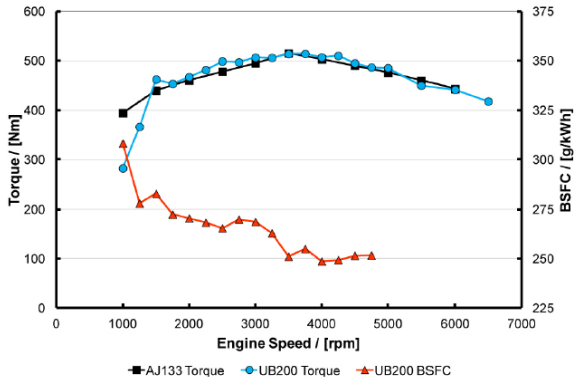

Figure 1-15. Final performance of Ultraboost engine (known as UB200) versus the initial project target torque curve taken from the Jaguar Land Rover AJ133 NA 5.0 litre V8 engine. Note shortfall in torque below 1500 rpm [59-60]

1.3.2 Electric Turbocharger

Electric turbochargers are sorted to electrically driven turbocharger or assisted turbocharger, which could improve the engine transient response and the low- end torque. However, due to the use of extra electrically driven supercharger, generator or motor, more complex devices are used in this type of boost technology, resulting in not easy to realize application in engines.

Electric turbocharger assistance (ETA) and Electric assisted turbocharger (EAT) are two main parts of electric turbocharger. In general, an electric motor or generator was combined within the bearing housing in a modified standard turbocharger. Figure 1-16 shows a type of electrically assisted turbocharger in Nicola's research. An electric machine rotor was fixed on the turbocharger by linked with the turbocharger shaft. In this way, the motor can drive the turbocharger through the shaft.

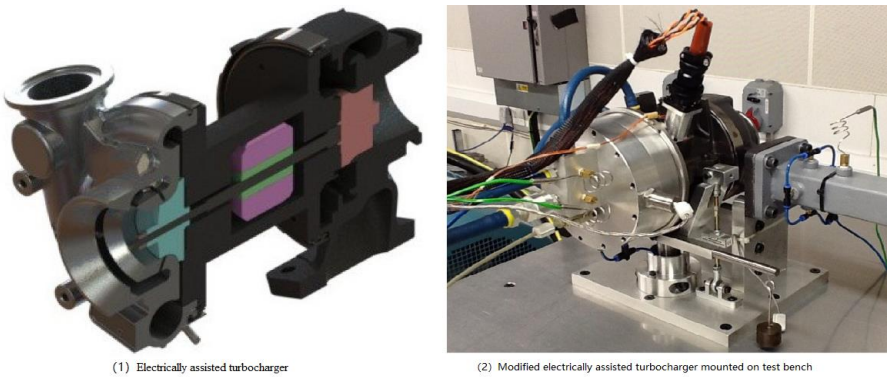

(1) Electrically assisted turbocharger (2) Modified electrically assisted turbocharger mounted on test bench

Figure1-16. Electrically assisted turbocharger and test bench [61]

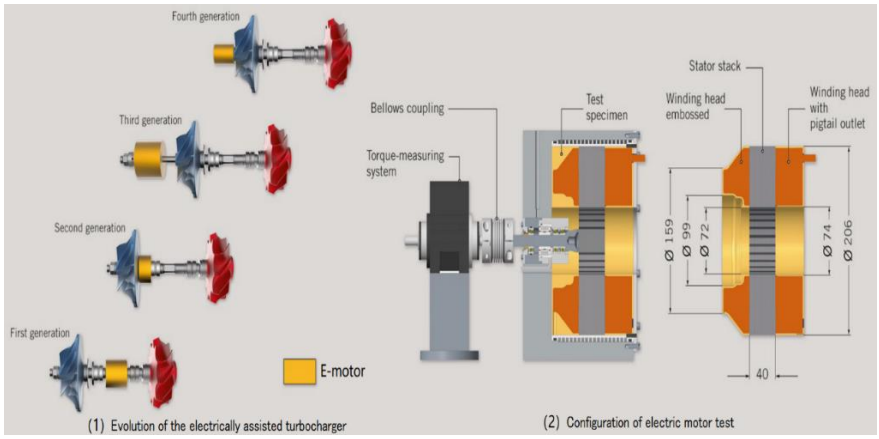

Figure 1-17. Electrically assisted turbocharger and test bench [62]

To solve the power delay of turbocharging and satisfy customers' demand of high-levels' deliver, MTU developed different types of electrically assisted turbochargers, and Figure 1-17 (1) shows the evolution of the developed electrically assisted turbocharger [62]. The E-motor size and mounted position have been constantly optimized from first generation to fourth generation. The main changes are mounted position and size of the E-motor. In the first and second generation, the E-motors were located between the compressor and turbine, installed in the turbocharger bearing points [63]. From the third generation, the locations were moved to outside the bearing between the turbocharger bearing points, in the front of compressor by expanding the bearing length. By this means with a media gap motor, high torque and low mass moment of inertia were achieved. To test these types of electrically assisted turbochargers, test stand was shown in Figure 17 (2). As a result, the turbocharging system and engine response were improved by using electrically assisted turbocharger (e-TC). In addition, it can expand engine performance characteristics and reduce consumption and emissions over a wide operation region.

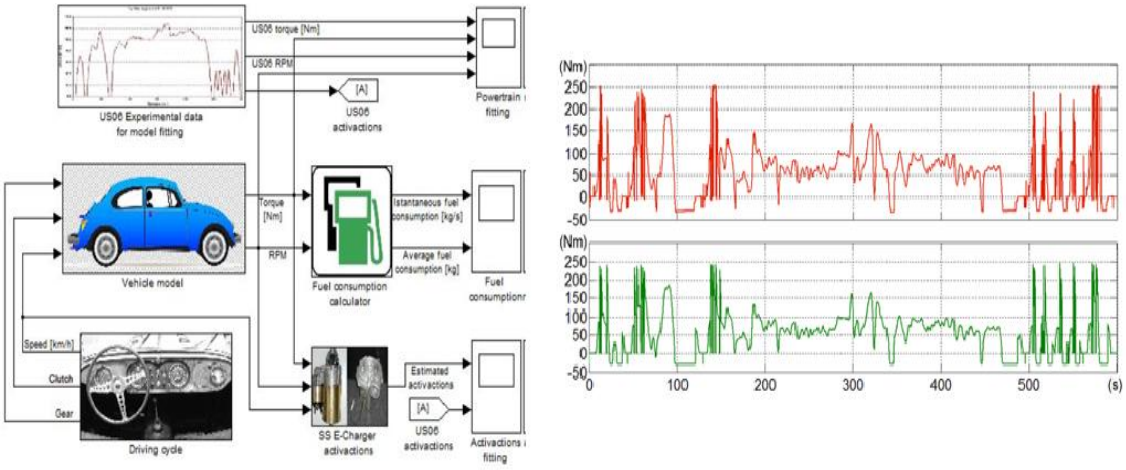

(1) Block scheme of the engine and transmission model. (2) Real (top) and estimated (down) motor torque

Figure 1-18. Electrically assisted turbocharger study by simulation method [65]

The electrically assisted turbocharger was effective to improve the dynamic characteristic of the vehicles and engines by using electric motor assisted turbocharger [64]. As a kind of Engine hybridization system, in order to increase the efficiency, drivability and battery lifetime, electric motor assisted turbocharger system should make all the parts work well, such as the motor, shaft inertia, compressor and turbine, especially by real time test method [65]. In that, the electric motor was used to assist the engine the achieve in low efficiency and low-end torque by battery, however, it is not linked to the vehicle directly, and the external cost of battery was not taken in consideration. Figure 1-18 shows a simulation model and the results of real (top) and estimated (down) motor torque.The powertrain model combined with engine model, vehicle model, transmission model, in which the vehicle speed was changing with time based on real time test cycle of US06 driving cycle. In this way, the vehicle consumption of the whole driving cycle could be obtained, and the real and estimated motor torques were also achieved. Thus, the motor operation and vehicle fuel economy could be evaluated by this means. Ibaraki [66] also developed a type of electrically assisted turbocharger to achieve better environmental properties and drivability at the low-speed engine operation mode. Balis [67] designed and develop a e-turbo to apply in SUV and light truck, with better low-end torque and improved fuel economy.

1.3.3 Turbocharging

As a boost technology, turbocharging, especial for exhaust turbocharging technique, has been widely used in recent years. It is a system to achieve high intake pressure via exhaust gas, higher than atmospheric pressure, compared to natural aspired (NA) engine. In a turbocharging system as shown in Figure 1-19, the system mainly includes a turbine, a compressor, and a shaft [68]. The turbine is

combined with the compressor by a shaft. The exhaust gas with high temperature and pressure enters the turbine housing to run the turbine impeller (wheel), resulting in a high-speed operation of the turbine, thereby a high-speed operation of the shaft. A part of exhaust gas energy is transmitted to turbine by this method. The reduced pressure and temperature of exhaust gas is transformed to the energy of turbine running. Then, by shaft, the compressor achieved the same operating speed of the turbine. Compressor as a machine device to increase the gas pressure by gas volume decreasing, the air of compressor inlet is boosted with increased gas temperature. As a result, the high-speed compressor does work on the low-pressure air of the compressor inlet, and an increased pressure is obtained at the outlet side of the compressor. At first glance, it maybe fell that turbine and compressor is the same, for their similar structure, however, the difference in their working ways is obvious. The turbine is a machine to extract (exhaust) energy from fluid flow by driving the turbine wheel, as a kind of mechanical rotary device [69]. The energy is converted to the moving of turbine impeller. In a turbocharging system, the turbine links to a compressor, and the energy is transferred to the working of compressor through a shaft. However, if the turbine is connected to a generator, the energy could be used to generating electrical power in thermal power plant or hydro power plant. Thus, the flow fluid could be gas, steam, and water.

A compressor is a device using its running impeller to increase the air pressure or flow of a fluid. In addition, the compressor needs external to drive it, such as thermal energy in a turbocharging system or electric energy in a motor driving system. During this work process, the shaft friction should be overcome, resulting in energy loss.

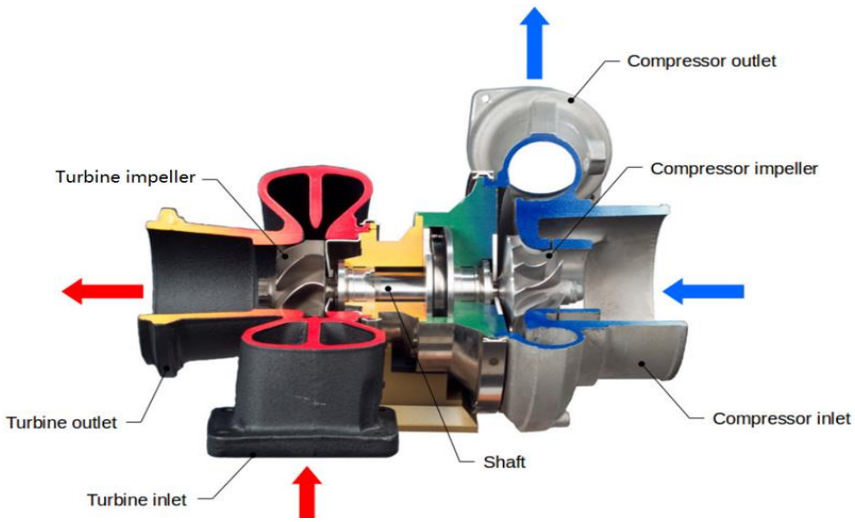

Figure 1-19. Turbocharger cutout view [68]

The turbines are mainly sorted into two types based on the direction of flow fluid into the turbine, radial flow type turbine and axial flow type turbine. However, in the current car market, the turbocharged engines are mostly combined with radial flow type turbine. Axial flow type turbines have also been

studied for engine application, though, they are used more in electric generator and fan jet engine of airplane as shown in Figure 1-20 [70-71]. Axial flow automotive turbocharger also has been studied by researchers. A kind of automotive turbocharger with an axial flow turbine was shown in Figure 1-21 [72]. This design was to reduce the shaft inertia, thereby achieving improved engine response, as small turbine diameter, light turbine weight is an approach of obtaining smaller inertia of turbine. Results showed that with a centrifugal compressor combined, the transient response time based on engine dynamometer was reduce by 25-40% compared to that of turbocharger with the radial inflow turbine. Anna has tried to use axial turbine in automotive, generally in marine and aviation application [73-74]. A Ford Ecoboost 1.6 L engine was selected for investigation with a special designed axial turbine combined turbocharger. Simulation results showed that the axial turbine obtained high efficiency in a wide range of operation with a symmetric volute design.

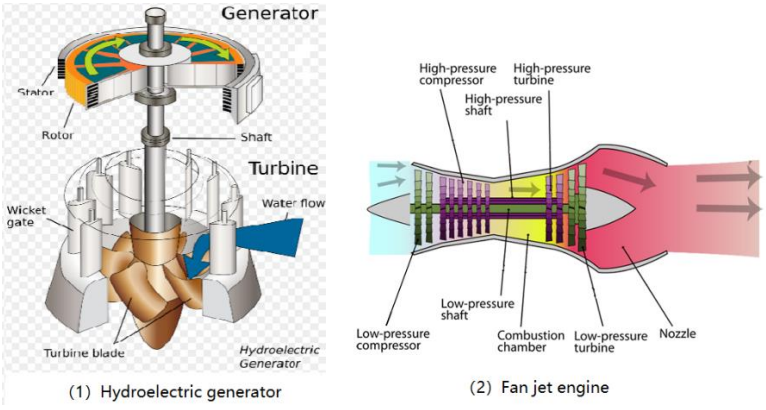

Figure 1-20. Turbocharger cutout view [70-71]

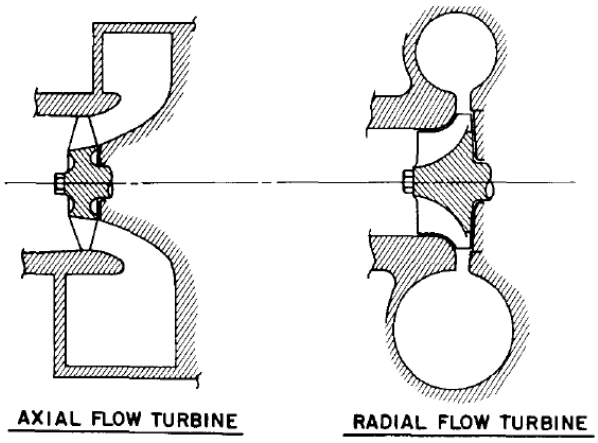

Figure 1-21. Turbocharger cutout view [72]

The selection of turbomachinery for special device application depends on the special speed Ns and diameter Ds, and the general characteristics are shown in Bale's diagram in Figure 1-22, with calculation results based on Equations (1) and (2) [74-75]. As a result, the axial turbine application is always under

the range of higher special speed Ns than that of radial turbine application. In addition, the diameter Ds of axial turbine operation range shows smaller than of radial turbine.

$$Ns = \frac{\omega\sqrt{\frac{\dot{m}}{\rho}}}{\Delta h_{t,id}{}^{3/4}} \tag{1}$$

$$Ds = \frac{Dm\ \Delta h_{ts,id}{}^{1/4}}{\sqrt{\dot{m}/\rho}} \tag{2}$$

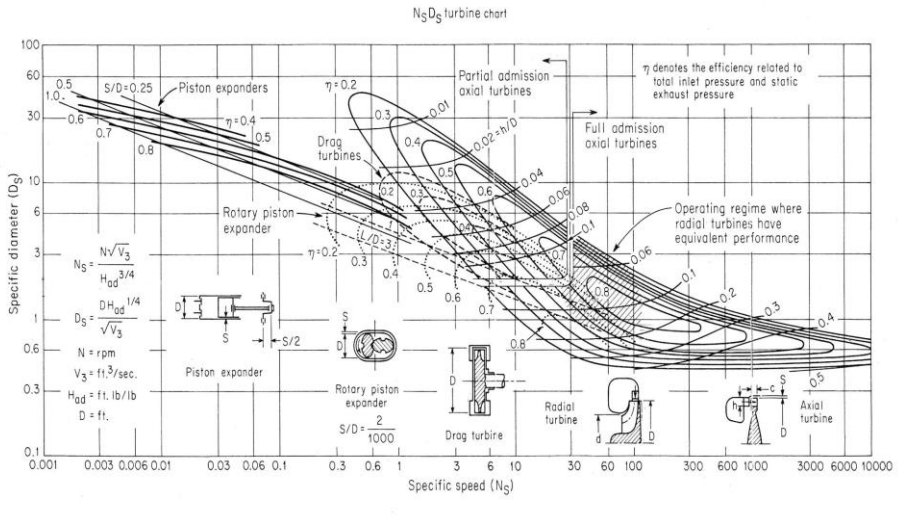

Figure 1-22. Bale's diagram of Ns and Ds [74-75]

Exhaust gas turbochargers combined with radial turbines has been widely used in current automotive market. Figure 1-23 shows a turbocharged engine system, including an engine, a turbocharger, a charge air cooler, an exhaust gas cooler. In general, the boosted air accompanied by high temperature, a Charger Air Cooler is always added between the compressor and throttle to cool the air before entering the cylinder, as shown in Figure 1-23. The work of compressor is to increase the air pressure by doing work on the air, leading to reduced volume and increased density. It includes a conversion between dynamic energy and thermal energy, so the air temperature is increased. This increased temperature air enters the cylinder, leading to high-temperature unburned gas and high pressure in the cylinder. In this condition, knock occurrence could be increased easily special at high engine load. To avoid knock due to high combustion temperature in the cylinder, a Charger Air Cooler is installed downstream of compressor before the throttle. In this system shown in Figure 1-23, an exhaust gas recirculation (EGR) system was also added with an exhaust gas cooler to decrease the intake gas temperature.

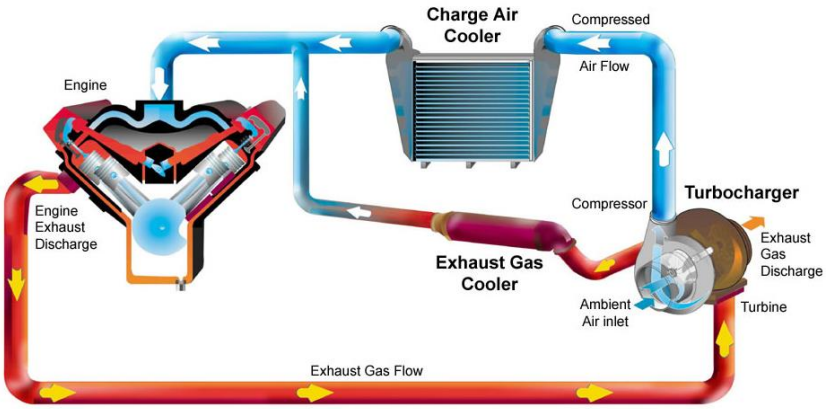

Figure 1-23. Schematic of turbocharged engine [76]

In the process of exhaust energy transmission in turbocharging system, turbine and compressor working efficiency are significant to utilizing the exhaust gas energy effectively. As the compressor is turned by the shaft combined turbine, it is major significant to improve the turbine performance in turbocharged engines. Thus, it is meaningful to study the efficiency improvement methods of turbocharging system.

1.3.4 Theoretical Calculation Formulas and Fundamentals of Turbocharging

1.3.4.1 Theoretical Calculation Formulas of Turbocharging

For a NA combined vehicle, the engine consumes fuel energy through the combustion of fuel in the cylinders, generating vehicle driving energy, which is accompanied by friction, thermal cooling losses, thermal exhaust gas losses, and other supply powers, as shown in Figure 1-24 [77]. It shows that only 10-15% of original energy (input fuel energy) is applied to drive the vehicle. The maximum efficiency of a gasoline ICE could just reach about 35%, with a large amount of energy escaping from the exhaust pipe to the atmosphere. The exhaust gas temperature is high to 950-1050℃ in gasoline engines with enthalpy energy. Turbocharged engines were produced to use the enthalpy energy by turbine collecting and transfer enthalpy energy and the compressor to boost the intake air, leading to higher intake pressure and air density. As a result, more engine output power is obtained via turbocharging method. Moreover, it downsizes the engine and causes less cooling loss with reduced fuel consumption and CO2 emission.

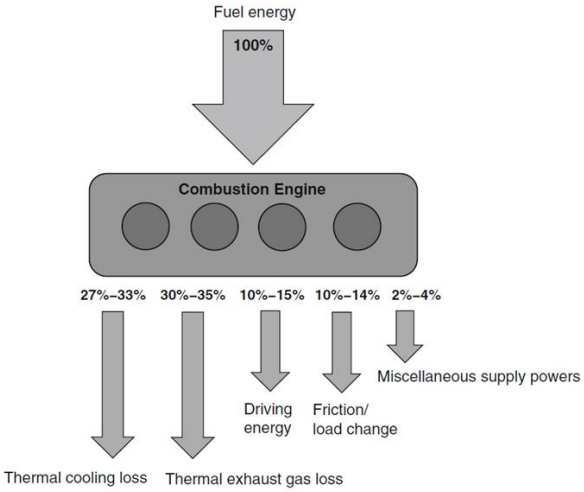

Figure 1-24. Energy percentage of automotive [77]

Exhaust gas is the essential flow fluid between engine and turbine, which is high-temperature and high- pressure flow gas and used by turbocharger. Therefore, the definition of exhaust gas temperature and pressure is important in the energy exchange calculation of turbocharging system. The total temperature of T_t (K) includes static temperature T_s (K) and dynamic temperature T_d (K).As the gas is with high speed in the exhaust manifold, the static temperature T_s (K) can be tested by sensor (thermocouple), however, due to the existence of viscous boundary layer, the dynamic temperature is the temperature at the wall with 0 gas flow velocity.

$$T_t = T_s + T_d = T_s + \frac{c^2}{2c_p} \tag{1.1}$$

c: the gas velocity;

c_p: the heat capacity at constant pressure

The total pressure of P_t is calculated based on isentropic gas equation in (1.2)。

$$P_t = P_s(\frac{T_t}{T_s})^{\frac{k}{k-1}} = P_s(1 + \frac{k-1}{2}M^2)^{\frac{k}{k-1}} \tag{1.2}$$

P_s: static pressure;

k=c_p/c_v: isentropic exponent of gas;

M: Mach number of gas (M=c/a);

a: the sound velocity.

As the temperature and pressure calculation in previous, the total enthalpy of h_t also includes two parts, specific enthalpy and specific kinetic energy.

$$h_t = h + \frac{c^2}{2} \tag{1.3}$$

h: specific enthalpy, J/kg

The exhaust gas specific enthalpy of h can be calculated by (1.4), including internal energy of exhaust gas u and the specific enthalpy of reference gas.

$$h(T) = c_p(T - T_0) + h(T_0) = u(T) + \frac{P}{\rho} = u(\mathrm{T}) + R_g T \tag{1.4}$$

*h(T0) ≡ 0 at T0 = 0 K.

The specific internal energy $u(T)$ is calculated based on (1.5)

$$u(T) - u(T_0) = c_v(T - T_0) = c_v \Delta T \tag{1.5}$$

Based on the previous calculation equations, $u(T_0)$ is equal to 0 when T_0 is equal to 0 K, as a result, $u(T) = c_v$T, h(T) = c_pT and the unit of T is K.

For turbocharging system, the calculation equations of the parameters are shown in below, which include mainly the speed of turbine and compressor, the working efficiency of turbine and compressor. The high-temperature and high-pressure of exhaust gas enters the turbine through expansion process in the turbine, leading to low-temperature and low-pressure exhaust gas. As a result, the specific enthalpy of the exhaust gas is utilized in the expansion process of exhaust gas and changed to be the kinetic energy of the turbine. The air of environment enters the compressor through compression process in the compressor, resulting to boosted air with higher-temperature and higher-pressure. The expansion and compression processes are shown in Figure 24 [77].

The exhaust gas state changes from state 3 at the turbine inlet (P_3, T_3) to state 4 at the turbine outlet (P_4, T_4) with a polytropic expansion process. The air state changes from state 1 at the compressor inlet (P_1, T_1)to state 2 at compressor (P_2, T_2) with a polytropic compression process. Due to the real expansion and compression processes are not isentropic process, the turbine and compressor working efficiency occurs in the turbocharging working process. The efficiency calculation equations are shown below.

The rotation speed ω of the turbocharger shaft is calculated by the following equation.

$$\Delta\omega = \frac{\Delta t(T_t - T_c - T_f)}{I} \tag{1.6}$$

T: the torque; Δt: the time step; I: the moment of inertia of the shaft

The changes in gas enthalpy and entropy in the turbine and compressor are shown in Figure 1-25. As the enthalpy changes are not isentropic processes, they are polytropic processes. For turbine, it is an enthalpy increase process with temperature decrease, however, for compressor, it is an enthalpy decrease process with temperature increase. With respect to entropy, they are a process of increasing entropy as shown below.

Turbine: $$h_4 = h_3 - \Delta h_{34}\eta_t \tag{1.8}$$

Compressor: $$h_2 = h_1 + \Delta h_{12}\frac{1}{\eta_c} \tag{1.9}$$

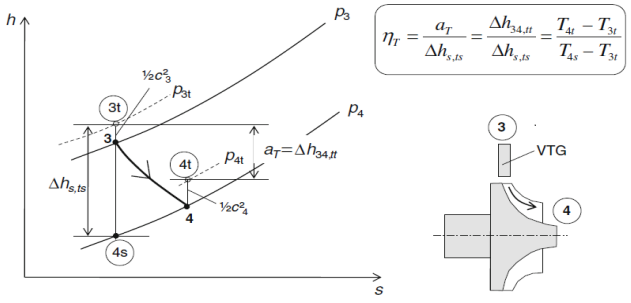

(1) Expansion process in the turbine stage in h-s diagram

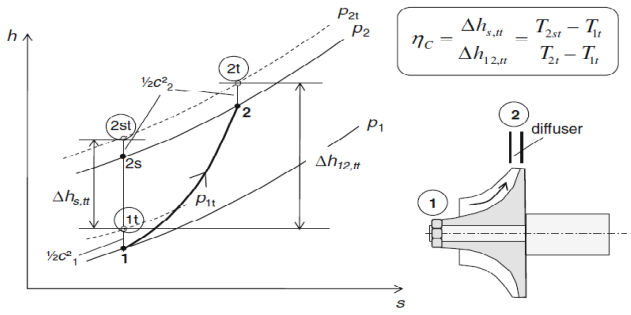

(2) Compression process in the compressor stage in h-s diagram

Figure 1-25. h-s diagram of expansion process in the turbine and compression process in the compressor stage in h-s diagram [77]

Due to the existence of friction and heat loss during the turbine and compressor operation conditions, it needs more energy for this working process compared to ideal process. They are polytropic enthalpy change processes rather than isentropic processes. The definition of efficiency is the ratio of the

isentropic total enthalpy change to polytropic total enthalpy change.

According to the h-s diagram in Figure 1-26, the efficiencies calculation equation of compressor and turbine are shown below.

Turbine: $$\eta_t = \frac{\Delta h_{34,tt}}{\Delta h_{s,ts}} = \frac{T_{4t} - T_{3t}}{T_{4s} - T_{3t}} = \frac{1 - \left(\frac{T_{4t}}{T_{3t}}\right)}{1 - \left(\frac{P_{4s}}{P_{3t}}\right)^{\left(\frac{k-1}{k}\right)_g}} \quad (1.8)$$

Compressor: $$\eta_c = \frac{\Delta h_{s,tt}}{\Delta h_{12,tt}} = \frac{T_{2st} - T_{1t}}{T_{2t} - T_{1t}} = \frac{\left(\frac{P_{2t}}{P_{1t}}\right)^{\left(\frac{k-1}{k}\right)_a} - 1}{\frac{T_{2t}}{T_{1t}} - 1} \quad (1.9)$$

However, for actual application, the turbine efficiency is not easy to calculate based on Equation (1.9) due to the difficulty to obtain the experimentally accurate temperature at the turbine side, especially the turbine outlet temperature. This error could be so large (the high-temperature exhaust gas) that the efficiency calculation result could be large mistake based on the tested data. Therefore, to find and use the parameters that can be accurately measured is significant to calculate the turbine efficiency. To avoid the large temperature error, a method to use the parameters of compressor operation is shown below. The calculation of turbine efficiency includes the friction of the shaft.

System $$\eta_{total} = \eta_{t-m}\eta_c = \frac{W_c}{W_t} = \frac{\dot{m}_i \times C_{cp-in} \times T_{c-in} \times \left\{\left(\frac{P_{c-out}}{P_{c-in}}\right)^{\frac{\kappa-1}{\kappa}} - 1\right\}}{\dot{m}_e \times C_{tp-in} \times T_{t-in} \times \left\{\left(\frac{P_{t-out}}{P_{t-in}}\right)^{\frac{\kappa-1}{\kappa}} - 1\right\}} \quad (1.10)$$

Compressor $$\eta_c = \frac{\left(\frac{P_{c-out}}{P_{c-in}}\right)^{\frac{\kappa-1}{\kappa}} - 1}{\frac{T_{c-out}}{T_{c-in}} - 1} \quad (1.11)$$

Turbine $$\eta_{t-m} = \frac{\eta_{total}}{\eta_c} \quad (1.12)$$

W: power;

$\dot{m}$: mass flow rate;

P: compressor inlet and outlet pressure;

t: turbine;

c: compressor; m: friction

During turbine and compressor operation, the gas enthalpy changes occur. The difference of gas enthalpy between inlet and outlet is the enthalpy changes. For turbine, it's an enthalpy decrease process, however, part of it transfers to be used by the turbine, namely the effective turbine power depends on the turbine efficiency. Turbine power calculation equations are shown in equation (1.13) and (1.14), the ideal power and efficiency turbine operation lead to the actual turbine power. In the equation, the P_4/P_3 is the pressure ratio between turbine inlet and outlet. As a result, turbine inlet temperature, pressure ratio, mass flow rate and efficiency decide the turbine power.

Turbine: $$W_t = \eta_t \dot{m}_t \left|\Delta h_{t,s}\right| \tag{1.13}$$

$$W_t = \eta_t W_{t,ideal} = \eta_t \dot{m}_t c_p T_3 \left[1 - \left(\frac{P_4}{P_3}\right)^{\frac{k-1}{k}}\right] \tag{1.14}$$

To calculate the compressor power, the friction of the shaft should be considered. In that, turbine power transfers to compressor by shaft, and a shaft transfer efficiency is defined as η_m, as shown in equation (1.15). In addition, the compressor power could be calculated by compressor efficiency, air mass flow rate, compressor inlet temperature, and pressure ratio between compressor inlet and outlet.

Compressor: $$W_c = \eta_m W_t = \eta_m \eta_t \dot{m}_t c_p T_3 \left[1 - \left(\frac{P_4}{P_3}\right)^{\frac{k-1}{k}}\right] \tag{1.15}$$

$$W_c = \frac{W_{c,ideal}}{\eta_c} = \frac{\dot{m}_c \Delta h_{c,s}}{\eta_c} \tag{1.16}$$

$$W_c = \frac{\dot{m}_c c_p T_1}{\eta_c}\left[\left(\frac{P_2}{P_1}\right)^{\frac{k-1}{k}} - 1\right] \tag{1.17}$$

The enthalpy changes calculation of turbine and compressor are shown below, in which the temperature is the total temperature, including the dynamic part of temperature in equation (1.19).

Turbine: $$\Delta h_t = c_p T_{total,in}\left(1 - PR^{\frac{k-1}{k}}\right) \tag{1.18}$$

Compressor: $$\Delta h_t = c_p T_{total,in}\left(PR^{\frac{k-1}{k}} - 1\right) \tag{1.19}$$

Turbine inlet temperature $T_{total,\ in}$

$$T_{total,in} = T_{in} + \frac{c_{in}^2}{2c_p} \tag{1.20}$$

Here, *PR* is the pressure ratio, c_p is the specific heat of the inflow gas, T_{in} is the static inlet temperature, and c_{in} is the inlet flow velocity.

For turbocharged engines，it is mainly determined by the boost air supplied to the intake manifold coming from the compressor of turbocharging system. Pressure ratio of the compressor as a critical factor of turbocharging system to obtain a high boost pressure air. Many methods were applied to improve pressure ratio of the compressor, such as a high mechanical efficiency of the bearing system in

$$\pi_C = \frac{P_2}{P_1} = \left(1 + \frac{c_{p,g}}{c_{p,a}}\left\langle\frac{\dot{m}_T}{\dot{m}_C}\frac{T_3}{T_1}\eta_{TC}\right\rangle \cdot \left[1 - \pi_T^{-\left(\frac{k-1}{k}\right)_g}\right]\right)^{\left(\frac{k}{k-1}\right)_a} \qquad (1.21)$$

low-end torque, a high exhaust gas temperature before the turbine, a low charge-in density after the compressor, a large mass flow rate [77-79].

The overall efficiency of the turbocharger ：

η_{TC}= η_m η_T η_C;

η_m :mechanical efficiency（friction）;

η_C -the compressor efficiency;

η_T - the turbine efficiency;

π_T- Pressure ratio of turbine

1.3.4.2 Operation Map Characteristics of Turbocharger

For designed turbochargers, the operation efficiency is related to pressure ratio and turbine speed. Figure 1-26 shows the characteristics of shaft friction combined turbine efficiency changing with pressure ratio under different turbine speed. In general, there is a maximum turbine efficiency point for a turbine speed, as the designed working point. This efficiency $\eta_m\eta_T$ is the total efficiency which could be used by the compressor part. At low turbine speed, the pressure ratio is small and mass flow rate is also low, leading to low oil temperature in the bearing. This low oil temperature in the bearing results in large bearing friction, thus small mechanical efficiency. It means that the bearing friction has significant effect on the total turbine efficiency $\eta_m\eta_T$ of turbine, and bearing friction is affected by oil temperature. In addition, oil temperature in the bearing increases with turbine speed or shaft speed. However, the too high turbine speed leads to increased bearing friction. In that, from a certain turbine speed, the turbine total efficiency decreases due to the high mechanical efficiency with rising bearing friction. Thus, the characteristics of turbine total efficiency are shown in Figure 1-26.

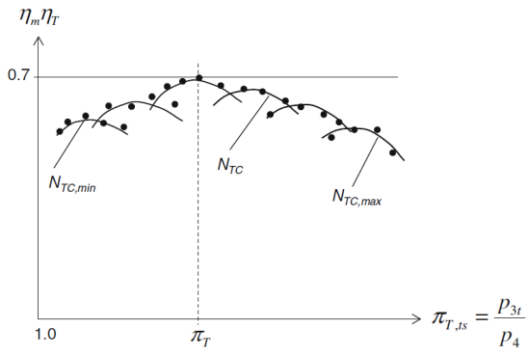

Figure 1-26. Turbine efficiency and pressure ratio [77]

Another part of turbocharging system is compressor, the operation characteristics are shown in Figure 1-27. It is a corrected mass flow rate versus pressure ratio graph, in which the surge line, choke line, efficiency island, and different turbocharger speed lines are plotted on the same graph. The corrected mass flow is calculated by reference temperature and pressure. In general, the reference temperature and pressure are account for the effects of ambient conditions, and these corrected mass flow rate and corrected speed is calculated by equations (1.22) and (1.23). The various turbocharger speed lines are depended on corrected mass flow rate, increasing with larger corrected mass flow rate.

$$\dot{m}_{Corrected} = \dot{m}(\frac{P}{P_{ref}})\sqrt{\frac{T}{T_{ref}}} \tag{1.22}$$

$$N_{Corrected} = \mathrm{N}\sqrt{\frac{T}{T_{ref}}} \tag{1.23}$$

The efficiency islands shown in Figure 1-27 reveal that the maximum compressor efficiency region is located at the central of turbocharger speed lines, namely, the range of both the middle of corrected mass flow rate and pressure ratio. In addition, the surge line and choke line are on the upper left, which represents the safe operation boundary on the working area of compressor map. Surge phenomenon is unstable condition of compressor operation due to lower corrected mass flow rate. This unstable condition may lead to severe vibrations of the axisymmetric oscillation of compressor flow. The vibrations could result in compressor damage due to large amplitude vibrations in compressor blades, bearings, connection pipes, resulting in compressor system damage and low reliability [82]. At surge point, the flow in the compressor is vibrate and detrimental. Thus, surge phenomenon should be avoided during the compressor selection and operation. Figure 1-28 shows how the surge phenomenon happens. At different compressor speeds, the surge points occur under the smallest corrected mass flow rate as shown in Figure 1-28 (1) [83], namely for the range with high gas pressure ratio and low mass flow rate. Compressor works by low-energy gas suction on the left side and high-pressure discharge on the right side in Figure 1-28 (2) [83]. The kinetic energy of compressor impeller is converted to the gas energy

(pressure head) through gas hurling in the radial direction. The point 1 is the air suction end with lowest energy, meanwhile, point 3 is the air energy maximum point. If as much as possible energy is imparted to air, reaching the100% compressor speed and 100% pressure, it will lead to too high backpressure to overcome, resulting in flow stalling near point 3. It means the gas kinetic energy at point 3 will transfer to be pressure due to flow stalling near point 3. As a result, the larger energy at point 3 than point 2 and point 3 leads to air flow reverse and backflow through impeller. Thus, compressor cannot work to boost the air. However, the air backflow will relieve the air energy at point 3, and the compressor begins to work again. The compressor surge occurring conditions or compressor working conditions are continually repeating occurrence and recovery. Thus, surge is a kind of cyclic variation phenomenon. This cyclic variation could cause so severe damage to the compressor parts that the it is significant to avoid surge occurrence in compressor operation.

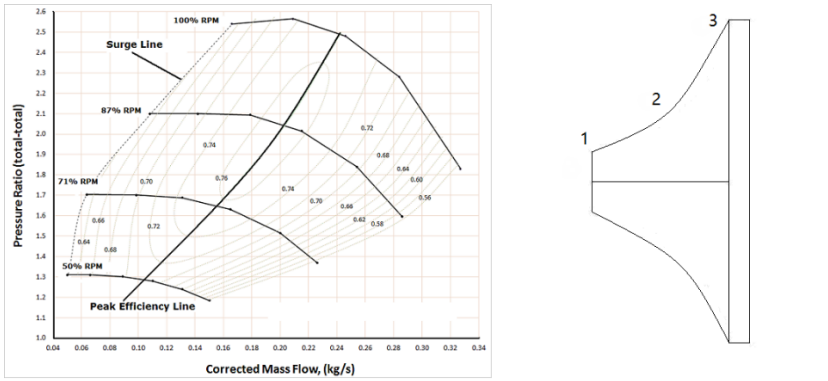

(1) Sample of compressor map (2) Schematic of compressor impeller

Figure 1-27. Compressor operation characteristics [80]

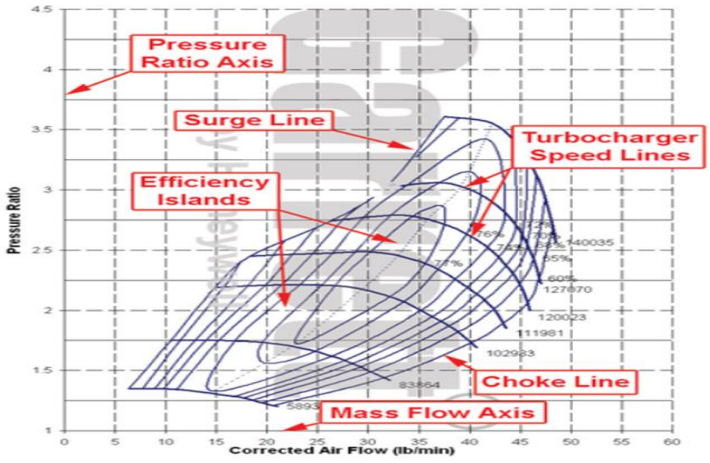

Figure 1-28. Compressor surge point characteristics [83]

The choke line (stonewalling) of compressor operation map is an abnormal operation condition of compressor. In general, centrifugal compressors could occur choke phenomenon under low pressure ratio with high flow rate conditions [83-86]. In compressor map of Figure 1-27, the choke line always

exists at the lower down range of the map. On the compressor operation map, the choke line means the allowed maximum mass flow rate at different compressor speeds for the used compressor. For compressor output, any further increased compressor output will not happen at the outside range of the choke line. The choke operation points happen when the resistance of flow in the compressor discharge line drops significantly below the normal levels [83]. The low resistance to flow in the compressor leads to low back pressure, resulting in increased gas velocity in the compressor. Moreover, at this operation points, this gas velocity increases continually until it reaches maximum value, namely sonic velocity. In fact, gas velocity is not able to exceed the sonic velocity. As abnormal operation phenomenon of the compressor choking, the parts of compressor, such as blades, rotors, will be damaged especially for long time running at choke points. In other words, choke points are dangerous to compressor. In order to avoid compressor choking, a certain operation limit needs to be set to prevent too low flow resistance happening. Some researchers name it an anti-choke value of compressor operation [83].

1.3.5 Types of Turbocharging System

Turbocharging systems have been widely used in turbocharged engines in recent years, however, due to the urgent needs to reduce fuel consumption and emissions, different types of turbocharging systems were developed to satisfy the future application, such as two-stage turbochargers, twin-turbo turbochargers, EGR combined turbochargers, and variable geometry turbochargers (VGT).In addition, turbocharger matching with a certain engine is also significant for turbocharged engines. The main of turbocharger matching is the pressure ratio and mass flow rate of turbocharger with mass flow rate and power required by the engine, namely the turbocharger operation map matching with engine performance characteristics. Korakianitis [87] investigated the turbocharger matching by theoretical calculation-based turbocharger matching and experimental tests. Results showed that theoretical turbocharger matching is convenient and useful, however, essential tests is also necessary to confirm the effect of different turbochargers on both the overall design-point and off-design-point performance. Moreover, the turbocharger performance is mainly decided by the compressor and turbine specification, and different engine operations maybe match well with different types of turbochargers. Meanwhile, compressor is more sensitive to matching with engine than compressor. Base on previous analysis, different engines should be matched with various turbochargers. For better using of turbochargers, researchers have developed different types of turbochargers to apply in engines.

Two-stage turbochargers and twin-turbo turbochargers have been applied in engines of current vehicle market due to the urgent need of less fuel consumption and CO_2 emission in recent years. Figure 1-29 shows two-stage and twin-turbo turbocharged engines. For two-stage turbocharger in Figure 1-29 (1), the intake system is combined with two sequential turbochargers, which the size of two turbochargers

are different (small size and big size). The intercooler is installed at the downstream of the compressor in these two turbochargers. In addition, both of these two turbochargers are fitted with bypass valve which allow no obvious pressure drops when just the primary TC is used in engine operation [87]. In fact, it is a graded turbocharging system, in which, the boost pressure continues to rise from the first stage to the second stage. The small size one is a high-pressure turbocharger, and the large size one is a low-pressure turbocharger. As a result, a higher intake pressure is achieved by this method. The advantages of two-stage turbocharger include better boosting characteristics at low engine speed, steady and transient engine conditions. The smaller size turbocharger is installed at the high-pressure stage, leading to better turbine response and easier acceleration of the vehicle due to the low moment of inertia [89]. MAHLE Powertrain has developed two-stage turbocharging system to enable better transient response and higher torque. Moreover, reduced real world fuel consumption benefits is also obtained by a reduction in full load fuel enrichment [90]. Based on an analytical model, Galindo [91] studied the effects of two-stage turbocharging system on engine pumping losses, and results shows that the reduced pumping loss and increased thermal efficiency by using two-stage turbocharger compared to single-stage turbocharger. However, one of the disadvantages of two-stage turbocharger system is the complexed and challenged nature of matching procedure and cost, resulting in no wide application so far [92]. The control of two- stage has become a key issue in wide speed of its application, and nonlinear model predictive control (NMPC) offering a high-potential in the control of two-stage turbocharger [93-95].

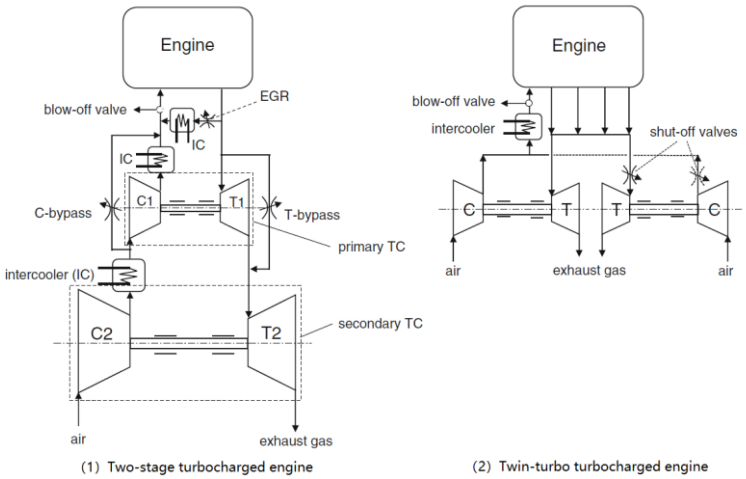

Figure 1-29. Two-stage and twin-turbo turbocharged engines [78]

Twin-turbo is known as a good solution to increase the response of turbocharged engines with many selections of layout in the engine compartment [96]. The application of twin-turbo is always in multi-cylinder double-number engines (6-cylinder engine, 8-cylinder engine), such as the 2.5-liter Biturbo V6, Nissan VG30DETT, 335i BMW, M276 DELA-30 of Mercedes Benz [97-100]. For example, for a V6

gasoline engine as shown in Figure [97], two parallel turbochargers are installed in the engine as the layout shown in Figure 1-30. In 6- cylinder engines, a group of three cylinders are connected to one turbocharger with different exhaust lines, and the exhaust gas enters the two parallel turbine housing and drive two small-size turbochargers. The two turbochargers are working independently at the same time [100]. The main effect of twin-turbo turbocharger is the reduced moment of inertia due to two small turbochargers application, thus leading to high response of the turbocharger.

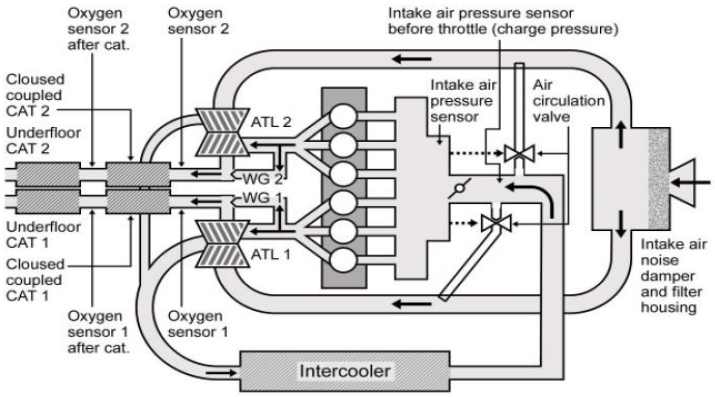

Figure 1-30. Twin-turbo turbocharged V6 engine [97]

Twin-entry turbocharger is a turbocharging system, in which the turbine is a kind of asymmetric twin-entry turbine. The twin-entry means the volute of the turbine combined with two entrances (two scrolls) in the axial direction. In addition, these two scrolls have different throat areas, one smaller one compared to the other one as shown in Figure 1-31 [101]. The reason for this design is to obtain reduced NOx emissions, meanwhile improved fuel economy of turbocharged engines. In fact, the small area scroll increases the exhaust pressure (backpressure), and the large scroll area decreases the exhaust backpressure [102-105]. The exhaust backpressure affects the exhaust gas recirculation, leading to the changes of internal exhaust recirculation. The increased backpressure increases the fraction of residual gas in the cylinder, thus depressing the oxygen concentration in the mixed gas reduce the combustion production of NOx. However, the reduced throat area of the turbine increases the backpressure by enhancing the flow resistance with worse scavenging condition, which should be avoided, thus larger throttle area is required in turbocharged engines. This condition is difficult to comprise in turbocharging system application. The design of using twin-entry turbocharger in Figure 1-31 increases the backpressure for enough EGR rate by the small throat area. In addition, the large throat area deceases the back pressure to achieve sufficient flow capacity (better scavenging) with more engine power output [101].

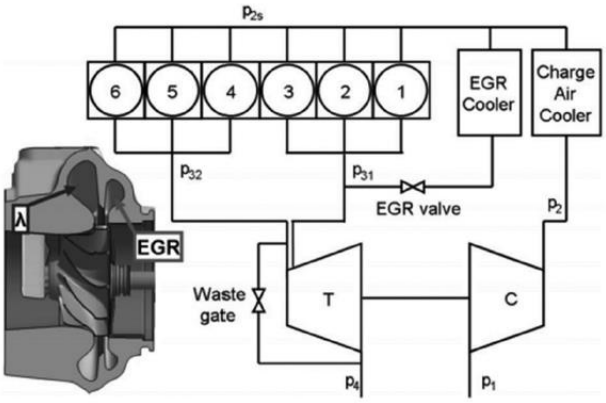

Figure 1-31. Twin-entry turbocharged engine [101]

1.3.6 Advantages and Disadvantages of Turbocharged Gasoline Engines

Turbocharging system with advantage to increase the intake air density have widely applied in the internal combustion engines for engine downsizing. In recent years, many vehicles on the market have combined turbocharged engines, and even Mazda, which is proud of its naturally aspirated engines, has developed and applied turbochargers as shown in Figure 1-32 [106].

Figure 1-32 Mazda CX-9 Turbocharged SKYACTIV G 2.5T [106]

One of the advantages of turbocharged gasoline engines is to increase the engine power. Formula（24）is always used to calculate the engine power of a four-stroke cycle engine, in which the parameters affecting the engine could be found, such as volumetric efficiency, air density and engine volumetric capacity. For engines with the same displacement, the volumetric efficiency, and air density is the key to increase the engine power. This is the reason why boosting the intake pressure could increase engine power output, thus downsizing the engine with small engine displacement. Turbocharged engines allow for smaller engine sizes to produce much more engine power relative to their size [107-108].

$$P = \frac{n_f \cdot n_v \cdot N_e \cdot V_d \cdot Q_{LHV} \cdot \rho_{air} \cdot \left(\mathrm{F}/\mathrm{A}\right)}{2} \quad (1.24)$$

n_f: fuel conversion efficiency;

n_v: volumetric efficiency,

Ne: Engine speed, [rot/s];

V_d: engine volumetric capacity (swept volume), [m^3];

LHV: low heating value, [J/kg];

ρ_{air}: air density, [kg/m^3];

F/A: fuel air ratio;

Better fuel economy of turbocharged engines is another pro compared to conventional engines. In idle engine condition, small size engines need less fuel consumption to maintain the idle operation due to less rotational and reciprocating mass. The cooling loss and friction loss in the engine operation process are reduced due to its small size compared to normal engine [109-110].

The higher efficiency of turbochargers combined engines is another advantage compared to the conventional engine. Turbocharger system is to use exhaust gas energy to drive the turbine in which the used energy is typically lost in NA engine, thus the overall efficiency of the engine is improved through the recovery of exhaust gas energy [111]. In the research of Reddy [112], results showed that the volumetric efficiency was increased at low power conditions and decreased at medium and high engine power output. The brake efficiency increased with the output power continuously with increased intake pressure. Meanwhile, the increased cylinder pressure also improved the combustion efficiency. All of these led to the increased thermal efficiency.

Worse engine response at transient engine conditions is a main disadvantages of turbocharged gasoline engines, which is also called turbo lag. It means that due to the shaft inertia, turbochargers, especially large turbochargers, take time to spool up and provide targeted intake pressure. To operate turbine, to achieve high boost pressure which means more air is used for fuel combustion thereby improving fuel efficiency [113-114]. However, turbocharged engines are characterized by transient operating problems, poor engine response during load or speed increase, lacking sufficient exhaust energy to operate the turbine efficiently [115-116]. More seriously, turbocharger transient operating problems can cause severe deterioration in emissions during acceleration and load changes [117]. Under low loads, the cylinder and manifold wall temperatures are lower than higher loads. Therefore, when the load is increased, the high temperature exhaust gas is used to heat the wall for a certain period of time which leads to lower exhaust gas temperature before the turbine. Due to this, the actual supercharging pressure cannot meet the demand for increased engine load or speed, thus, to reduce the time delay of turbine is important in turbocharging system application.

Power surge is another disadvantage in turbocharging system applications with high unsteady operation of the compressor, especially the large -size combined turbocharger, reaching the boost threshold of the compressor operation. It always happens at low flow rate required to high engine load, leading to compressor operation unsteady, which may result in compressor damage [118-122]. The maps of compressor and turbine are only tested at steady engine conditions however, the surge phenomenon is coming from oscillating flow inside the turbocharger. Then, the surge also appears at vehicle acceleration and deceleration conditions. Deep surge could be very seriously characterized with a sudden high drop in the pressure delivery, meanwhile large pulsating flow that may be very harmful to lead to the compressor or bearing operation failure [122-124].

Knock occurrence turns to be easily in turbocharged gasoline engines. Due to the damage to the engine, knock has become the barriers to improve the thermal efficiency of SI engine, especially in the high boost gasoline engines [125-128].The unburned end gas lead to the auto-ignition and detonation which results in knock as the knock occurrence theory [125]. Researchers has found some knock occurrence model, such as higher in-cylinder soot emission correlated and carbon particles induced super-knock with high peak pressure and pressure oscillations [129], mega knock [130-131], surface ignition, lubricated oil, and fuel/oil mixing induced low-speed pre-ignition (LSPI) [132-133] or deto-knock [134] in turbocharged gasoline engines, especially for GDI engines under the low-speed high-load operation conditions. These knock occurrences could result in unsteady engine operation conditions, thus avoid knock phenomenon is important.

The higher exhaust gas temperature of gasoline engines compared to that of diesel engine is one of the restrictions for the fuel economy of turbocharged gasoline engines. The exhaust gas temperature can be high to 950- 1100 ℃, which could destroy the turbine, resulting in useless of the turbocharging system.

1.3.7 Techniques to Improve the Turbocharged Engine Performance

Turbocharged engines using exhaust gas energy to run the turbine and increasing the boost pressure, still have its own disadvantages as introduced in previous. Researchers have developed method to improve the performance of turbocharged engines and the disadvantages as flows.

To reduce the turbine response (turbo-lag) of turbocharging system, small size turbines with low inertia and variable geometry turbochargers (VGT) have widely applied in diesel engines to improve the turbine performance at transient engine conditions and increase the engine output power [135]. IHI [136] developed new design concepts to increase the turbine rotation at low engine speed by decreasing turbine size and altering the turbine impeller shape thus obtaining enough boost pressure for required torque. As

a technology with great potential to improve fuel consumption, different types of turbocharging systems have emerged. The VGT is a type of turbocharging system combined with variable geometry（gas flow channel）inside the turbine, thus changing the back-pressure in the turbine. VGT is another technology to improve the low engine speed performance. Ebisu [137] used VGT to increase the engine thermal efficiency of gasoline engines. The simulation result shows 2%-3% fuel consumption decreases under JC08 driving condition. Moreover, it also demonstrates the advantages of increased output power and reduced emissions with new turbocharging system. An experimental study reveals 5-10% more brake power is achieved for an engine with turbocharger following with less CO and HC emissions compared to the engine without turbocharger [138]. With a turbocharger, NOx and CO_2 emissions also decreased in a single-cylinder diesel engine based on experimental test [139]. MHI [140] also developed a new type of VGT turbocharger using high-temperature resistance technology to improve fuel consumption by increasing the temperature of exhaust gas for low pollution cars.

Turbocharging combined with other advanced technologies shows great potential for improving fuel consumption and emissions. The valve timing can also affect the particulate emissions of direct-injection turbocharged engine [141]. A 3-cylinder turbocharged gasoline direct injection engine employs variable valve action (VVA). It had obtained 18% CO_2 emission reduction as compared to the conventional engine in the study of Kirwan [142].

Downsized turbocharged gasoline engines run at higher mean effective pressure (MEP) compared to NA engines for the same torque output which may lead to knocking at high engine load. It is dangerous for gasoline engines, especially heavy knock which causes damage to the engine. To avoid knocking, cooled exhaust gas recirculation (EGR) is introduced to retard the combustion and increase the knock limit and spark advance hence resulting in low fuel consumption [143]. In addition, EGR can reduce NOx emissions and improve the engine thermal efficiency effectively [144-145].

New exhaust energy recovery methods were also launched during the past several years to improve the turbine performance, thereby the engine performance. Heat storage medium is one of these applications. Phase change medium such as water which absorbs heat energy by vaporization process generates steam to assist in turbine working. This steam improved turbocharging thermal efficiency by about 2% basing on simulation results [146].

1.3.8 Porous Material Utilization in Engines

Porous mediums with complex and variable internal structures have attracted attention and been widely applied in many research areas recently, such as catalytic reactors, thermal energy storage, and

[147,148,149]. In these studies, the heat exchange between porous media and other media or energy (such as water as phase change material, engine exhaust, solar energy) is one of the most important and common application of porous mediums with large surface areas and variable porosity. Such porous mediums can change the flow and heat exchange conditions [150]. Porous material with fixed porosity was studied by Chandrasekhara, in which a flow model was founded to evaluate the velocity distribution among porous beds [151,152]. Transfer and Vafai [153,154] studied the heat transfer of porous medium and developed that Rayleigh numbers had a significant effect on the heat transfer coefficient. Large surface areas and enhanced conductivity features of porous medium have been used to develop energy storage and conversion devices [155]. A porous substrate microchannel heat sink was used to improve thermal performance, porosity and fin thickness. These factors in-turn were optimized using simulation method [156]. In order to study the heat transfer conditions within the interface region of porous material, the Darcy number, Reynolds number and porosity of porous media were studied. This indicated that the change of boundary conditions has a significant effect on the velocity and temperature changes [157,158]. A porous microchannel heat sink was designed to reduce the drop of pressure and thermal resistance. The model simulation illustrated a high marked reduction of pressure drop [159]. Porous media with a relatively high surface area and a small pressure loss of porous structure (less energy loss) have the advantage of heat exchange or storage.

Porous materials have been used to store and reuse engine exhaust heat, however, the high temperatures and pressures of exhaust gases limit the selection of material. The material used to store the energy of the exhaust gases must have high temperature resistance. In addition, the medium should exchange heat with the exhaust gas effectively because the interaction duration of exhaust gas and medium is relatively limited. Porous materials with larger surfaces such as silicon carbide and silicon can withstand high temperature and therefore attracted many researchers. In recent years, porous materials such as SiC ceramic honeycomb (SCH), porous mullite-bonded silicon carbide and porous silicon nitride-bonded silicon carbide have been studied due to their high thermal conductive features [160]. Research on the thermal conductivity changes in porosity and on the components of porous material has shown that if porosity changes from 30% to 74%, thermal conductivity could vary from 2 to 82 W/(m·K) and Y2O3-La2O3 sintered SiC has a range of 169-206 W/(m·K) for thermal conductivity. Moreover, SiC in a honeycomb structure has been used in engines as a particulate filter with smaller pressure loss [161,162,163]. Therefore, it is possible to use porous SiC and Si as heat storage materials (HSM) [164].

1.4 Thesis Objectives and Approaches

Porous materials have the potential to be used as heat storage medium in engines [165-170]. To

improve the engine response of turbocharged engine and obtain further reduced fuel consumption, a kind of porous Si-SiC material porous is applied and evaluated to investigate the possibility of improving engine performance in a turbocharged gasoline engine, the main objectives studies are shown as follows.

1) For a better understanding of the used porous material, the characteristic parameters of porous Si-SiC material are studied, such as substrate surface area, substrate surface volume, heat capacity, heat transfer, pressure loss [171]. To easily evaluate the effects of porous material on performance of turbocharged engines, models of porous Si-SiC material are developed and calibrated, including structure model, heat transfer model and pressure loss model [172].
2) The used porous Si-SiC material is installed before the turbine, as a kind of heat storage material to store and reuse the energy of exhaust gas. The changed exhaust temperature and exhaust pressure affected by the added porous Si-SiC material are studied under engine steady and transient engine conditions. Moreover, the turbine response is investigated at engine load recovery conditions.
3) The porous material installed at the upstream of turbine could affect the exhaust temperature and pressure, thereby the engine performance. Thus, the effects on fuel economy under steady and transient conditions are studied
4) To improve the performance of VGT application in gasoline turbocharged engines under high engine load, porous Si-SiC material is applied to reduce the turbine inlet temperature, thus obtaining the expanded engine stoichiometric combustion region and the increased maximum engine output power.

The characteristics of porous material are calculated and analyzed in micron level by scanning electron microscope (SEM) and computed tomography (CT). The developed porous material model and engine model are developed by experimental data. The effects of porous material on engine and turbine performance are investigated by simulation method.

1.5 Outlines

The outlines of this dissertation are shown as follows: Firstly, Chapter 1 introduces the background and motivation of this research, meanwhile, the pros and cons of the advanced techniques of engines and the fundamentals and types of boost techniques are also introduced. Porous material characteristic studies and model development and validation are shown in Chapter 2, including porous material model of structure, heat transfer pressure loss, engine model, Worldwide harmonized Light-duty vehicles Test Cycles (WLTC) model. Then, the models are applied in the following research. In Chapter 3, the porous material is installed before the turbine to investigate the effects on turbine and engine response. The

engine fuel consumption is investigated under both steady conditions (same load) and transient conditions (WLTC driving cycles) in Chapter 4. Due to the drawbacks of variable-geometry turbochargers (VGT) application in turbocharged gasoline engines, Chapter 5 introduce the possibilities of using porous material to improve the high-temperature reliability, stoichiometric combustion region and peak torque. Finally, the conclusions and future prospect are proposed in Chapter 6.

Chapter 2 Experiment and Model Development of Porous Material and Engine

2.1 Porous Material Introduction

The structure of material combined with pores (voids) is named porous material or porous medium [173]. In general, the characteristic of pores or voids is typically filled with a fluid channel for liquid or gas, in which the skeletal material is usually a solid [174].The porosity maybe one of the main parameters, except for the properties of permeability, tensile strength, electrical conductivity, tortuosity.

Table 2-1. Properties of Porous Material

Characteristic Parameters	Properties	Unit
Material	Si and SiC	-
Density	2500	kg/m^3
Porosity	90	%
Heat Capacity	2930	J/kg-K

The expanded heat exchange surface areas and increased thermal conductivity are also characterized to apply in heat storage or cooling. The total volume of porous material includes the volume of substrate material and air in pores, in which the porosity determines the substrate volume. In addition, the substrate surface area is also related to porosity and substrate skeleton bone thickness. In general, the heat exchange between solid (skeletal material) and gas (pore) is heat transfer, and typically occurs by convection. Heat transfer coefficients, transfer surface area, and temperature difference between solids and gases are main parameters to calculate the heat transfer [175]. Substrate surface area plays an important role in the amount of heat transferred per unit of time. Moreover, skeletal material determines the heat capacity of the porous material.

Meanwhile, the porous material is fragile during installation, transportation, and use, especially for high porosity. The broken porous material may damage the high-speed running turbine. Then, it is important to find suitable material and porosity of porous material to apply in turbocharged engines. The catalyst to converted the harmful substances (CO,NOx, HC) in the exhaust gas into harmless substances [271]. It has similar structure with porous material used in this research which has been widely used in engines. As the working temperature restriction of the catalyst, and the higher exhaust temperature of turbine inlet than the turbine outlet, the catalyst working could be improved by installed in a porous material, especially during cold start condition.

A kind of porous material is used as heat storage medium in this study and the characteristic parameters are given in Table 1. The compositions of the used porous material are silicon and silicon carbide (Si and SiC). The porosity is an important parameter for material with porous structure, and the porosity of the used porous material is 90%, namely, the ratio of substrate volume and gas flow channel volume is 1/9. The density of this material is 2.5 g/cm^3. The heat capacity is 2930 J/kg-K which is an important parameter for heat storage medium. The substrate volume and substrate surface area are the Si and SiC volume and surface area used in this study as shown in Figure 1 in which the diameter of the used porous material is 130mm with a length of 100 mm.

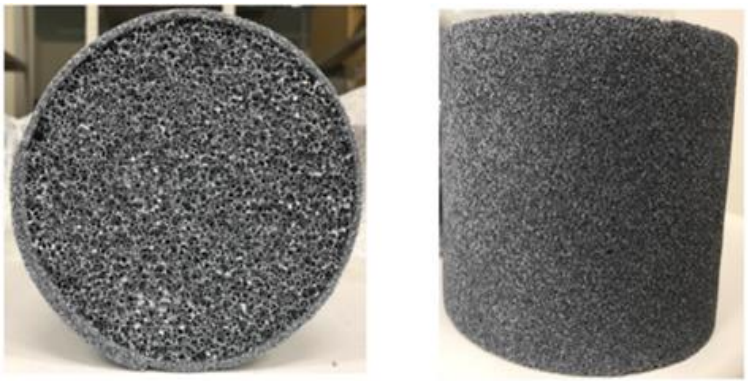

Figure 2-1. The structure of porous material Si-SiC

2.2 Model Development and Validation of the Porous Material

2.2.1 Model Simplification of Porous Material Si-SiC

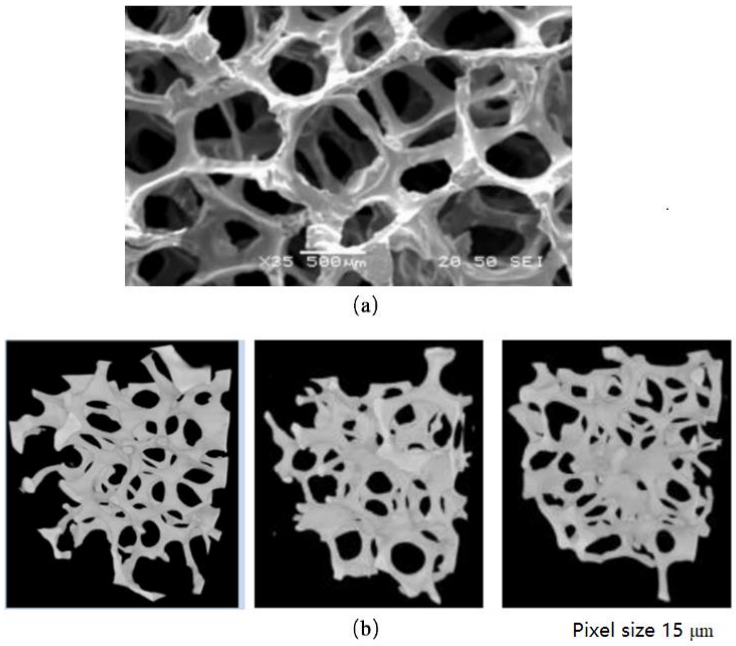

Figure 2-2. Micron level structure analysis of Si-SiC by SEM and CT

To be able to identify and define the used porous Si-SiC material, the porous Si-SiC material was analyzed through micron level structure analysis. Figure 2-2 is the micron level structure images of Si-SiC by scanning electron microscope (SEM) and computed tomography (CT). The porous structure of the used porous Si-SiC material is obvious shown in Figure 2-2, in which the skeletal material is solid with pores around it.

The characteristic parameters based on SEM and CT image analysis are shown in Table 2-2. The results coming from the basic images shown in Figure 2-2 are initially indicating the pixel size rather than the actual numerical size. As it's three-dimensional of porous material, the pixel size is also tested by three images in Figure 2-2 at three directions (X,Y and Z) shown in Table 2-2, in which Z represents the layer number. By unit conversion and calculation, the skeletal material volume and skeletal material surface area are able to be calculated and shown in Table 2-3.

Table 2-2 Analysis results based on the SEM and CT

Orientation	Value	Unit
X	8.00×10^2	pixel

Y	7.00×10^2	pixel
Z	9.00×10^2	-
Pixel size	15.00	μm
Skeletal material volume	5.02×10^7	$pixel^3$
Skeletal material surface area	4.09×10^6	$pixel^2$
Percent Skeletal material volume	10	%

* Z= layers number

* Skeletal material surface area = the substrate surface of the heat storage material

* Percent Skeletal material volume = the substrate volume of the heat storage material

Table 2-3 Analysis results based on unit conversion

Parameter	Value	Unit
Substrate volume	1.70×10^2	mm^3
Substrate surface area	9.20×10^2	mm^2

In this research, the cylindrical structure porous Si-SiC material (D=130mm, L=100mm) shown as Figure 2-1 with characteristics shown in Table 2-3. In fact, it is difficult to define the structure in model development, however, it is possible to obtain a simplified model along with the same substrate surface area and substrate volume with the actual porous Si-SiC material. A simplified structure model is shown in Figure 2-4 and the porous flow channel of Si-SiC is simplified to straighten the line square channel, of which channel width and cell density are two main parameters in determining the properties of the square geometry. Figure 2-5 is a model simplified calculation flow chart to explain the calculation method of the substrate surface area and substrate volume for the model. Firstly, one cell of the model is focused on in which the unit of cell density is $/mm^2$ hence 1/cell density is the front total area of one cell [176]. The porosity of Si-SiC is 90% (namely the ratio between gas flow channel area and substrate area is 9/1), then the flow area and substrate area of one cell are 90% × front total area of one cell and 10% × front total area of one cell respectively. Moreover, gas flow channel also has surface area for heat transfer hence it needs to be calculated. The model calculation results were shown in Table 2-4 with little difference based on cell density (0.2042 $1/mm^2$) and substrate thickness (0.3591 mm) compared with the calculation results in Table 2-3.

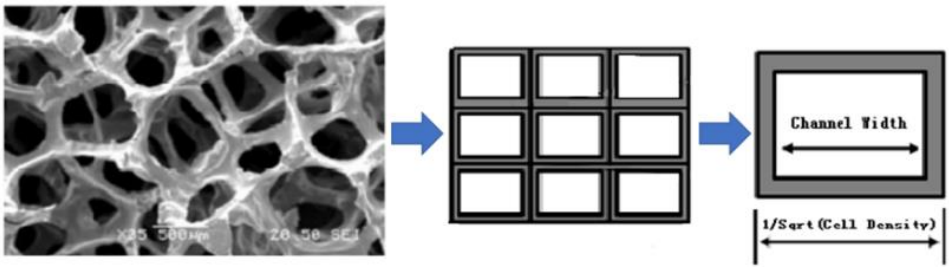

Figure 2-4. Structural model simplification of porous materials

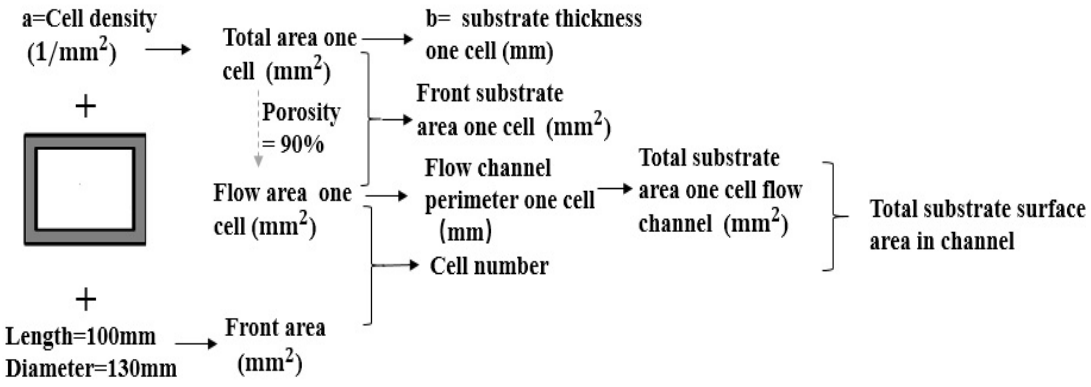

Figure 2-5. Total substrate surface area and substrate volume calculation method

Table 2-4. Substrate surface area and volume based on actual calculation and model calculation

Parameter	Based on Table 2	Based on Model Simplification	unit
Cell density	-	2.0420×10^{-2}	$1/mm^2$
Substrate thickness	-	3.5910×10^{-1}	mm
Surface area	7.1979×10^5	7.1975×10^5	mm^2
Substrate volume	1.3273×10^5	1.3273×10^5	mm^3

Table 2-5. Heat capacity calculation based on S/V ratio of different diameter

Diameter	Length	Substrate surface area	Substrate volume	Total Heat
mm	mm	mm^2	mm^3	J/k
90	100	3.45×10^5	6.36×10^5	4.66×10^2
100	100	4.26×10^5	7.85×10^5	5.75×10^2
110	100	5.15×10^5	9.50×10^5	6.96×10^2
120	100	6.13×10^5	1.13×10^6	8.28×10^2
130	100	7.20×10^5	1.32×10^6	9.71×10^2

The heat capacity varies with the size of the porous material. In this research, diameter and length of the porous material determine the size. In addition, the substrate volume and substrate surface area at different sizes are shown in Table 2-5. It is obvious that the heat capacity of the porous material increases with the increased diameter and length.

2.2.2 Model Validation of Porous Material Si-SiC

Commercial software GT-Suite was introduced as a convenient method to study the effect of porous material on exhaust gas, in which the porous structure parameters and thermal properties parameters

were used to simulate the actual porous material. Hence it is possible to define the structural parameters of porous materials and calculate heat transfer between exhaust gases and porous material. Moreover, a pressure drop model based on Re and pressure loss coefficient K is used to calculate the exhaust gas pressure loss shown as Figure 2-7.

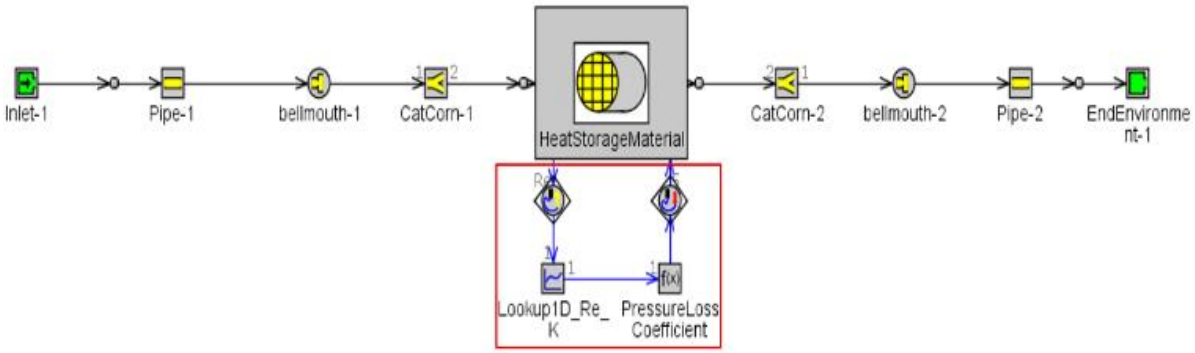

Figure 2-6. The calibration model of Si-SiC

The model accuracy needs to be checked by experiment. especially for temperature change conditions (engine transition condition). Therefore, porous material Si-SiC as heat storage material (HSM) was added at the downstream of engine exhaust manifold in Figure 2-7. Engine specifications are shown as Table 2-6. High temperature thermocouples（HOSKINS2300,φ1.0）were used to measure the inlet and outlet gas temperatures of HSM. In addition, it is important to use the high-response thermocouples in the calibration experiment, especially the temperature test at transient conditions. Two water-cooled absolute pressure sensors (Kister 4049A) were used to measure exhaust gas pressure.

A model of porous material was developed shown in Figure 2. The model includes a structure model, a thermal model, a pressure loss model which were calibrated by calculation and experiments results. Substrate surface area and substrate volume are two important parameters for porous material which represent the volume and surface area of Si and SiC in the used porous material for the diameter of 130mm and length of 100 mm. To maintain the same heat capacity and heat transfer surface area of the actual porous material, the structure model calibration method is to keep the same substrate surface area and substrate volume. Table 2 shows that the calculation results based on the actual structure and the structure model are with little calculation error.

The pressure loss calculation through porous material is based on Equation (1) and (2). The calculation results of pressure loss are in good agreement with the experimental pressure loss. For thermal model calibration, the outlet temperature of the porous material was tested at the process of engine load changing shown in Figure 2. As porous material is used as a kind of heat storage medium, it is important to check the outlet temperature at transient conditions. It can check the heat transfer and heat capacity

of the model. The calculation results of the outlet temperature matched well with the experiment temperature shown in Figure 3. Then the structure model, thermal model and pressure loss mode model can predict the outlet temperature of porous material and pressure with little difference which can be used in this work.

Table 2-6. Specifications of Engine

Engine	4-Cylinder. 4-Stroke.SI Engine
Bore	73mm
Stroke	74.2mm
Comp. Ratio	11
Displacement	1242cc

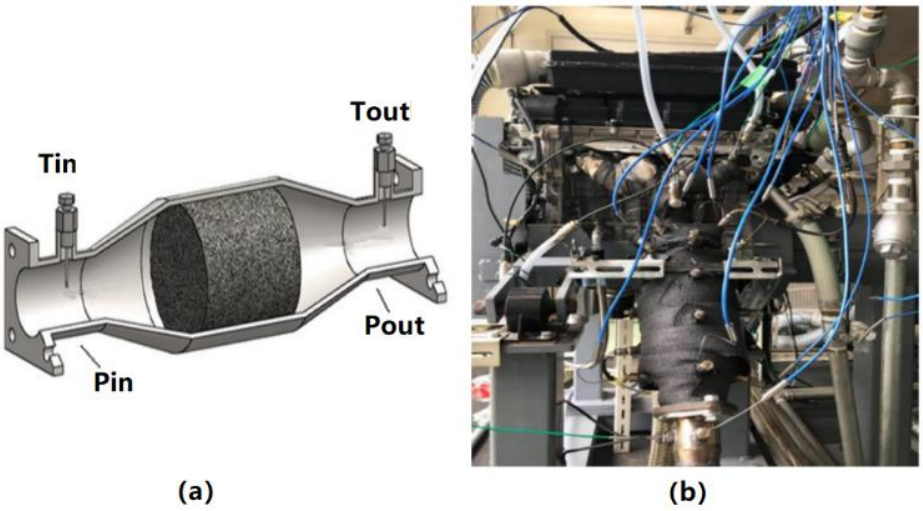

Figure 2-7. Experiment bench setup

Pressure loss model calibration

The gas pressure loss through porous material Si-SiC is related to the size of Si-SiC, namely the diameter and length. Furthermore, the pressure drops between the porous material inlet and outlet increased length and decreased diameter of porous material. Meanwhile, the Reynolds numbers range was 5000-29000 for exhaust gas flow, shown in Habib′ s study [177]. Therefore, based on Equations (2-1) and (2-2), the dimensionless constant Reynolds number (Re) vs pressure loss coefficient K was obtained in Figure 2-8 by experiment and calculation results. L is a characteristic linear dimension of the porous material, and as the structure of the used porous material is a uniform circular pipe, in this

research L is the diameter. The Reynolds numbers are the data at the entrance of HSM. It also shows that K does not changes largely with the increased Reynolds numbers. Then, the pressure loss coefficients K corresponding to the Reynolds numbers were obtained with a look-up table which is inserted into the model to calculate pressure drop due to the added porous material. Experimental and calculation results are shown in Figure 2-8 with small pressure loss and no significant differences.

$$\Delta P = P_{in} - P_{out} = \frac{1}{2} K\rho \left(\frac{\dot{m}}{\rho A_0}\right)^2 \qquad (2\text{-}1)$$

$$Re = \frac{\rho v L}{\mu} \qquad (2\text{-}2)$$

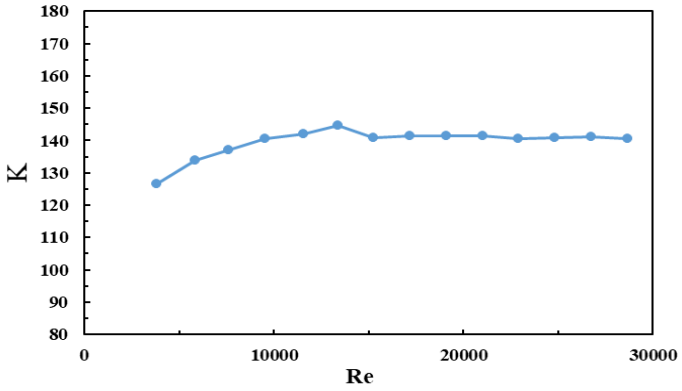

Figure 2-8. Re vs pressure loss coefficient K

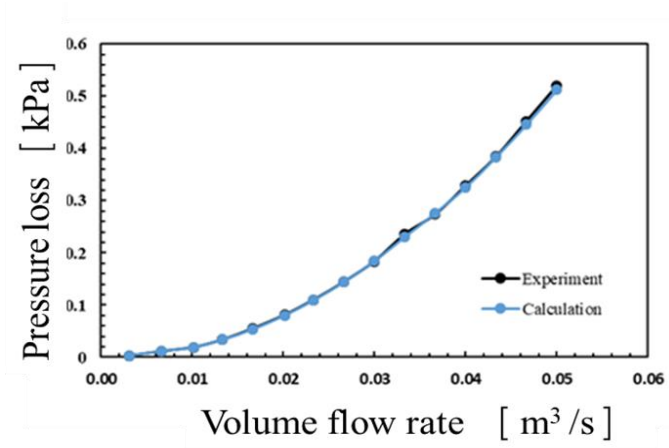

Figure 2-9. Comparison of pressure loss of experiment and calculation result

Thermal model calibration and results

In this study, the porous Si-SiC material is used as a type of heat storage medium to exchange thermal energy with exhaust gas. Therefore, to investigate the thermal properties related to thermal evaluation is necessary, such as Si-SiC, heat capacity and conductivity. In addition, the exhaust gas temperature varies

during engine load or speed changing conditions, which may represent a significant temperature difference at transient engine conditions. Meanwhile, the thermal properties of porous Si-SiC material may also change with different temperature. Pappacena [178] demonstrated that thermal conductivity of porous silicon carbide could reduce quickly from approximately 36 W/m K to 11 W/m K when the temperature had changed from approximately 0℃ to 1100℃. Mills [179] found that the heat capacity rose with the decreased thermal conductivity as temperature increased from 0℃ to 1500℃. Thus, the different temperatures correspond to different heat conductivity and thermal capacities are shown as Figure 8 [180].

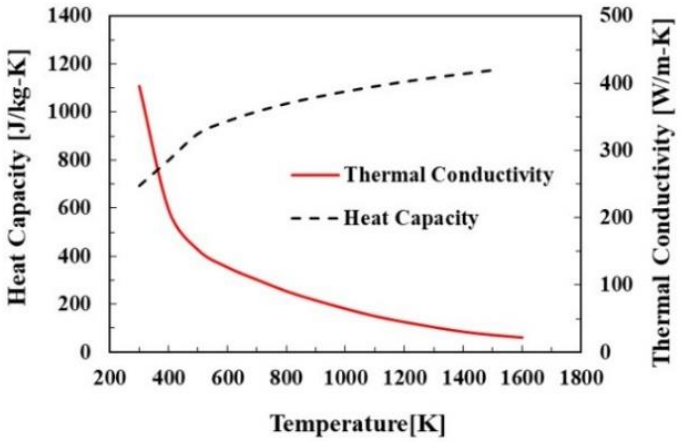

Figure 2-10. Thermal conductivity and heat capacity data correspond to different temperature.

To verify the accuracy of the thermal model, engine load changes when the HSM outlet temperature reaches a steady state. This means that the HSM has achieved thermal equilibrium with the exhaust gas and effects the temperature versus time curve. In these experiments, the temperature change curve after the load change was highlighted and the accuracy of the model was studied using five engine load conditions. The exhaust gas temperature was in the range of about 400 ° C to 850 ° C which makes the model applicable from low temperature to high temperature. For thermal model calibration, the outlet temperature of the porous material was tested at the process of engine load changing, as shown in Figure 2-11. As porous material is used as a kind of heat storage medium, it is important to check the outlet temperature at transient conditions. It can check the heat transfer and heat capacity of the model. The calculation results of the outlet temperature matched well with the experiment temperature in Figure 2-11. Then the structure model, thermal model and pressure loss mode model can predict the outlet temperature of porous material and pressure with little difference which can be used in this work.

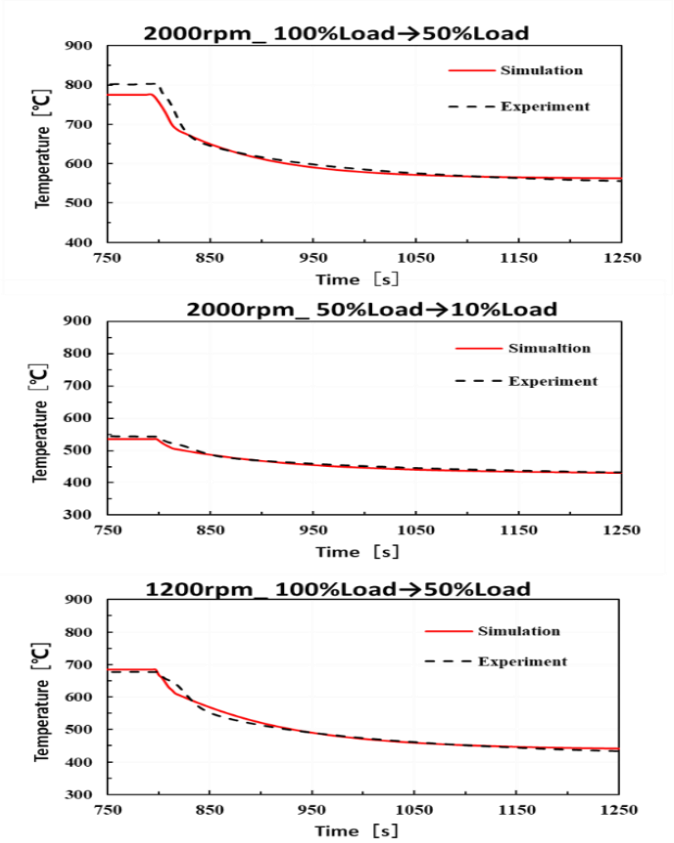

Figure 2-11. Calculation and experiment results of exhaust gas temperature after Si-SiC at engine load change conditions

2.3 Model Validation of the Engine

Table 2-7 shows the specifications of the turbocharged gasoline engine used in this study. In order to investigate the impact of HSM on engine fuel consumption, a GT-power model of this engine was calibrated using experimental data. Figure 2-12 shows engine torque test data (72 points) along with engine speed ranging from 650 rpm to 4400 rpm. The calculation results of BSFC using GT-power model are shown in Figure 2-13. It is shown that for most data, the errors were within 3%. The sub-models of HSM were implemented to the GT-Power model of this engine.

Table 2-7. Specifications of the target turbocharged engine

Induction type	Turbo charged
Displacement	1618 cc
Compression ratio	9.5
Number of cylinders	4
Bore	79.7 mm

Stroke	81.1 mm

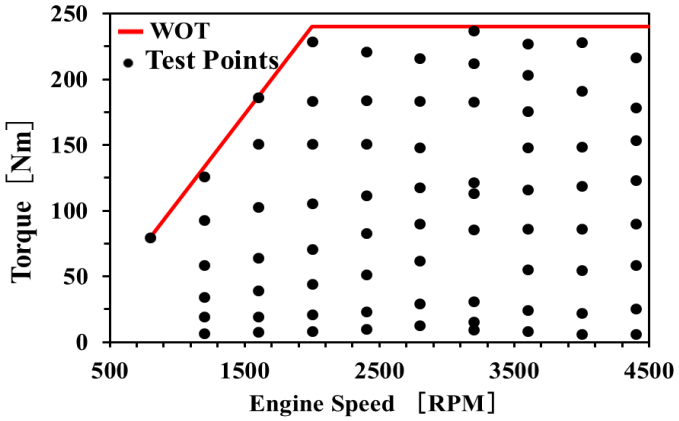

Figure 2-12. Experiment points of engine performance testc

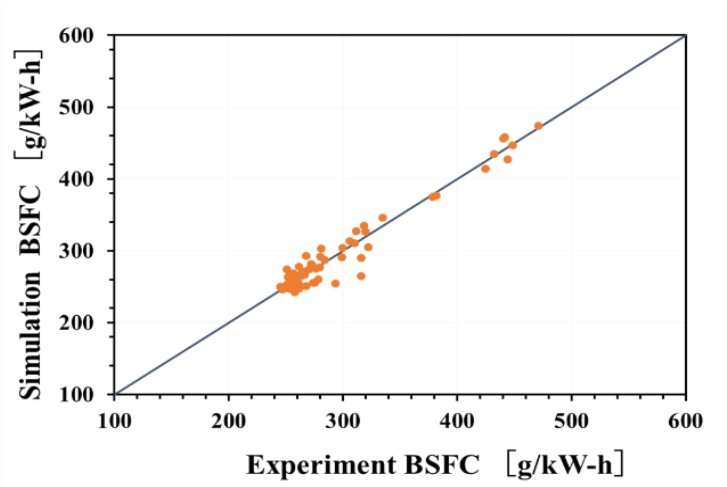

Figure 2-13. BSFC simulation results compared with experiment

2.4 Model Validation of WLTC Driving Cycles

The previous section presented the effect of HSM on fuel consumption under steady engine conditions. In addition, HSM can also come into effect at the engine load or speed recovery process, so it is necessary to evaluate the working of HSM at transient engine conditions. Worldwide harmonized Light vehicles Test Cycle is an effective and realistic comparison method to study the engine transient fuel consumption [235-239]. To use this method, a WLTC driving cycle model with engine maps was built and calibrated with experiments. The specifications of the target vehicle are shown in Table 2-8. The driving cycle map model is a type of simplified driving cycle model in which the full engine model is facilitated to a simplify engine model for fast and easy calculation in Figure 2-14. This model also includes the transmission and chassis models of the vehicle. The target of building this model is to verify the accuracy of the necessary data coming from the test bench such as the maps in the engine, running resistance data, CVT transmission control map and tire rolling resistance coefficient, etc. This paper just uses this model

to verify the validity of maps for engine calculation. The whole process of testing will not be described in detail.

Table 2-8 Specification of target vehicle

Body	Seating capacity	5
	Gross vehicle weight	1400 kg
	Max. torque	240 Nm/ 2000~5200 rpm
	Induction type	Turbo charged
	Displacement	1618 cc
	Compression ratio	9.5
	Number of cylinders	4
Drivetrain	Transmission type	CVT

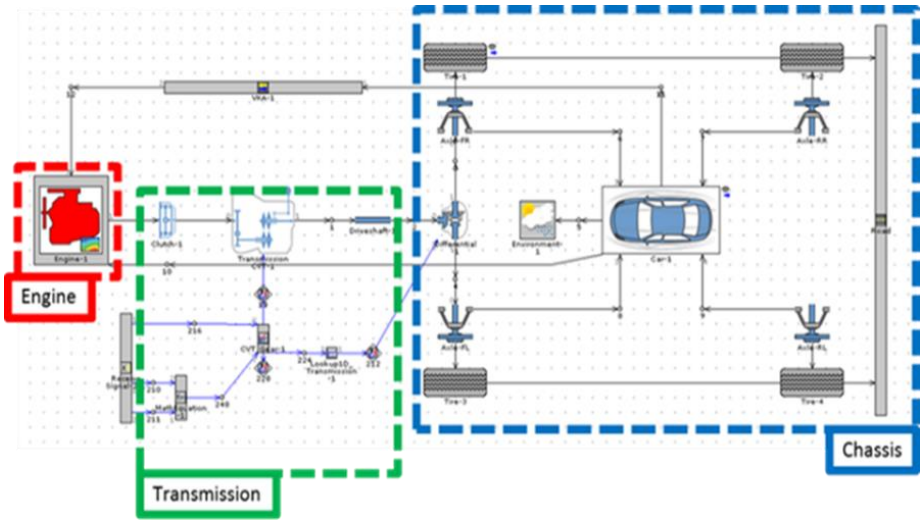

Figure 2-14. Driving cycle calculation model [270]

Figure 2-15 shows the fuel consumption of the WLTC driving cycle by the chassis dynamo and the driving cycle map model. The simulation is based on the vehicle speed of standard WLTC driving cycle and the simulation results are shown in Figure 2-15. The WLTC driving cycle has four vehicle speed regions, including low speed, medium speed, high speed and extra high speed which are shown at the top of the Figure 2-15. The blue line shows the simulation results of vehicle speed and there is no obvious difference compared to red line of target vehicle speed. The maximum error between the experiment and calculation is 2 km/h within 5% from the low to high vehicle speed which is shown in the Figure 2-15. The simulation results are matched well with the experiment. As a result, other engine performance parameters of the WLTC driving cycle such as engine speed, braking torque, and engine fuel flow were also obtained through experiments and simulations. Moreover, it was demonstrated that parameters in

the model were properly given such as the engine fuel consumption map, engine mechanical loss map, driveline transmission efficiency, tire rolling resistance, air resistance, and CVT gear ratio control map etc. Then, with this, by ensuring enough accuracy of the vehicle driving model, these results and parameters are used as input in the same engine model to study the effect of HSM on fuel consumption.

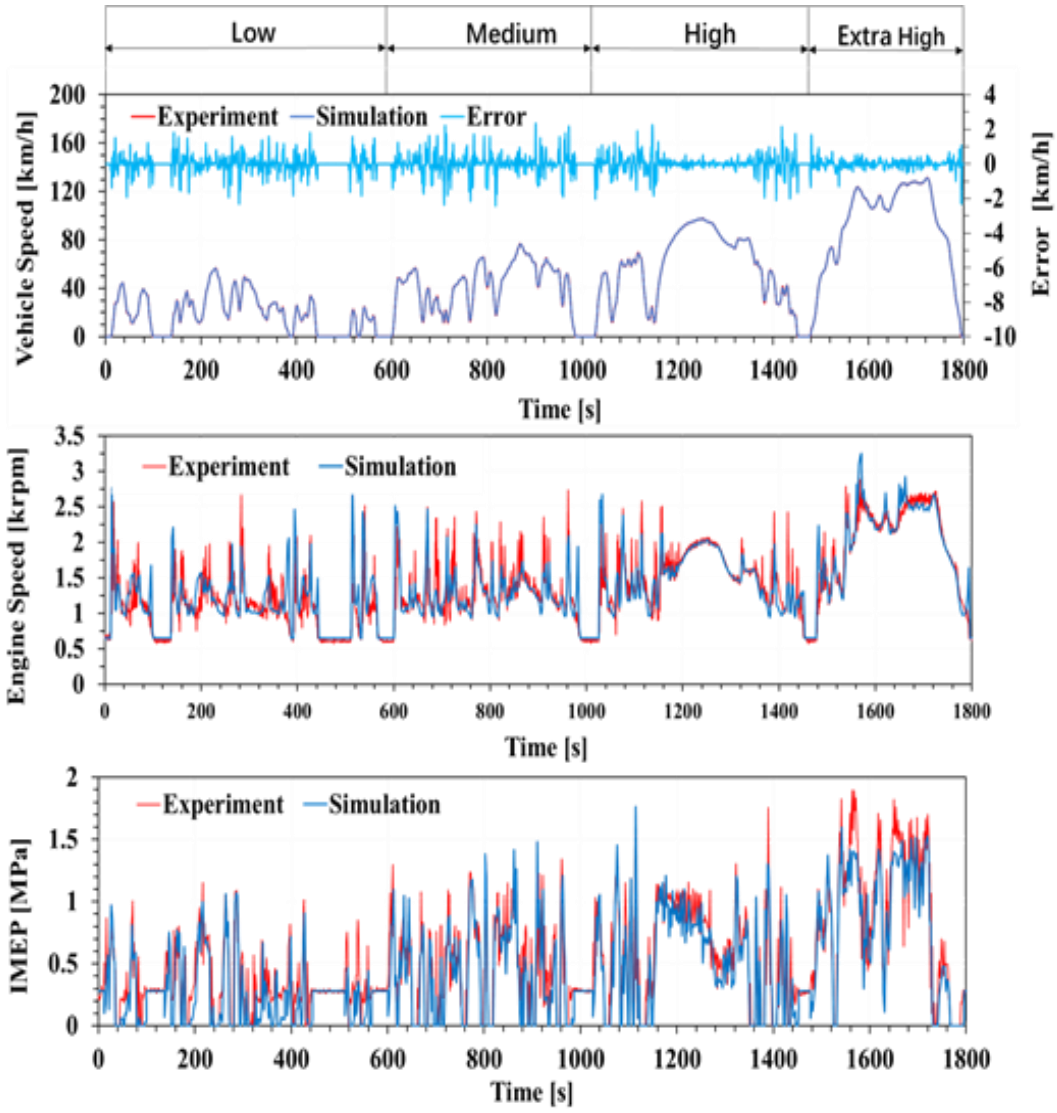

Figure 2-15. Difference between experiment and simulation of WLTC [270]

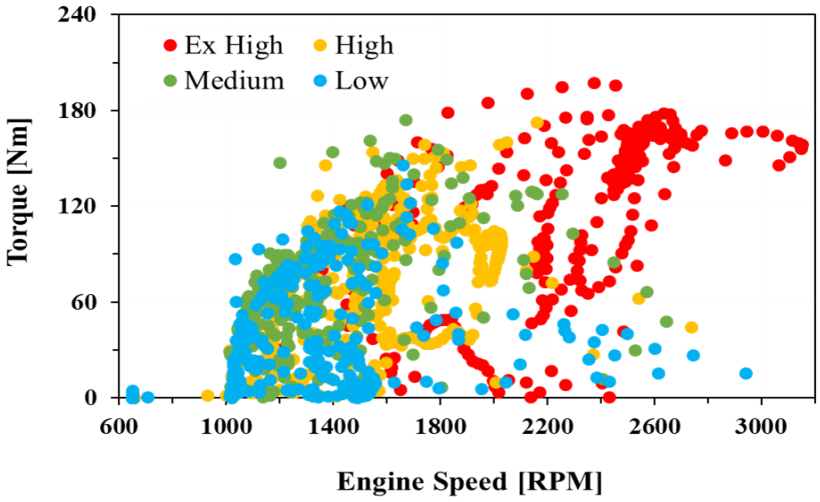

Figure 2-16. Engine running points in WLTC driving cycle [270]

For the WLTC driving cycle, the engine running points are shown in Figure 2-16. For this engine, the idle condition has the minimum engine speed with 650 rpm and the maximum engine speed is about 3200 rpm at the extra high region of the WLTC driving cycle. In addition, more engine operating points are located in the low to medium driving range. For engine speed, most engine operating points are between 1000 rpm and 2600 rpm. This means that studying fuel consumption is great significance, especially in these vehicle driving areas and engine operating points.

In this section, the objective is to study the effect of HSM on fuel consumption of the engine under the WLTC driving cycle. The reliability of the necessary maps used in calculation had been verified. Thus, in the full engine model, it is feasible to input the engine speed and torque, etc. as the target parameters to run the simulation using transient calculation model which represents the engine operating points in WLTC driving cycle. Thereby the obtained engine speed and torque till 1800 seconds are used as the input data for the transient operation of the engine and the calculation was carried out through the full engine model. Figure 2-17 shows the calculation results of the normal engine model compared to measure data. By comparing measured engine speed and simulation engine speed of the normal engine (or fuel flow rate), it illustrates the calculation accuracy of the model. Then, with the same engine model, HSM model is added before the turbine to calculate and study the influence of HSM on engine fuel consumption under the engine conditions of the WLTC driving cycle. Simulation results are given in Figure 2-17.

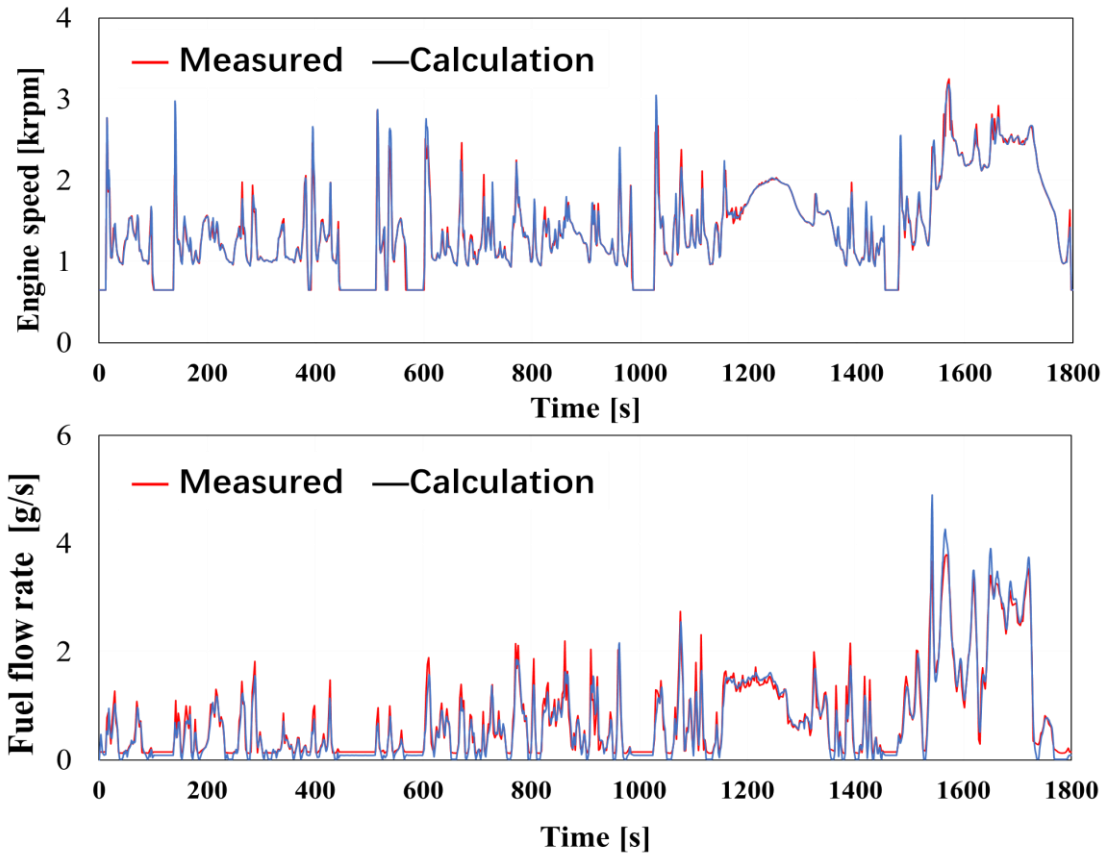

Figure 2-17. Comparisons between calculated and target values using full engine mode under WLTC driving cycle of engine conditions

2.5 Porous Material Application Setup

Table 2-18 shows the specifications of the turbocharged engine used in this study. It is a kind of 4-cylinder turbocharged gasoline. To study the effect of porous material on the turbocharged engine performance especial for turbine performance, the installed position of porous material Si-SiC on the engine is shown in Figure 2-18. The heat storage medium (HSM) was added before the turbine at the downstream of the engine exhaust manifold. Then HSM can affect the exhaust gas pressure and temperature by its porous structure and the ability to store and utilize

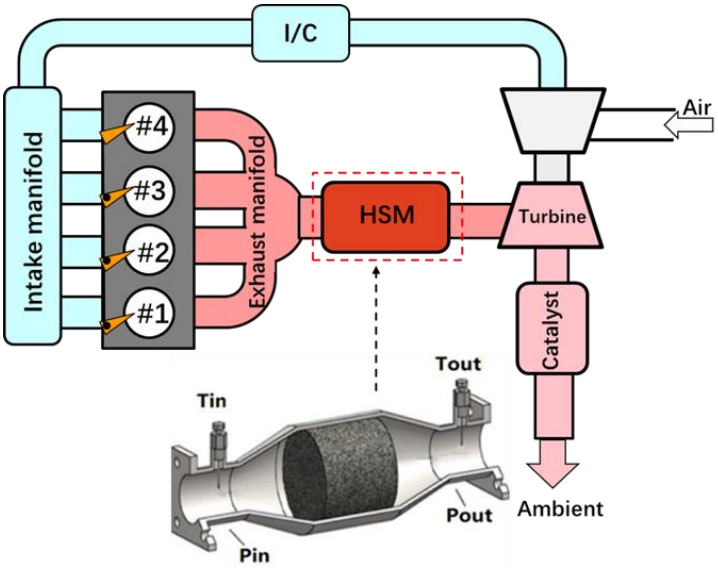

Figure 2-18. Engine setup with HSM

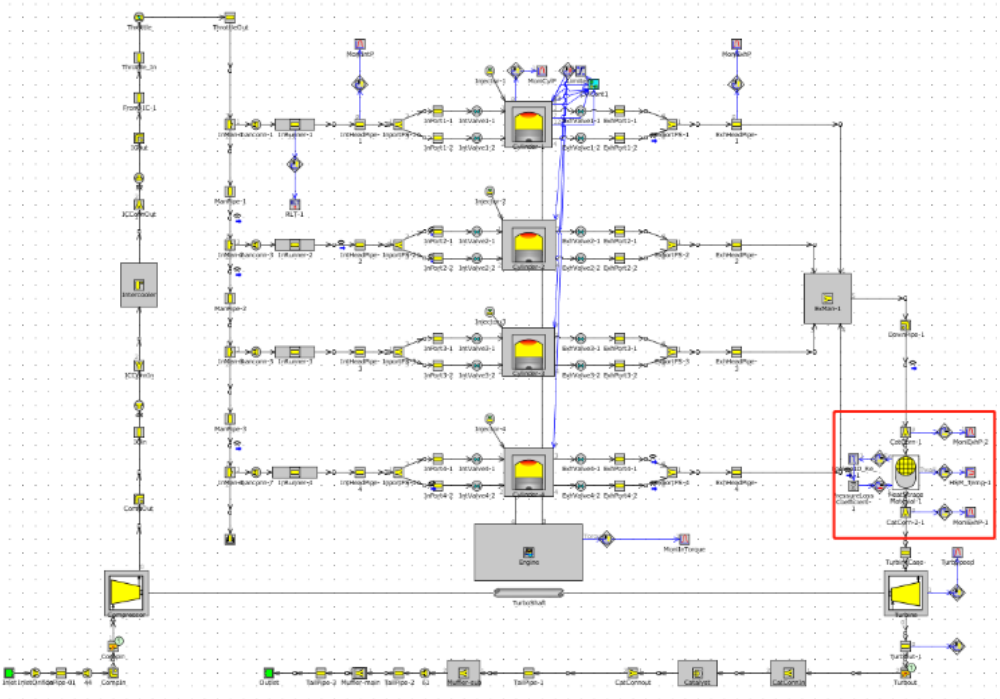

Figure 2-19 Model of turbocharged engine with porous material model

the exhaust gas energy. Figure 2-19 shows the setup of HSM in turbocharged gasoline engine, in which the porous material model is installed before the turbine with structure model, heat transfer model and pressure model. Then, the combined model can be used to study the effects of porous Si-SiC on engine and turbine performance.

2.6 Summary

In this chapter, the porous Si-SiC material is prepared to apply in turbocharged gasoline engines.

The specific properties of the used porous Si-SiC material were investigated by micro-structure analysis. The SEM and CT methods are introduced to calculate the skeletal surface area and skeletal volume. Then, it is able to obtain the actual structure parameters of the porous material.

To define and develop the model of the porous Si-SiC material, the physical parameters and thermal properties were studied, such as porosity, substrate surface area, substrate volume, thermal capacity, conductivity. In addition, the pressure drops through the used porous material due to the effects of porous material were tested for the pressure loss model application. The thermal model was to evaluate and simulate the gas temperature changes at different engine conditions, especially the transient conditions with exhaust temperature changing.

The engine model is convenient to use in the investigation of engine performance. Then, a model of the target engine model was calibrated at different conditions. The BSFC was typically tested with high accuracy. To study the fuel consumption under transient conditions, WLTC driving cycle model was developed and validated for the following study.

As a result, the engine model was combined with the developed porous material. Thus, it could be used in the studies below.

Chapter 3 Effects of Porous Material on Engine Response

3.1 Response Drawbacks and Improvement Techniques of Turbocharged Engines

The poor performance under transient engine conditions is the typical problem in turbocharged engines. There is a time delay to research the target under the changing load or speed conditions compared with NA engines. For engine system, the main reason is that it takes time to fill the air inlet manifolds and exhaust manifolds to increase the boot pressure [181]. For turbocharging system, the main obstacle is the necessary time of the turbine rotating increasing as well as the energy used by compressor operation. In fact, only a part of the target exhaust energy could be used and delivered to the compressor at the beginning. In addition, a part of the exhaust energy is required to overcome the inertia and friction of the turbocharging system. Thus, it is the time required to generate the target pressure. For vehicles, it occurs as a sense of no enough power under the vehicle acceleration conditions. The time required to change the engine power corresponding to the increased throttle angels by the acceleration pedal [182]. As a result, the turbo lag is resulting from inertia, friction, and engine load.

The worse response problem is also existence at the rapid change in the required engine power output, in which the input signal and output power are not synchronized. This response also leads to poor vehicle driving sense, and engine designs to reduce the turbo lag show in a number of ways [184]. The reduced bearing frictional losses of turbocharging system by using a foil bearing in place of conventional oil bearing is able to decrease the system response time [185-186]. It is efficient to improve the turbine response by using lighter and smaller parts of the turbocharging system due to the reduced rotational inertia of the turbocharger, namely small size or low weigh turbocharger. Variable-nozzle turbochargers could change the turbine inlet back pressure to corresponding to different engine conditions [187-190]. The variable geometry turbine (VGT) has been widely used to improve the engine transient response and peak torque at low engine speed [191]. The multiple turbochargers sequentially or in parallel was designed to reduce the turbo-lag and improver the engine transient conditions [192]. The improved waste-gate response has been widely applied in turbocharged engines which could be used to increase the load step transient response of a turbocharged spark ignition engine by the changed exhaust gas mass flow rate running into the turbine [193]. E-Tronic Turbocharger was also designed to analyze the reduced turbo lag [194]. The introduced anti-lag system was added to help reduce lag [194].

Figure 2-16 shows the gasoline engine response time during load step from 100 kPa BMEP to full load at 1500 rpm under different boost systems [181]. The systems include a mechanical supercharger,

an electrically driven supercharger (VTES), a turbocharger, a supercharger and a conventional naturally aspirated system [183]. The response time was plotted in the same Figure 3-1. Results shows that the mechanically supercharged engine, electrically driven supercharger were demonstrated to decrease the engine response time obviously.

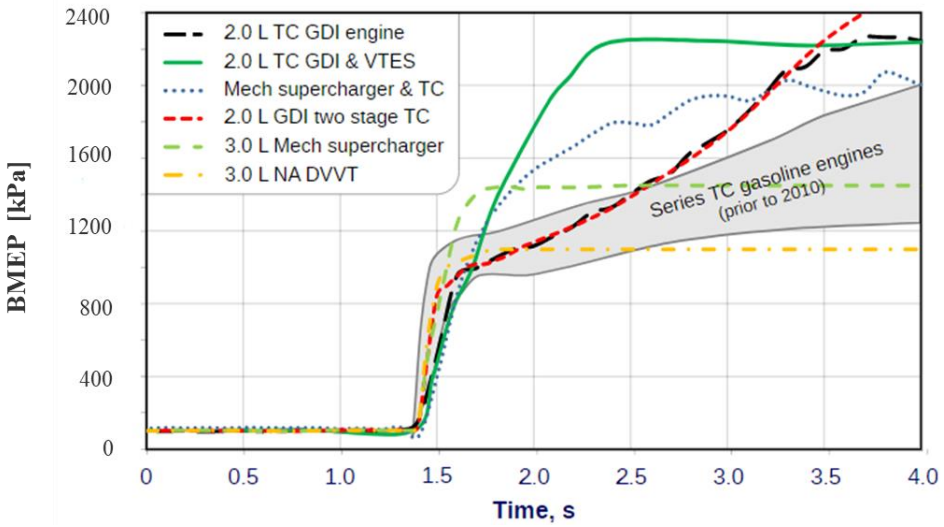

Figure 3-1. Gasoline engine transient response for several boosting options (Load step from 100 kPa BMEP to full load at 1500 rpm) [183]

A turbocharger system is a method that uses exhaust gas energy to operate turbine to achieve high boost pressure which means more air is used for fuel combustion thereby improving fuel efficiency [115,116]. However, turbocharged engines are characterized by transient operating problems, poor engine response during load or speed increase, lack of sufficient exhaust energy to operate the turbine efficiently [117-119]. More seriously, turbocharger transient operating problems can cause severe deterioration in emissions during acceleration and load changes [120]. Under low loads, the cylinder and manifold wall temperatures are lower than higher loads. Therefore, when the load is increased, the high temperature exhaust gas is used to heat the wall for a certain period of time which leads to lower exhaust gas temperature before the turbine. Due to this, the actual charging pressure cannot meet the demand for increased engine load or speed. Thus, it is necessary to study the method to reduce the time delay of turbine.

For a gasoline turbocharged engine, advanced technologies have been developed to improve the transient torque and driving sense by reducing the turbocharger lag. This consists of supercharger, turbocharger with electrically driven supercharger, electrically assisted turbocharger and variable geometry compressors and turbines [194-195].

For turbocharging system, pressure ratio of the compressor is a critical factor to obtain boost pressure and the calculation formula is shown as Equation (1). Many methods have been proposed to improve pressure ratio of the compressor such as high mechanical efficiency of the bearing system, high exhaust

gas temperature (high enthalpy of exhaust gas) before the turbine, low charge-in density after the compressor and large mass flow rate [116-118].

$$\pi_c = \frac{p_2}{p_1} = \left(1 + \frac{c_{t.p.in}}{c_{c.p.in}} \left\langle \frac{Q_t}{Q_c} \frac{T_{t.in}}{T_{c.in}} \eta_{total} \right\rangle \left[-\pi_t^{-\left(\frac{k-1}{k}\right)_e} \right] \right)^{\left(\frac{k}{k-1}\right)_a} \quad (1)$$

η_m -mechanical efficiency, η_c-the compressor efficiency,

η_t - the turbine efficiency, π_t-pressure ratio of turbine,

π_C- pressure ratio of compressor, P- pressure,

T-temperature, k- specific heat ratio, Q- mass flow rate,

c_p -ratio of the heat capacity at constant pressure, e-exhaust gas, a- air,

1- turbine inlet, 2-compressor inlet

To improve the engine response under transient conditions, the porous Si-SiC material was added before the turbine. By simulation method, the effects of porous Si-SiC material on exhaust gas was investigated. The turbine performance was thereby affected due to the changed exhaust gas temperature and pressure. To evaluate the effects on exhaust pressure and temperature at steady conditions and transient conditions, a better understand of the porous Si-SiC material work on turbine performance was obtain. The reduced exhaust pressure pulsation and temperature was demonstrated. A high response of the engine was achieved at the engine load recovery conditions.

3.2 Effects of Porous Material on Engine and Turbine Performance

In the previous chapter, the model of porous Si-SiC material and engine were validated. The two models were combined together to investigate the effect of Si-SiC on turbine and engine performance by simulation method. It is a 4-cylinder turbocharged, direct injection gasoline engine. The engine turbocharger specifications and GT-suite model are shown in Table 3-1 and Figure 3-2, respectively. This part tries to conduct a preliminarily study on the feasibility of using HSM in turbocharged engines to improve the performance of turbocharged engines.

With high temperature resistance about 1500 ℃, the used porous Si-SiC material could be added the upstream of turbine for application. The porous structure leads to small pressure drop of the exhaust gas which means little exhaust gas energy loss. Due to the cycle characteristics of the 4-cylinder turbocharged engines, the pressure and temperature vary with time or engine operation cycles. In fact, the exhaust pressure and temperature pulsations will occur both at steady conditions and transient conditions. The large surface area characteristics of the added porous Si-SiC material could exchange heat with the exhaust gas quickly, namely strong heat exchange capability inside the porous material. It

is known that the heat flow is from high temperature to low temperature. As a result, the outlet exhaust gas temperature (turbine inlet temperature) was adjusted through the applied porous Si-SiC material. In this process, the porous Si-SiC material worked as heat storage medium, and the heat capacity characteristics of the medium have been studied in previous chapter.

Table 3-1. Specifications of Turbocharger

Turbine type	No wastegate turbine
Mass Multiplier	0.68
Maximum Pressure Ratio	4.8
Maximum Speed (Reduced)	7100 RPM/K^0.5
Wheel Diameter	29.2 mm

At transient engine condition or quick engine load changing conditions, the porous Si-SiC material as heat storage medium could also affect the turbine inlet temperature. It is obvious that the higher turbine inlet temperature may achieve a quicker building of turbine speed and the boost pressure at the beginning of the engine load recovery. Kocsis's studies [196] increased the exhaust gas enthalpy (higher pressure and temperature) by a new designed exhaust line. Results showed that the boost pressure aided in quicker building up speed because a higher turbocharger rotor's angular acceleration was induced by the designed exhaust line. In addition, Newton PJ [197] demonstrated that the reduced flow pulsation could increase the turbine operation efficiency based on experimental and computational investigations.

3.2.1 Effects of Porous Material on Exhaust Pulsation at Steady Condition

The exhaust gas flow is a kind of thermal fluid with high frequency component due to the exhaust valves opening and closing. In addition, the frequency and amplitude are two main parameters related to exhaust gas pulsation. Moreover, engine combustion frequency is approximately equal to frequency of exhaust gas fluctuation while the amplitude changes with the engine load [198-199]. At the same time, the exhaust pressure pulse frequency has been confirmed to have small effect on the pressure fluctuation amplitude [200-201]. However, the main pressure trace seems to have a close relation to the mass flow rate feature including the high frequency component [201,202,203]. Then exhaust gas flow fluctuation (pulsation amplitude and frequency) was considered and engine exhaust gas flow pulsation characteristic parameters were computed by equation (3-1) in which engine exhaust flow pulsation frequency f is related to engine speed N (r/min) and cylinder number n. Moreover, there exists a frequency reduction

parameter β which is related to angular frequency ω, gas flow velocity v and characteristic length scale L. Dimensionless parameters St was also introduced to describe the fluctuation of exhaust gas flow [204] which was used to evaluate unsteady effects of the turbine stage. However, the current study only considers changes in the amplitude of the pulsation and ignores the change in frequency. Though it may have phase-shifting for adding HSM in front of turbine compared to the original. For a porous structure studied in this research, based on Darcy's Law [150], the fluid velocity varies throughout the pore space, due to the connectivity and geometric complexity of porous medium. In this process, pressure loss led to weakened amplitude of the pressure pulsation, and energy exchanges between fluid and heat storage medium resulted in reduced temperature pulsation. These all led to a reduced pulsation of the exhaust gas before coming into the turbine. The more stable flow could cause a more stable operation of the turbine. In turn, the intake and exhaust can be more stable. As a result, the porous material made an impact on the exhaust characteristic, leading to a reduced exhaust pulsation.

$$f = \frac{1}{2} \times \mathrm{N} \times \frac{1}{60} \times n \tag{3-1}$$

$$\beta = \frac{\omega L}{v} \tag{3-2}$$

$$\omega = 2\pi f \tag{3-3}$$

When it comes to turbine performance, mass flow rate, pressure ratio and gas temperature are the main parameters to induce turbine performance to happen. Turbine entrance mass flow rate pulsation curve keeping pace with exhaust gas pressure fluctuation can characterize exhaust pulsation. Moreover, as the main parameter in turbine map it controls the turbine action building and performance under transient and steady engine conditions. It is easy and applicable to estimate the pulsation based on the mass flow rate amplitude. For engine cycle, engine valve open-close characteristics resulting in mass flow pulsation, lower mass flow pulsation induced a higher turbine efficiency. Thus, in the same steady engine condition (2000rpm, 183N.m), the amplitude of exhaust gas mass flow pulsation before the turbine was compared between with and without HSM shown as Figure 3-2. It shows that the pulsation behavior was dramatically weakened owing to HSM system. Thus, it turns to encompass the turbine pressure ratio and efficiency which represent the turbine performance. Similarly, with HSM, the pulsation amplitude of turbine efficiency also obtained an improvement at the trough of turbine efficiency pulsation. Moreover, the turbine efficiency changes with engine speed and load. In those, an improvement about 5% of turbine efficiency with HSM was founded for lower engine speed (1200rpm, 125N.m).

The HSM does create more turbine power for better using of exhaust gas by turbine efficiency improvement. In steady engine condition, brake specific fuel consumption (BSFC) also decreases about

1% (2000rpm,183Nm) due to the smaller pulsation of turbine inlet gas with HSM.

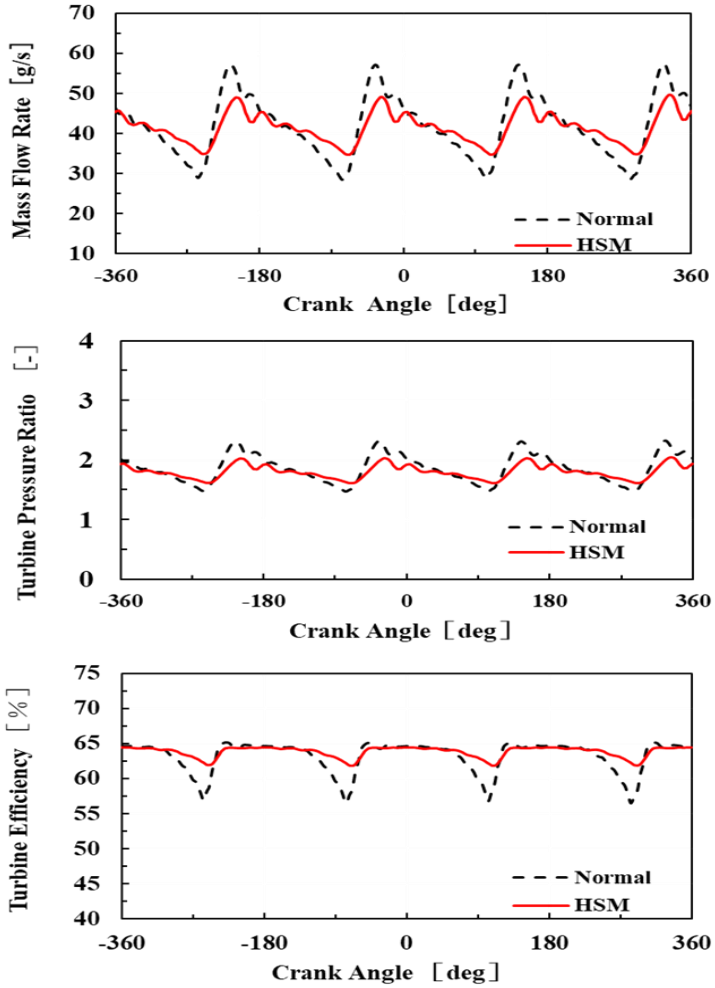

Figure.3-2 Comparation the effect of pulsation flow on turbine performance with HSM

3.2.2 Effects of Porous Material Engine Performance at Transient Condition

For turbocharged engines, turbine response speed is always the research topic since it leads to the instantaneous boost pressure as well as engine torque. Moreover, engine target torque building up process comprises of engine cold start and torque recovery. The time is decided by turbine response speed relating to turbine efficiency and the turbine entrance exhaust gas enthalpy. Then, if the exhaust gas enthalpy (temperature and pressure) rises, especially for the target torque building up process, it will obtain a steeper torque gradient for the torque building up curve with time. In this study, the Si-SiC is

utilized as heat storage media to store and reuse the exhaust gas energy.

The purpose of this section is to investigate the possibility of porous heat storage material Si-SiC for the improvement of turbocharged engine response performance under engine transient conditions. Understanding the criterion of turbine response performance is necessary. Higher turbine efficiency leads to better turbine response performance for effective use of exhaust energy. Smaller turbine blade inertia and lower exhaust gas flow pulsation etc. along with porous structure can weaken the exhaust gas flow pulsation as it was confirmed in the previous section. However, under transient conditions, it is still unknown whether the turbine efficiency can be improved by exhaust heat storage of HSM. Therefore, turbine efficiency calculation method is applied directly. For turbocharged system, the exhaust gas drives the turbine movement and the rotating shaft drives the compressor to compress the air to achieve intended intake pressure. However, in this process, the movement of gas and the transfer of energy involve heat loss and friction loss especially the accuracy of temperature measurement of turbine outlet is insufficient due to a large temperature difference compared with gas temperature for heat loss. Meanwhile, the gas temperature before and after the compressor does not change much under low temperature condition thus, the turbine efficiency is always calculated based on total efficiency and compressor efficiency which are related to inlet and outlet gas pressure P, temperature T and gas specific heat ratio κ . However, it is not easy to evaluate the turbine performance by calculation. A simpler method, the building up speed of the turbine speed and torque are used in this study.

As the size of Si-SiC is selected (D=130mm, L=100mm), the heat capacity of it is a definite value. However, the energy stored in porous Si-SiC is from high-temperature exhaust gas, which is not permanent but is continuously released. Engine torque recovery process can realize effectively in the order of energy absorption and release in the transient engine condition. In addition, the engine load rising processes after different periods of dwell time (time from load drops to a load rise, namely fuel cut-off duration) are investigated shown as Figure 3-4. The definite operation process is shown in Figure 3-3. There is no fuel cut-off single at the beginning of this operation process, as the HSM needs time to store exhaust energy at high load conditions before working. After inserting fuel cut-off single, the HSM start to release energy and heat the exhaust gas. In this study, with the same target value (3200rpm and 237N.m) of the engine, from the first row to the third row, the dwell time (fuel cut-off duration) from 2s, 3s, and 4s respectively and attention is paid to torque, boost pressure, exhaust pressure and temperature of HSM inlet/outlet. It should be noted that the heat storage media has achieved heat balance (heat storage process) with exhaust gas before a fuel cut off signal during dwell time. In order to study the effects of dwell time on HSM working, the same throttle angle action was used in the simulation. In the engine load recovery process such as 2s dwell time condition, the torque increasing curve is always higher before reaching the target torque by using HSM compared with normal engine which means that

engine load transition time is shortened by about 2s. Meanwhile, the engine boost pressure is also at a higher level. In that case, the HSM releasing energy to exhaust gas by heat exchange to maintain the turbine speed at relative higher speed which induces a short time to build target boost pressure by a higher turbocharger rotor's angular acceleration. As a result, the turbine response performance is improved in the transient engine condition with extra energy invested from previous cycles by HSM. With HSM, it is turbine inlet temperature to be increased to induce a quicker turbine response and intake pressure increasing at the beginning of load recovery. The simulation results of exhaust gas temperature, HSM inlet, HSM outlet and turbine inlet without HSM, are shown in Figure 3-5. The temperature of HSM outlet is much higher than the other two at load restarting point which is the reason of turbine response improvement by HSM releasing energy to exhaust gas. However, for a short time, the HSM inlet temperature became higher than HSM outlet temperature. Because HSM was always exchanging energy with exhaust gas before engine exhaust gas temperature returning to be higher than temperature of HSM substrate. During this load recovery process, the HSM outlet temperature was higher compared to normal engine (without HSM). Meanwhile HSM inlet temperature had a higher temperature than normal engine turbine inlet temperature invariably for heat loss of HSM. With small pressure drop of HSM, exhaust pressures between HSM inlet and outlet has little difference. With HSM, the exhaust pressure also has a similar rising curve with torque and boost pressure compared with no HSM. This is the reason of HSM working in load recovery process.

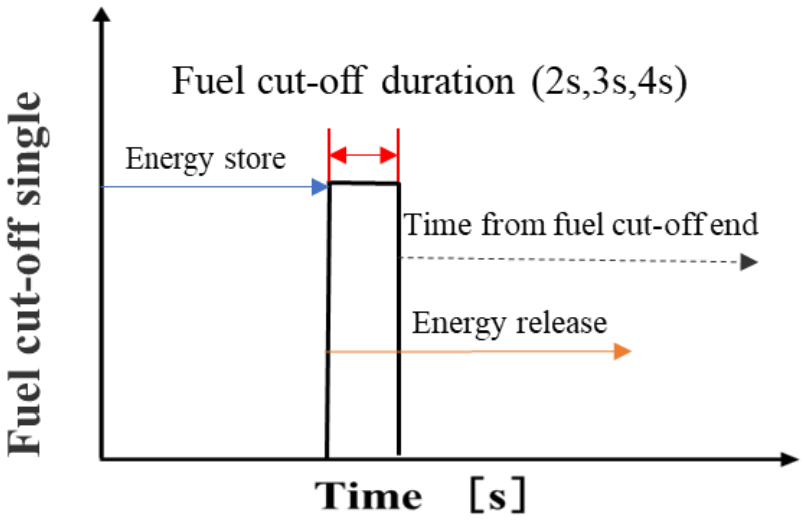

Figure.3-3 Transient test conditions c

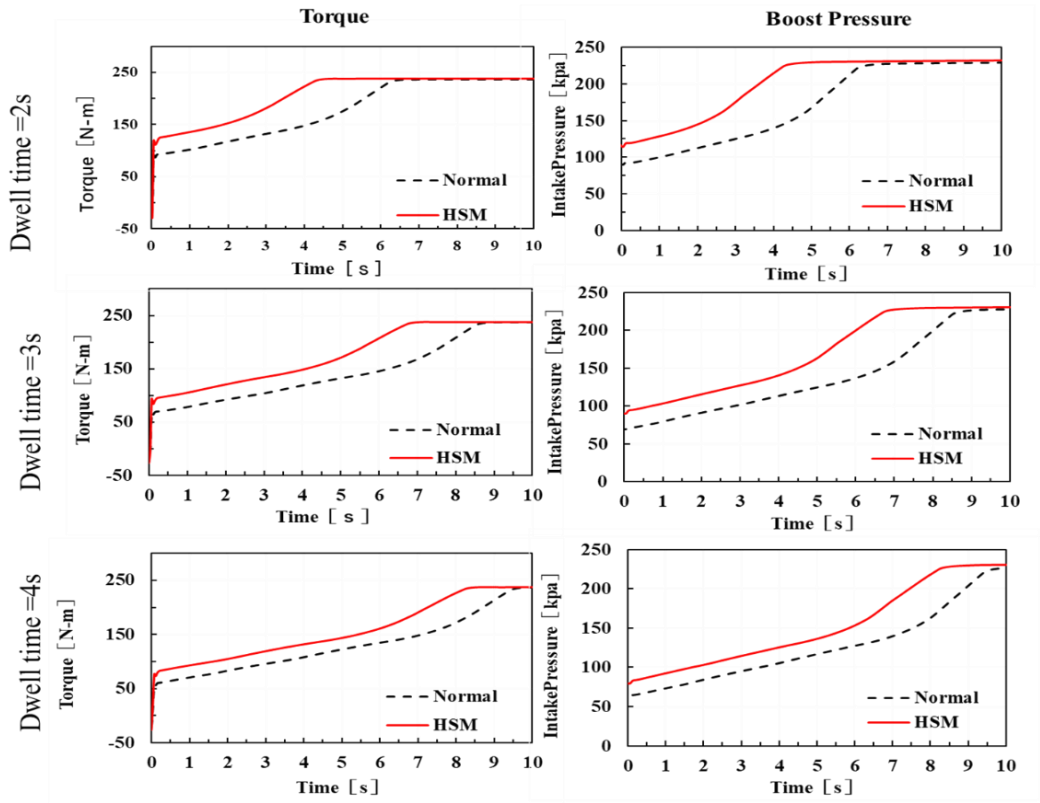

Figure.3-4 The recovery of engine torque and boost pressure with HSM compared to normal engine

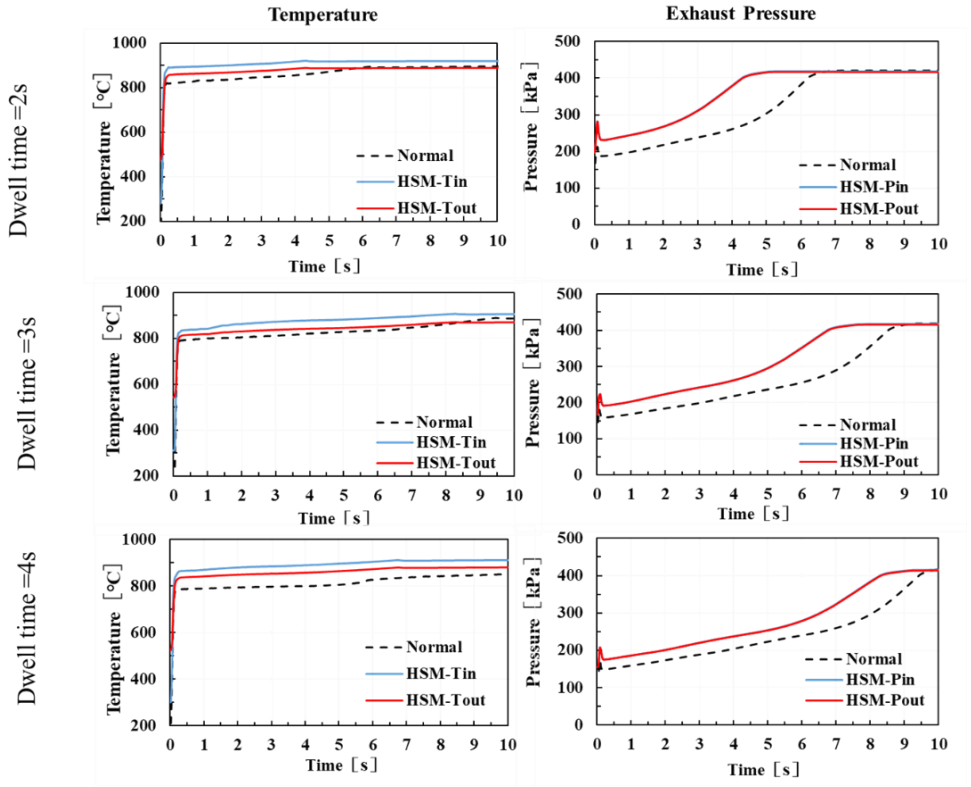

Figure.3-5 Engine transient temperature and pressure performance with HSM compared to normal engine

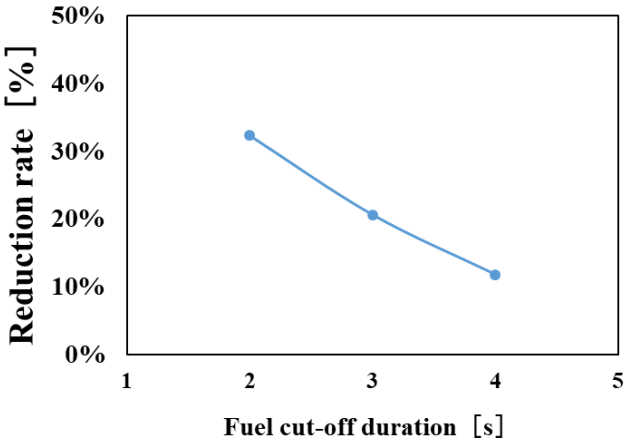

Figure.3-6 Engine response time reduction rate

For given size of Si-SiC, it acts effectively when its temperature is higher than exhaust gas flowing through it. The effectiveness duration is worth studying on the heat storage materials Si-SiC application by changing dwell time. It is obvious that the torque building up speed improvement was weakened by the dwell time changing from 2s to 4s, and it even begins to be ineffective at 4s-long dwell time as seen in Figure 3-5 for limited heat capacity of Si-SiC. It means that the effectiveness duration of porous Si-SiC as heat storage material changes with dwell time. Moreover, a long-time transient testing is necessary which will be implemented in a later study. To Analyze the engine response improvement with different dwell time with HSM compared to normal engine, the engine response time reduction rate is defined as reduction time/normal time. The engine response time reduction rate with different fuel cut-off signal is shown in Figure 3-6. Results shows it decreased with increasing of dwell time (fuel cut-off duration), in that, HSM stored energy was continuous reduction during fuel cut-off duration. However, as the HSM must store energy at first before working, it could lead to bad cold start conditions of the engine. The reason is that the temperature of HSM is lower than exhaust gas under cold start conditions, then the exhaust gas had to release energy to heat HSM which means more heat loss. The less exhaust energy led to the worse turbine operation in this condition, with more time to reach the target engine torque.

As a result, with porous heat storage material Si-SiC, it induces higher turbine efficiency by pulsation amplitude of turbine inlet gas flow. The exhaust gas thermal energy can be stored and reused by heat storage material Si-SiC at transient load recovery condition of gasoline turbocharged engine. This in-turn offers higher turbocharger rotor's angular acceleration to enhance the transient performance and a higher turbine response.

3.3 Summary

The verified HSM model was added to the turbocharged engine to investigate the effect on turbine performance with simulation method. Results show that two factors are essential for the improvement of engine performance in which the turbine efficiency becomes better by decreasing pulsation amplitude with porous Si-SiC. The turbine efficiency improved about 5% with HSM of lower engine speed (1200rpm, 125N.m) and BSFC decreases about 1% (2000rpm,183N-m) due to the smaller pulsation of turbine inlet gas with HSM.

Furthermore, engine takes less time (reduced by about 0.8s with a 1s dwell time of 3200rpm) to reach target torque and intake pressure. This means a higher turbine response at load recovery condition because the high load exhaust gas thermal energy is stored and reused by heat storage medium Si-SiC. These results proved that it is feasible and beneficial to use porous Si-SiC as storage material for exhaust gas energy recovery.

Chapter 4 Effects of Porous Material on Fuel Economy of Turbocharged Gasoline Engine

4.1 Fuel Consumption Reduction Methods of Turbocharged Engines

In recent years, due to the increasingly stringent regulations on fuel consumption and exhaust emissions, more and more advanced technologies have been continuously developed and applied in internal combustion engines, such as lean burn, new type of injectors, mixed fuels, dual-injection and engine downsizing technologies [206-211].Engine downsizing has become a kind of widely accepted technology for fuel consumption improvement, especially turbocharged engines. The engine output torque is based on the air supplied by intake system. With a turbocharged system, the intake pressure is boosted to increase intake air density, thus increasing the air mass flow rate. More air means more fuel utilization for the stoichiometric operation leading to increasing of engine power directly for a given engine displacement which contributes to reducing the engine displacement [212]. Moreover, it also expands the range of engine utilization with different turbine sizes. A 1.5-litre turbocharged engine may provide the same power of 2.0, 2.5 and 3.0 liters naturally aspirated (NA) engine. Small size engine causes less heat and mechanical loss which benefits the engine fuel consumption improvement. For the same power requirements, gasoline engine downsizing technology leads to about 20%-60% engine size reduction and 8%-10% brake specific fuel consumption (BSFC) decreasing in throttling losses [213].Grant Lumsden [214] designed a 1.2 L turbocharged engine to replace a 2.4 L NA engine which got higher torque, simultaneously 25%- 30% on-road fuel consumption benefits. Turbocharged engines use exhaust gas energy to run the turbine and increase the boost pressure. However, at low speed, an engine experiences turbo lag and is unable to get large torque due to low exhaust energy. Researchers of IHI (technical paper, no name in it) [215] developed new design concepts to increase the turbine rotation at low engine speed by decreasing turbine size and altering the turbine impeller shape thus obtaining enough boost pressure for required torque. As a technology with great potential to improve fuel consumption, different types of turbocharging systems have emerged. Variable geometry turbocharger (VGT) is another technology to improve the low engine speed performance. Ebisu M [216] used VGT to increase the engine thermal efficiency of gasoline engines. The simulation result shows 2%-3% fuel consumption decreases under JC08 driving condition. Moreover, it also demonstrates the advantages of reducing emissions with a turbocharging system. An experimental study reveals 5-10% more brake power is achieved for an engine with turbocharger following with less CO and HC emissions compared to the engine without turbocharger [217].With a turbocharger, NOx and CO_2 emissions also decreased in a single-cylinder diesel engine based on experimental test [218]. Researchers from MHI

[219] also developed a new type of VGT turbocharger using high-temperature resistance technology to improve fuel consumption by increasing the temperature of exhaust gas for low pollution cars. Turbocharging combined with other advanced technologies shows great potential for improving fuel consumption and emissions. The valve timing can also affect the particulate emissions of direct-injection turbocharged engine [220]. A 3-cylinder turbocharged gasoline direct injection engine employs variable valve action (VVA). It had obtained 18% CO_2 emission reduction as compared to the conventional engine in the study of Kirwan [221]. Downsized turbocharged gasoline engines run at higher mean effective pressure (MEP) compared to NA engines for the same torque output which may lead to knocking at high engine load. It is dangerous for gasoline engines, especially heavy knock which causes damage to the engine. To avoid knocking, cooled exhaust gas recirculation (EGR) is introduced to retard the combustion and increase the knock limit and spark advance hence resulting in low fuel consumption [222]. In addition, EGR can reduce NOx emissions and improve the engine thermal efficiency effectively. [223, 224].

Other exhaust energy recovery methods are also launched during the past several years. The heat storage medium is one of these applications. Phase change medium such as water which absorbs heat energy by vaporization process generates steam to assist in turbine working. This steam improved turbocharging thermal efficiency by about 2% basing on simulation results [225]. Without phase change, heat storage medium has characteristics of high thermal conductivity and large heat transfer area. Porous materials such as SiC ceramic honeycomb (SCH), porous mullite-bonded silicon carbide and porous silicon nitride-bonded silicon carbide has been used as a heat storage medium for its porous structure and large heat thermal conductivity [226]. It is the high porosity of porous material which induces large surface area for heat exchanging that enhances the heat transfer between fast-flowing fluid and heat storage medium. Research showed that the thermal conductivity of porous SiC alters from 2 to 82 W/(m-K) when the porosity of SiC is varied from 30% to 74% [227]. SiC sintered and other material (additives) such as Y2O3–La2O3 can improve the thermal conductivity up to 206 W/(m·K) [228]. Pressure drop through SiC porous material decreases with pore size and increasing porosity [229]. For these characteristics, porous material has been used as a heat exchange medium to enhance heat transfer by improving the effective thermal conductivity [229]. Moreover, the strength and heat resistance are important for application. Research shows 1-205 MPa strength of porous SiC when the porosity ranges from 9% to 91% with a fracture toughness of 0.3–4.3 MPa m1/2 [230]. It also maintains heat-resistant stability up to 1600-1700℃.

To study the engine fuel economy, the worldwide harmonized Light Cycle (WLTC) is an effective cycle test method compared to steady engine testing [231]. Simulation and experiment methods have been used to investigate the engine fuel consumption and emission by this transient cycle test

[232,233,234]. Chiong [235] studied the effect of twin-scroll and single-scroll turbocharger on turbine performance and fuel consumption. Results showed that twin-scroll turbocharged engine obtained about 2.7% reduction of fuel consumption due to the reduction in the exhaust gas pulsation compared to the single-scroll turbocharged engine. In this test, the target engine speed and target brake torque are pre-set for WLTC drive-cycle testing. WLTC is developed by the United Nations level based on the United Nations Economic Commission for Europe (UNECE) and now has been extended to other countries. It is a more realistic method to test the vehicle's fuel consumption and the impact on CO_2 emissions compared to other test cycles [235].

Previous studies have shown that porous material such as SiC has the potential to be used as a kind of heat storage medium to store energy [226-231]. However, porous Si-SiC material used as a kind of heat storage medium to recover exhaust gas energy which may improve the turbine performance has not been investigated. In previous studies of this research project, the characteristics of porous Si-SiC material have been investigated such as porosity, substrate surface area, and heat capacity [236]. It has been demonstrated that it is possible to use the porous material Si-SiC as a kind of heat storage medium to store and reuse the energy of exhaust gas of the gasoline engine and improve the engine performance at steady and transient engine conditions. This improvement of engine performance with HSM may also improve the fuel economy of the turbocharged gasoline engine. In this paper, further study was carried out to investigate the effects of HSM on the fuel consumption of a 4-cylinder turbocharged gasoline engine. Targeted torque as steady engine condition and WLTC driving cycle as transient engine condition were applied to investigate influence of HSM on fuel consumption of the engine. WLTC is an effective transient cycle test method to study the effects of turbine performance on the fuel economy of the engine and a model of WLTC driving cycle calculation was developed and calibrated by experimental data. Then by simulation method with HSM, the predicted fuel economy improvement of the engine was investigated compared to the original engine.

4.2 Effects of Porous Material on Fuel Consumption at Steady Conditions

This porous material can be used as a heat storage medium to store exhaust energy from high loads and reuse the stored energy under transient engine load recovery conditions. However, it is also meaningful to study the effect of HSM on engine performance under steady conditions. In this section, the fuel consumption at various engine torques (engine speed from 1600 rpm to 4400 rpm) was calculated with HSM and compared to the data of normal engine. The fuel consumption of the gasoline engine decreased with HSM shown in Figure 4-1. These data have some characteristics as follows. With

engine speeds ranging from 1600 rpm to 3600 rpm, the maximum BSFC (Brake Specific Fuel Consumption) improvement always occurs at the maximum engine torque. In addition, the maximum BSFC reduction also decreases as the engine speed increases. In these results, the reduction in BSFC could be as small as 0.2% at 2000 rpm (39 Nm), and the BSFC could be also reduced by 1.13% using HSM at 2000 rpm (229 Nm). To investigate the reasons, engine operating parameters were taken into consideration such as throttle opening angle, intake pressure, pump loss, turbine performance, exhaust pressure, temperature and energy balance.

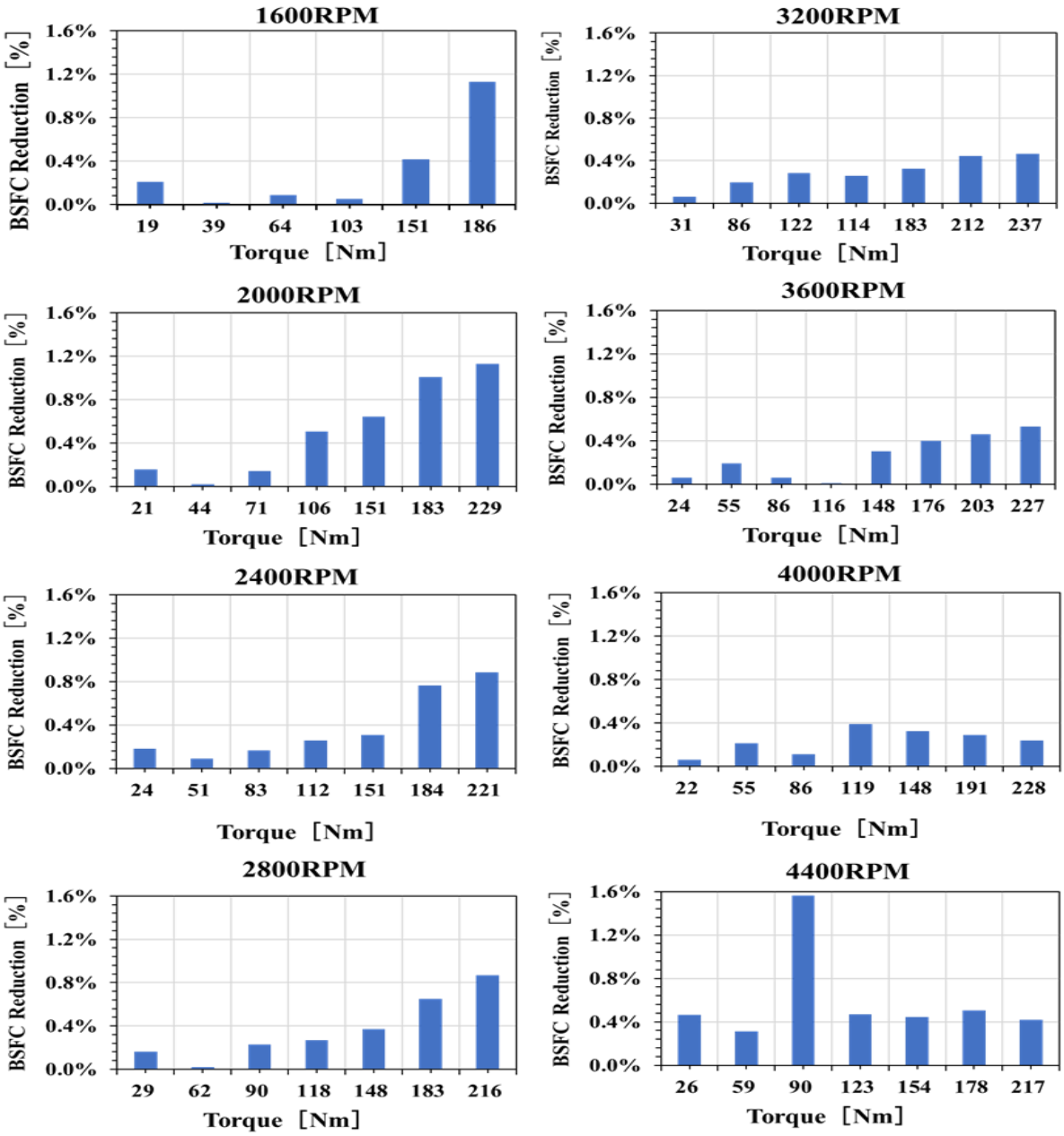

Figure 4-1. BSFC reduction with HSM compared to the normal engine

SI (spark ignition) engines always use a throttle to control engine load. For NA (natural aspirated) engines, pumping losses include intake throttle losses and intake/exhaust valve losses. These pumping losses vary with engine speed and load, where the throttle opening has a great effect on pump losses, especially for some engine loads [235]. Turbocharged gasoline engines control throttle opening angle before intake manifold and wastegate valve at turbine inlet to obtain target engine torque. The throttle opening angle changes the intake mass flowing into the cylinder namely the gas exchange condition with the cylinder. This gas exchange efficiency increases at higher engine load with the same engine speed with larger throttle angle. At the same engine speed, the pumping loss caused by the throttle decreases with the increasing of engine torque. It needs larger throttle angles (opening the throttle more widely) to get higher BMEP (brake mean effective pressure) compared to low load, also meaning less pumping loss resulted from wide opening throttle [235,237]. It means that wider throttle opening angles benefit to reduce pumping loss. However, the loss of intake and exhaust valves is particularly important for pumping losses at high speeds, especially for WOT (wide opening throttle). In turbocharged engines, the intake pressure is boosted by the turbine which utilizes exhaust gas energy. Moreover, because of restriction of exhaust gas flowing, the turbine was regarded as an exhaust valve by Müller [238]. For a target torque, wide opening throttle angle and lower exhaust pressure leads to lower pumping loss which results in lower BSFC.

To explain the effects of HSM on engine fuel consumption in detail, Figure 4-2 shows more data related to engine performance at engine speed of 2000 rpm and 3200 rpm under steady conditions. As a result, with the usage of HSM, BSFC of the engine could decrease under both high and low engine loads, however, the average reduction of BSFC under 2000 rpm engine speed turns to be higher than that under 3200 rpm engine speed. This is due to the high exhaust mass flow rate at high engine speed in which the effect of the fixed size HSM on the engine is relatively small. By adding HSM before the turbine, the turbine inlet pressure and temperature were reduced slightly compared to without HSM engine. However, the average turbine efficiency was increased by reducing pulsations during turbine operation, resulting in the same target torque at relatively low turbine inlet temperatures and pressures. In addition, the pressure loss by HSM must be taken into account although this pressure loss is small for the porous structure of HSM. This additional drop of pressure and temperature is unavoidable with the addition of HSM using pipe to store porous materials. Porous heat storage material was added to the engine by placing a pipe in the engine. Adding them caused more heat loss to the exhaust gas. The exhaust gas transferred heat with the porous material and reach thermal balance. Moreover, this thermal balance also occurred between the porous material and the pipe, and between the pipe and the surrounding environment. These led to HSM outlet (turbine inlet) temperature decrease eventually. However, using HSM to improve turbine efficiency and reduce pump losses will compensate for this heat loss, which can ultimately reduce fuel consumption. For example, the throttle opening increases about 10 deg for

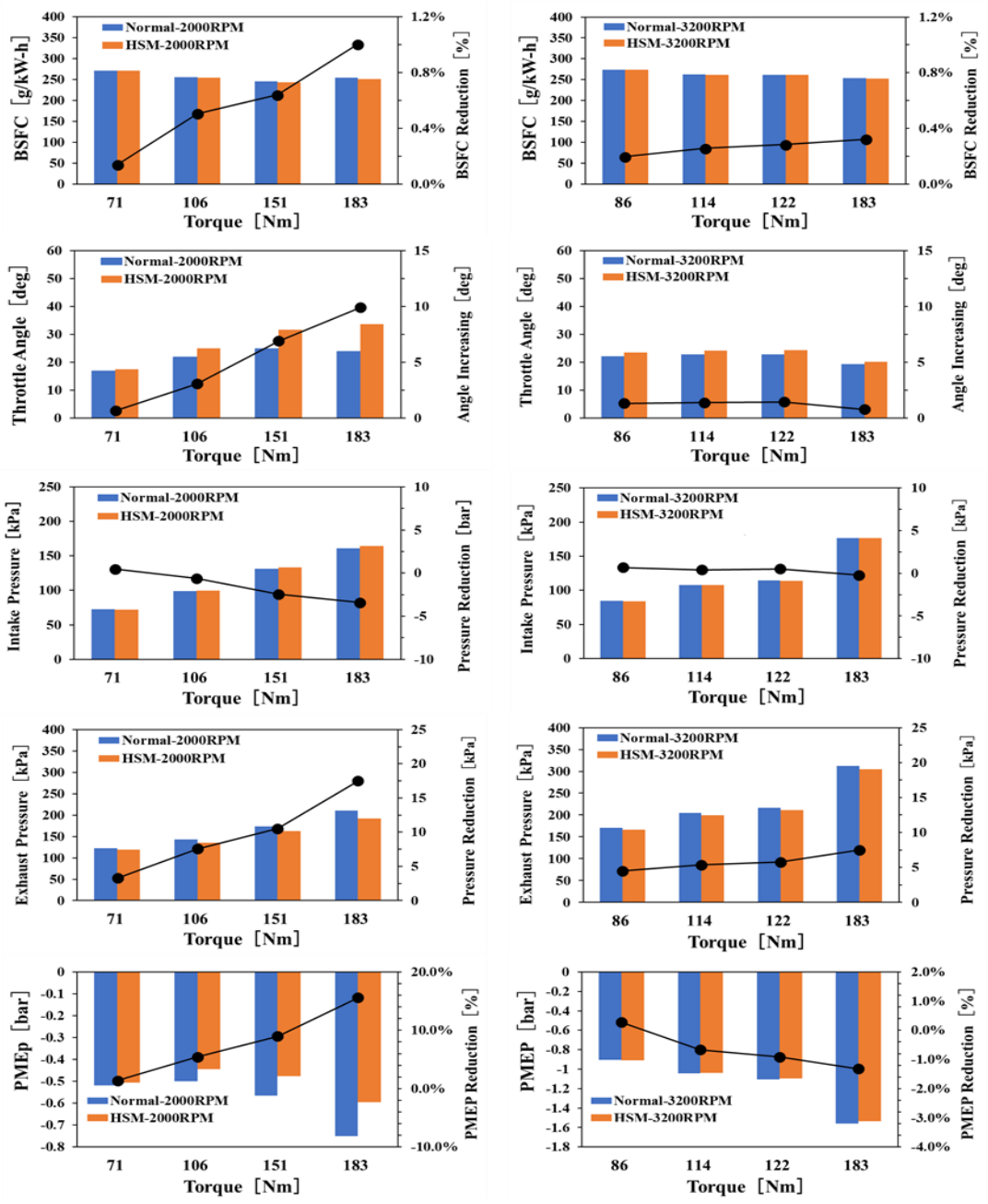

Figure 4-2. The throttle angle, intake pressure, exhaust pressure, PMEP analysis of BSFC improvement with HSM

183 Nm at 2000 rpm with HSM compared to compared to the normal engine. It means that a 16% reduction of pumping loss was observed and one of the reasons is wider opening throttle. With the pumping loss decreasing by using HSM, a lower intake pressure may achieve the same target output torque. In addition, HSM also caused turbine performance improvement. In other words, better turbine performance may induce larger intake pressure even with low turbine inlet temperature and pressure which can be seen in Figure 4-2 and Figure 4-3. At engine speed of 3200 rpm, the simulation results show some difference compared to 2000 rpm. The wider opening throttle angles with HSM of 3200 rpm

are smaller which leads to little change of intake pressure and the turbine inlet exhaust pressure reduction is also smaller. However, the engine still obtained BSFC improvement which resulted from a larger turbine efficiency and less pumping loss.

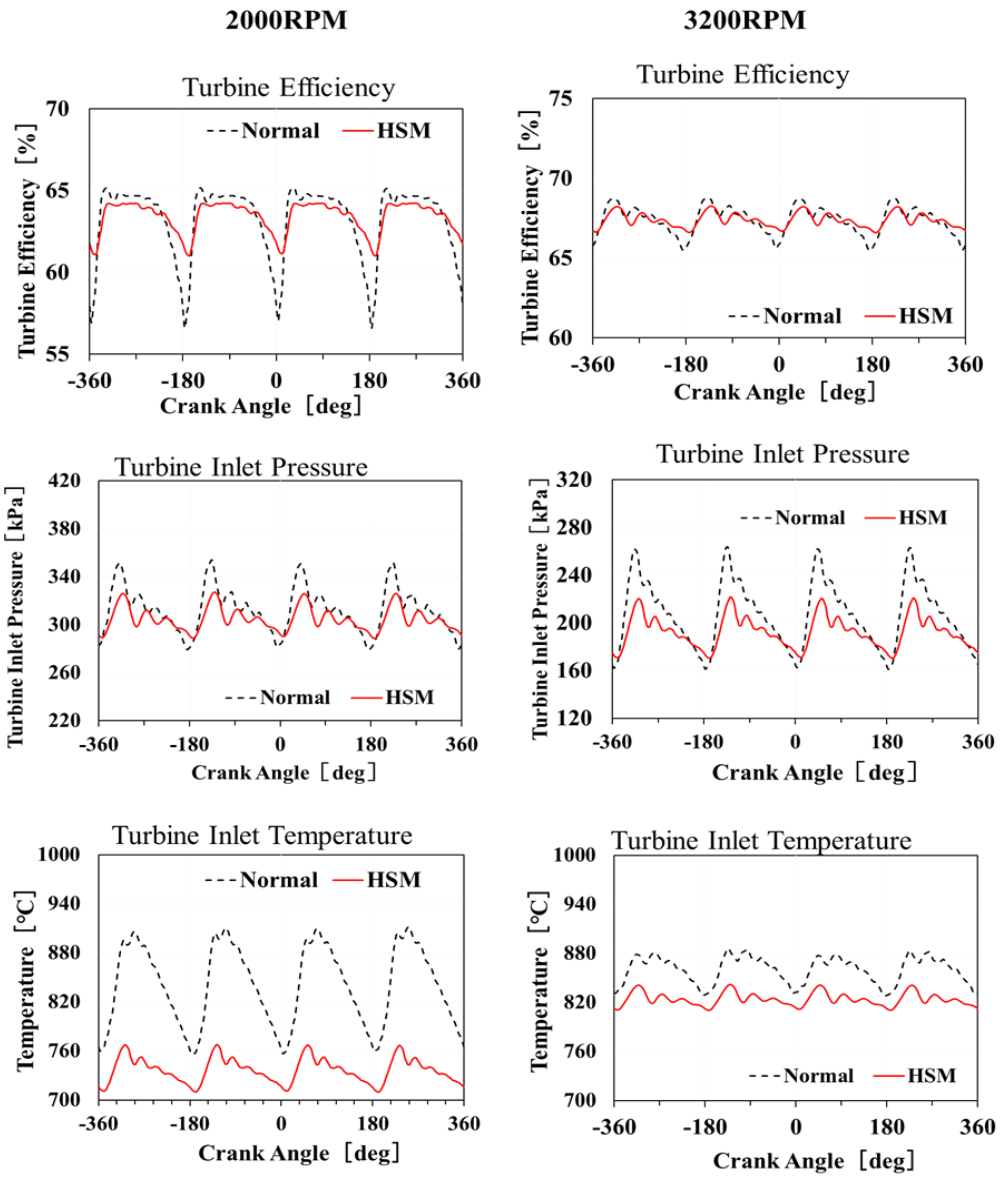

Figure 4-3. Turbine performance with HSM compared with normal engine

Figure 4-3 shows the efficiencies, inlet pressure and temperature of the turbine at the output torque of 183 Nm under engine speed of both 2000 rpm and 3200 rpm. It can be observed that with HSM the pressure and temperature fluctuations at the turbine inlet were lower. Nevertheless, the output work of the turbine maintains the compressor to yield the identical target intake pressure due to the rising of the turbine efficiency. There are inevitable temperature and pressure fluctuations at the turbine inlet due to the intrinsic cyclical supplying of exhaust gas from each cylinder of the 4-stroke engine. The turbine efficiency at 2000 rpm indicates a sharp decline leading to less output. However, the turbine works at

higher efficiency with HSM which benefits the intake pressure increasing. This eventually leads to BSFC decreasing.

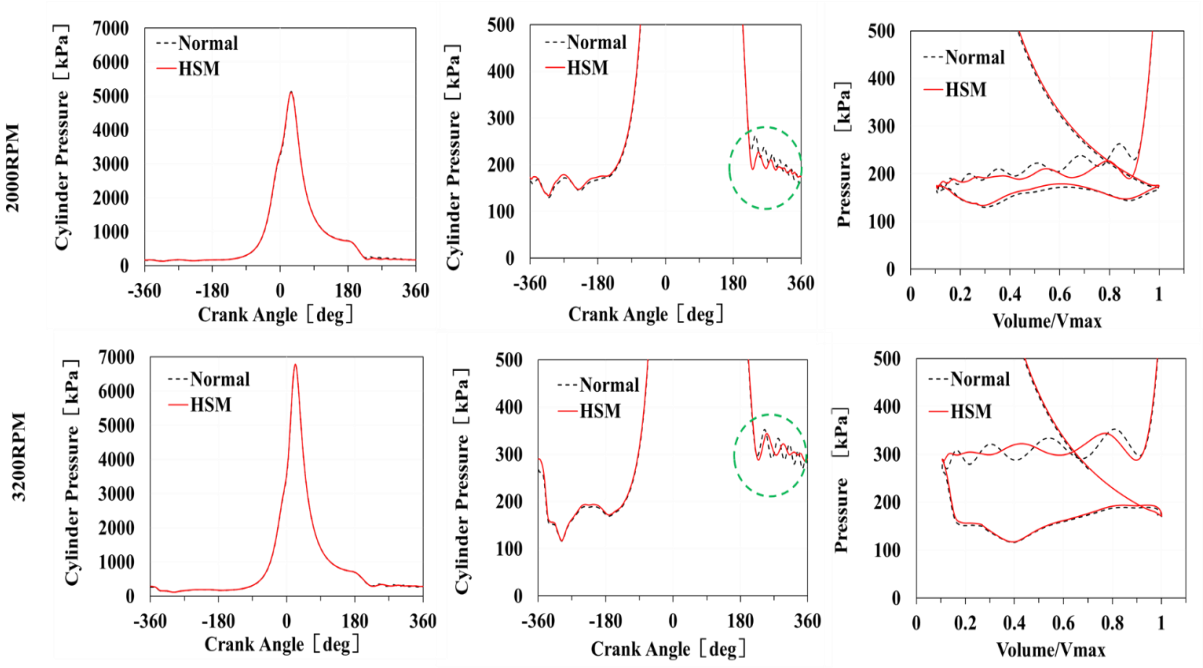

Figure 4-4. Cylinder pressure and log P-log V comparation for normal and HSM added engine

Table 4-1. HSM added engine performance parameters compared to normal engine

Parameter	Engine Speed	Normal	HSM
Throttle angle [deg]	2000 rpm	23.67	29.30
	3200 rpm	19.40	20.20
Intake pressure [kPa]	2000 rpm	160	164
	3200 rpm	176	177
PMEP [kPa]	2000 rpm	-76	-59
	3200 rpm	-161	-154
Turbine average efficiency [%]	2000 rpm	63.92	65.33
	3200 rpm	67.41	67.52
Indicated efficiency [%]	2000 rpm	34.80	35.19
	3200 rpm	35.79	35.85

In order to explain the effect of HSM on engine performance more clearly at steady engine condition, pressure and LogP-LogV diagram of the same engine torque at 2000 rpm and 3200 rpm are shown in the Figure 4-4. In the exhaust stroke, the cylinder pressure pulsation with HSM is lower. Finally, the parameters are summarized in Table 4-1. Throttle opening angle, turbine average efficiency, PMEP and

indicated efficiency were improved due to HSM addition as compared to normal engine. These variations were also beneficial for decreasing pumping losses, thereby reducing fuel consumption.

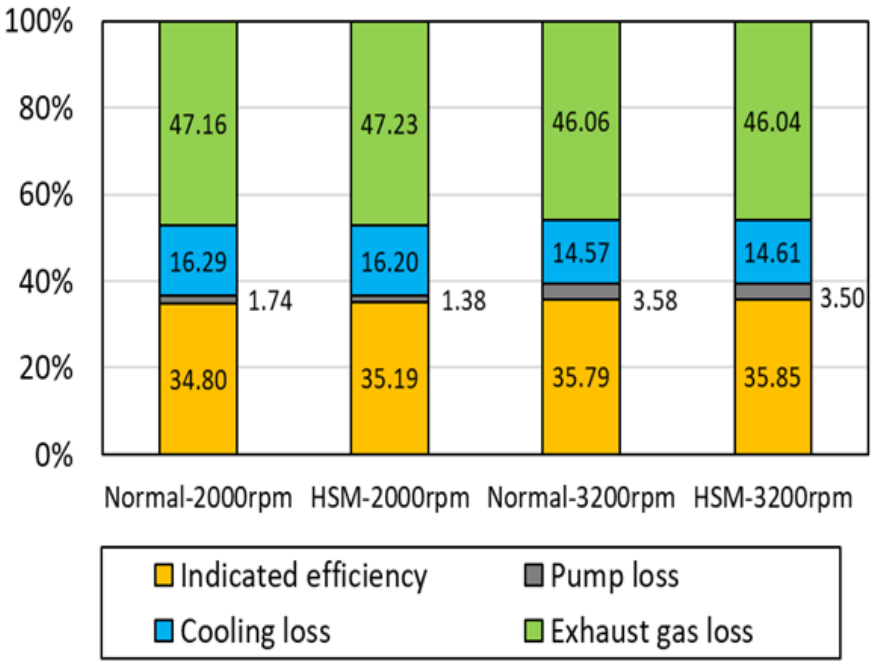

Figure 4-5. Engine heat balance with HSM compared to normal engine

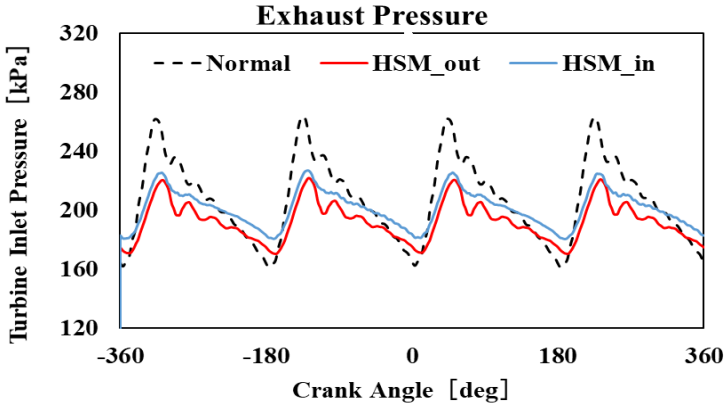

Figure 4-6. Exhaust pressure with porous material compared to normal engine

Furthermore, an analysis of the influence of HSM on engine performance under the same engine torque of 183 Nm at 2000 rpm and 3200 rpm with heat balance analysis is shown in Figure 4-5. At 2000 rpm, it is obvious that the decrease of pumping loss is the main reason for BSFC reduction. However, at 3200 rpm, a little reduction of BSFC was found and the pumping loss decrease was also small. In that, the used fixed-size porous material had a smaller effect on engine performance at 3200 rpm compared to 2000rpm due to less pumping loss decrease and less turbine efficiency improvement. Another evidence of pumping loss reduction compared to normal engine is the changed exhaust pressure. Exhaust

pressure with porous material is shown in Figure 4-6, in which the inlet pressure and outlet pressure of exhaust pressure pulsations are both less than the pressure pulsation of the normal engine. This leads to the pumping loss reduction compared to that of normal engine.

4.3 Engine Performance at Transient Conditions with HSM Under WLTC Driving Cycle

A direct method to study the effects of HSM on engine fuel consumption is to see the engine fuel flow rate under the WLTC driving cycle. Thus, the engine fuel flow rate is given in Figure 4-10. It can be seen that the fuel consumption rate curve of the normal engine is higher than that of the engine with HSM. It shows higher turbine inlet temperature with HSM after vehicle speed dropping down in the Figure 4-10 compared to the normal engine. This is beneficial to engine load recovery and can receive high turbine response resulting from higher turbine inlet temperature with HSM compared to the normal engine. Moreover, it is a continuous response process which causes the follow-up boost pressure to reach the target value faster.

The energy storage of HSM is beneficial to the turbine response under transient engine condition, thereby reducing engine response time for engine load recovery. The fuel consumption reduction with HSM is related to turbine efficiency increment and pumping loss reduction. Results of Figure 4-11 show that turbine efficiency changes with time, in which obtained higher turbine efficiency with HSM is indicated compared to the normal engine. The improvement of turbine efficiency is due to the small temperature and pressure fluctuation which is similar to the analysis of steady-state engine conditions. In addition, the extra heat energy releasing from HSM also leads to higher turbine efficiency at transient engine conditions from high load to low load engine.

For easier explanation, red, green, and black periods are marked. The red marked periods are in the process of engine load decreasing from high to low and considering the idle load, it is obvious that the HSM engine got higher turbine efficiency at these time regions. This is because the temperature of HSM was higher than exhaust gas which released energy to heat exhaust gas leading to higher turbine efficiency. Moreover, green marked periods, they were in continuous process of falling engine load and rising again and the HSM added engine also was along with higher turbine efficiency. In these periods, the temperature of HSM is higher compared to exhaust gas temperature, especially for the trough periods of the pulsation and HSM was a heat source that could assist to heat exhaust gas. This extra energy refers to the recovery and reuse of exhaust gas energy. This is thereby to reduce the fuel consumption which can be seen in the fuel flow rate of Figure 4-6. However, for marked black periods, the turbine efficiency

of the HSM engine was of little difference in consumption at transient engine conditions with HSM compared to steady engine conditions. It demonstrated that the exhaust gas energy was stored and reused by HSM under transient engine condition.

In these transient conditions, the turbine inlet temperature changes with time as shown in Figure 4-7. When HSM is added, the temperature appears to be lower than that of normal engine during most time of WLTC during cycle. However, results also indicate that the turbine inlet temperature of the engine with HSM is higher than that of the normal engine at the initial stage of engine recovery process, though it is surpassed quickly. The reason is that the energy stored in HSM at high exhaust temperature condition was reused to provide energy for exhaust gas which led to the less exhaust temperature decreasing compared to normal engine. However, the PMEP and exhaust temperature of normal engine turned to be higher compared to the HSM engine. These two marked periods are the high and extra high vehicle speed regions of the WLTC driving cycle with large engine speed and load, especially for the extra vehicle speed region. In this period, the HSM-added engine obtained larger throttle angle which lead to smaller PMEP, thereby the reduction of fuel consumption which is validated by the fuel consumption rate and PMEP data in the Figure 4-7.

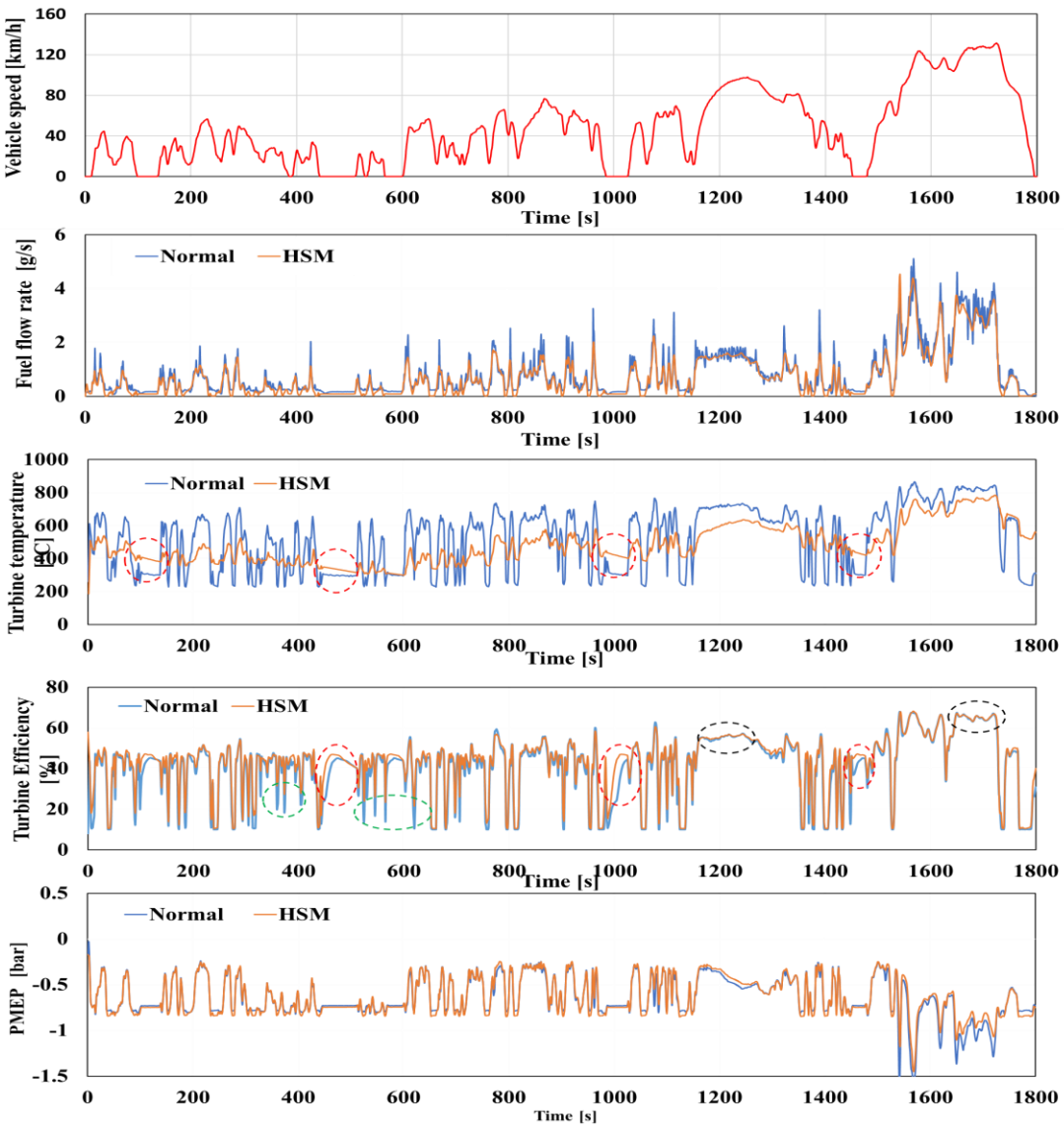

Figure 4-7. Engine performance of vehicle driving cycle with HSM compared to normal engine

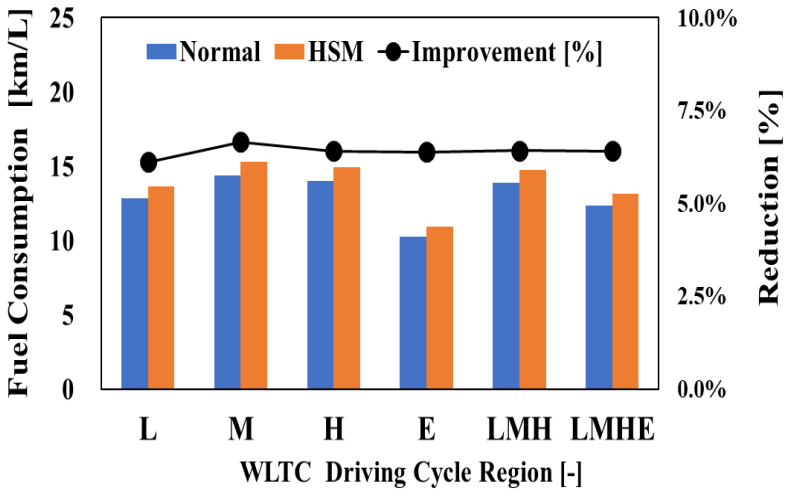

Figure 4-8. Engine performance of vehicle driving cycle with HSM compared to normal engine

To observe the fuel consumption changes using HSM more clearly, the fuel consumption (km/L) in different WLTC driving cycle regions is given in the Figure 4-8. To see the column diagram of the fuel consumption, it shows that with HSM, the fuel consumption for different WLTC driving cycle regions was reduced from about 5.9%–6.6%. The fuel consumption was reduced by 6.6% at the medium vehicle speed region of WLTC driving cycle. The main differences in these regions are engine speed and load as shown in the Figure 2-16. It means that the exhaust mass flow rate changes at different WLTC driving cycle regions. In this research, the HSM was used to affect the exhaust gas temperature and pressure of exhaust gas. In addition, in this step of the research, the HSM is a kind of fixed-size porous heat storage material (same heat capacity). As a result, the exhaust gas flow rate changes at different WLTC driving cycle regions in the Figure 4-8. Using the same size HSM, this caused the HSM to have different effects on different exhaust mass flow and reduced fuel consumption in different WLTC driving cycle areas. At the red circles of exhaust temperature in Figure 4-8, the turbine inlet temperature with HSM is higher than that of normal engine. This is an evidence to confirm that the stored exhaust energy was reused. Moreover, the time of these regions is different during different regions of vehicle speed, in which the longest one is under medium vehicle speed. At this region, the fuel consumption reduction is also the largest one as shown in Figure 4-8. The basic reason is different exhaust mass flow rate at different engine speed and load, and the fixed-size porous material has differential impacts on them. As a result, based on the simulation results of WLTC driving cycle, the HSM engine can reduce the engine fuel consumption effectively compared to normal engine under transient conditions.

4.4 Summary

In a turbocharged gasoline engine, the porous Si-SiC material was used as heat storage medium, and the effects of porous Si-SiC material on engine fuel consumption was investigated under steady and transient conditions (WLTC driving cycle) by numerical simulation. The main conclusions are as follows:

1) Under different steady engine conditions (engine speed from 1600 rpm to 4400 rpm), engine fuel consumption was investigated with HSM compared to the normal engine. It demonstrated that with HSM, the engine indicate efficiency increased due to lower pumping loss resulting from increased turbine efficiency. This BSFC reduction changed with engine speed and load, and the higher BSFC reduction was at medium engine speed.

2) Under transient engine condition in the WLTC driving cycle, calculation results showed fuel consumption reduction in all the four vehicle speed regions of the WLTC driving cycle. The largest effect of fuel consumption improvement happened at medium speed of WLTC driving cycle by

about 6.6%. This is due to higher turbine efficiency, PMEP reduction, exhaust energy storage and reusing with HSM under transient engine conditions.

3) The porous Si-SiC material can be applied to the turbocharged gasoline engine and improve the fuel economy of the turbocharged engine.

Chapter 5 Effects of Porous Material on Variable Geometry Turbocharged Engine Performance

5.1 VGT Application Drawbacks in Turbocharged Gasoline Engines

The turbocharged engines have been widely used and accepted for engine downsizing and improvement of fuel economy. However, they still have some serious drawbacks for traditional turbocharged engines, in which the long-time engine transient response (turbo lag) and the worse engine torque characteristic at low engine speed are two main issues [240]. As the turbocharging technologies developing, the variable geometry turbochargers were investigated and applied to engines, such as the diesel engine of truck [241]. The turbine mass flow area is able to be controlled by changing the turbine vanes or rack position of the VGT. In that the back pressure (turbine inlet pressure) of the VGT turbine can be changed by the opening and closing of VGT vanes. The closing of VGT vanes leads to a narrow gas flow channel which can increase the exhaust gas velocity and increase the turbine inlet pressure [242]. This increased turbine inlet pressure can improve the turbine performance, moreover, the engine torque at low engine speed [243]. With the VGT vanes angle changing, the engine performance at full load and part load conditions was also improved by VGT along with great importance of cold-start emissions reduction [243]. The time of the turbocharged engine to the target torque at transient engine condition (turbo lag) was got effective improvement by using VGT compared to fixed-geometry turbochargers [244]. For these potential benefits, the variable geometry turbochargers have been developed on many types. Dual-Volute-VTG was a kind of VGT design with two gas flow channels at the turbine inlet [245], which showed advantages to improve the overall engine performance by residual gas reduction and exhaust gas back-pressure reduction compared to a single-scroll VGT. Similarly, variable Flow Turbocharger (VFT) is another type with a simple and new structure which obtained high reliability compared to other types of VGT [246].

The VGT engines have advantages, such as a smaller engine responses time at transient engine conditions, fuel consumption improvement, higher engine output power at higher engine speed, compared to the normal turbocharged engines. These benefits have impelled commercial of VGT in the turbocharged engines for many years. However, for spark ignition (SI) engine using, variable turbines are still in the way of technology development, and not mature enough for gasoline engine application. The main reason is the higher exhaust temperature in the gasoline engines [242]. The exhaust temperature of the gasoline engines may be high to more than 1000 ℃ which is about 200 ℃ higher than diesel engines [247]. This high temperature can damage the complex structure of the VGT which

leads to bad high-temperature reliability of the variable components in gasoline engines. Andersen [244] demonstrated that the VGT working function became worse in the high exhaust temperature working regions for metal to metal friction and the mechanism to stick for soot build-up especial for long-time application. The exhaust gas temperature always increases with the increased air flow rate, the retarded combustion phasing, the higher air fuel ratio. In that, the conflicts in temperature limits of VGT application typically occur at high engine speeds and loads with large air mass flow rate which are usually near to the operation conditions of peak power at various engine speeds. The high turbine inlet temperature leads to that it is difficult to increase the peak power in the case of the theoretical equivalent ratio due to turbine safe operation temperature restriction [244]. The common practice is to sacrifice fuel economy while maintaining a safe temperature limit.

Due to high turbine inlet temperature challenge for VGT application in gasoline engines, researchers have paid attention to it and focused on many methods, such as the high-temperature durability material, the new design concepts and the turbo-cool turbocharging system, enrichment changing from c, etc. A kind of advanced turbocharger material for the components of the variable structure has been used on in Porsche 911 Turbo which obtained high-temperature reliability with high costs for sports car application [248]. Yasuaki developed a kind of heat resistant material with higher strength and more reliable sliding of the VG linkage for using with exhaust temperature high to 950 ℃ [249, 250]. Tetsui [251] and Kenji [252] developed TiAl and HERCUNITE-S NSHR-A5N respectively for high temperature using of VGT. Arikawa [240] used a coolant circuit with turbine housing design which could cooling the turbine and improve the high-temperature durability, and a water-cooled exhaust manifold component was added on the exhaust manifold to enhance the cooling performance of the high temperature exhaust gas. They led to the turbine inlet temperature reduction which was beneficial to safe application of VGT. However, it decreased the engine exhaust temperature without any energy compensation which led to a loss of available exhaust gas energy resulting in lower turbine power and higher fuel consumption. As a compensation method, exhaust gas recovery (EGR) was used to improve the engine economy due to knock suppression [253]. In addition, as a general method to reduce exhaust temperature, the air fuel rate changing from stoichiometric to enrichment is another effective method to reduce the exhaust gas temperature [254]. However, it obtains lower turbine inlet temperature by more non-reaction masses with incompletely burned CO, thereby worse fuel economy [255]. Aisin Seiki [256] has designed a new kind of variable flow turbocharger (VFT), which tried to resolve the problems of gasoline engine applications by CFD method. By a kind of advanced replacing material, a simpler structure was developed and used to cope with higher exhaust temperatures compared to other types of VGT.

The VGT is a promising technology to meet the tighter regulations of the engine fuel economy and emissions with better transient performance compared to normal turbocharger in the future [257-259].

Despite many methods and efforts have been applied to improve the technologies and equipment of the VGT for the gasoline engine application, however, the implementation of the VGT in gasoline engine has been very limited especial for the high temperature of exhaust gas [260]. It becomes to be necessary and important to investigate the VGT application method in gasoline engines by using new concepts. In that it may be a more effective method to reduce the exhaust gas temperature directly along with no fuel consumption increase. In this paper, a kind of porous material was applied before the VGT which also was used as a kind of porous heat storage medium (HSM). It has been demonstrated that the HSM could improve the turbine performance and engine fuel economy. Moreover, it can reduce the exhaust gas temperature which is a benefit for VGT heat resistance compared to normal VGT engines. For these characteristics of the porous heat storage medium, it was used in the variable geometry turbocharged gasoline to improve the VGT durability at high engine loads, and the fuel consumption reduction was also investigated by using porous heat storage medium. By simulation method, the results showed that the turbine inlet temperature of the VGT was reduced successfully at steady engine conditions of different engine loads and engine speeds. At the same time, the fuel economy and peak torque were also improved by using HSM and VGT compared to normal turbocharged gasoline engine. It can be an effective method to improve the VGT application durability in the turbocharged gasoline engines.

5.2 VGT Application Improvement in Turbocharged Gasoline Engines by Porous Material

5.2.1 Method to Improve High-Temperature Reliability of VGT Gasoline Engine

There are 5 main methods in these years' research to improve the high-temperature reliability of the VGT gasoline engine. Firstly, a simpler structure design of the variable geometry structure is aiming to obtain high reliability, such as variable flow turbocharger [261]. The second method is more advanced material with high-temperature reliability used for the variable geometry structure [262] which increases the cost of VGT. The third one is to add a water-cooling channel on the exhaust manifold to directly reduce the exhaust temperature [240]. The fourth one is more fuel injection (rich combustion), which results in insufficient combustion and higher exhaust energy loss leading to more fuel consumption. In this paper, a new method by using HSM is proposed to reduce the VGT inlet temperature and increase the VGT life while reducing the fuel consumption of the engine.

5.2.2 Effects of Porous Material on VGT Engine Performance at Steady Condition

In this section, the effects of HSM and VGT on engine performance were investigated at the steady conditions. The HSM was predicted to be able to decrease the turbine inlet temperature. In fact, the turbine inlet temperature of the turbocharged engine is determined by many factors, such as engine load, compression ratio, air/fuel ratio. In general, the higher engine loads lead to higher exhaust temperature. Due to the safe operation temperature of the turbine, to protect the turbine and maintain the high temperature stability in the engine load increasing process, one used method is to change the air fuel ratio from stoichiometric to enrichment. In that combustion temperature in the cylinder could be reduced by rich burn when the turbine inlet temperature reaches the limit. However, this approach goes against to recent emissions restrictions especial for CO_2 reduction goals [263]. Moreover, it will bring more fuel consumption. An interference of turbine inlet temperature limit and low fuel consumption occurs in normal turbocharged gasoline engine at high engine load.

In this study, the use of porous material is predicted to decrease both the turbine inlet temperature and fuel consumption. Then a GT-power model of the studied turbocharged gasoline engine was calibrated by experiment. Figure 5-1 shows the calibration conditions and results. The engine speed ranges from 800 RPM to 4000 RPM, and due to turbine inlet temperature limit (900℃), the engine torques are the highest torques at the corresponding engine speed. For engine speed of 2000 RPM, 3200 RPM and 4000 RPM, the maximum torque is determined by turbine inlet temperature limit. Results shows that simulation results of turbine inlet temperature and brake specific fuel consumption (BSFC) have little difference with experiment data. Then, the HSM model was added into the GT-power model of the target engine. Simulation method was used in this study.

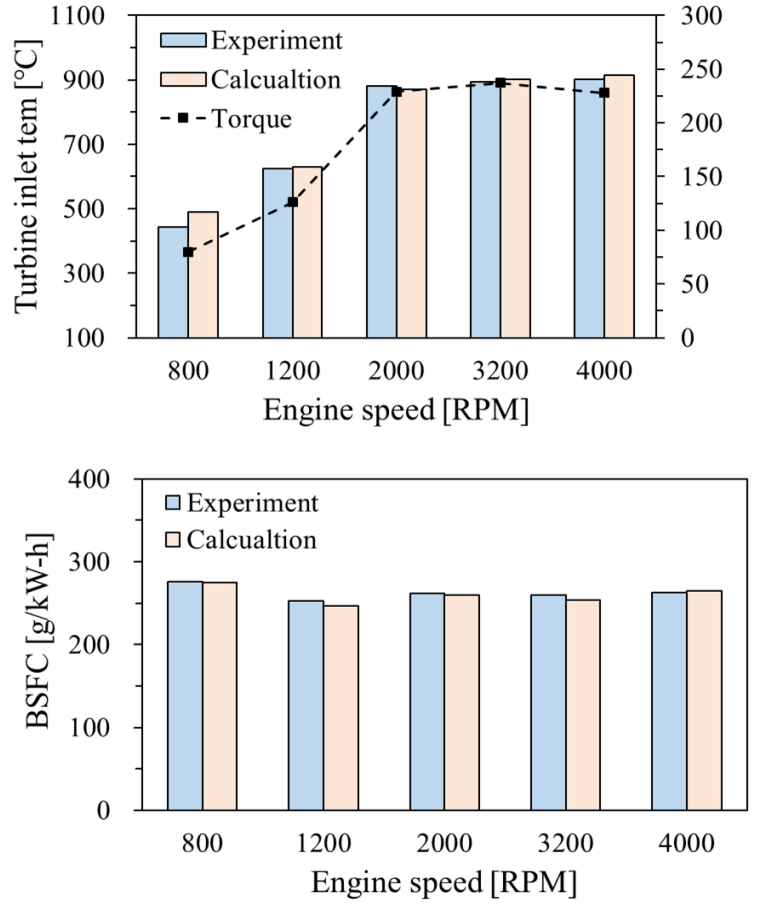

Figure 5-1. Experiment and simulation results of turbine inlet temperature and BSFC

To investigate the effects of HSM and VGT on engine performance, especially the turbine inlet temperature and BSFC, the research conditions are shown in Table 5-1. The normal one is the engine using a fixed geometry turbine, and the HSM one is the engine with the HSM added before the turbine. The case of VGT is the engine compounded with VGT instead of the fixed geometry turbine, and the HSM-VGT is the engine combined with HSM and VGT. For comparison, the effects of throttle full opening and part opening were also studied in the cases of HSM-VGT and Normal-HSM. The reason is that for VGT engines, with a same throttle angle, the turbine working pressure ratio can be increased by closing the angle of the variable vanes. As a result, higher engine loads will be achieved despite having the same throttle opening angle, which is another way for VGT engines to control engine load. Based on the above analysis, to minimize losses of throttle, the throttle could be set to full opening, and the vanes angle could be adjusted to achieve the target load. This may be able to reduce engine fuel consumption by reducing pumping losses. Then, in this research, the fuel economy of the VGT engine was investigated with the throttle full opening and part opening with the same engine torque.

Table 5-1. The test conditions

Case	Normal	HSM	VGT	Throttle Full Opening	Engine Speed ［RPM］	Torque ［Nm］
1	✓	×	×	×	3200	183
2	✓	✓	×	×		
3	×	×	✓	×		
4	×	✓	✓	×		
5	×	×	✓	✓		
6	×	✓	✓	✓		

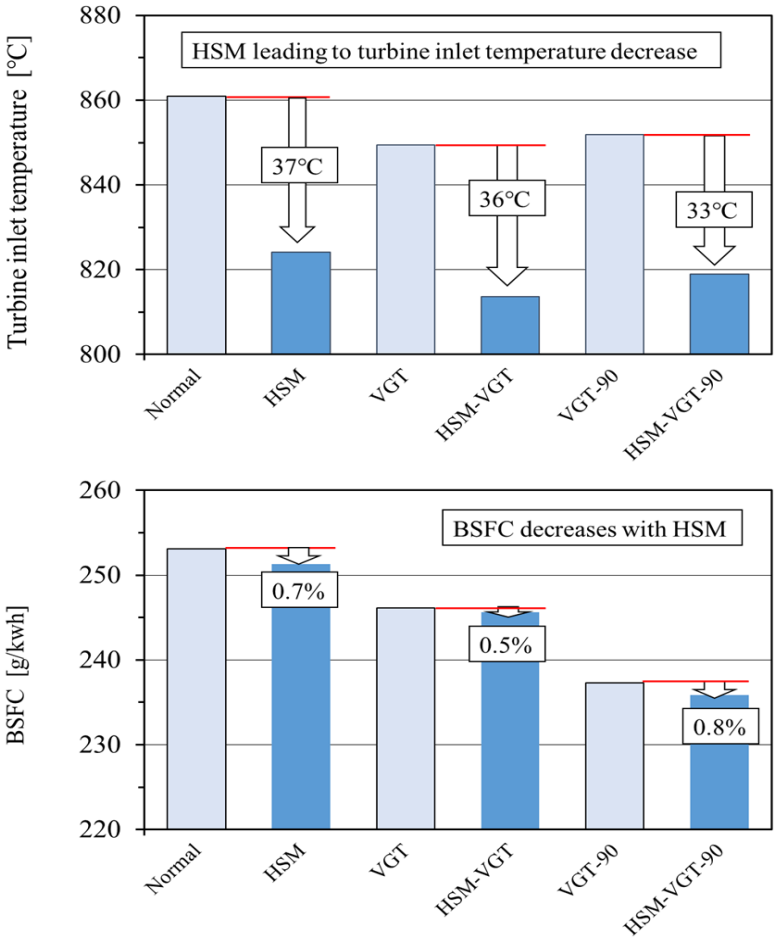

Figure 5-2. The effects of VGT and HSM on turbine inlet temperature and BSFC

The simulation results of turbine inlet temperature and BSFC are shown in Figure 5-2. According to the conditions shown in Table 5-1, the turbine inlet temperature was reduced by 37 ° C, 36 ° C and 33 ° C by using HSM, respectively, compared to normal engine (fixed geometry turbine) and VGT engine without HSM. In addition to lowering exhaust temperature, the use of porous material was also

demonstrated to reduce fuel consumption both using HSM and VGT compared to normal engine. The analysis of these results is shown below.

To analyze the turbine inlet temperature, it is necessary to understand the energy source and influencing factors of the exhaust temperature. Firstly, fuel combustion in the cylinder generates energy. This energy is the source of the engine output torque (power) as well as cooling loss, pump loss, and exhaust energy. For the same target torque of a turbocharged gasoline engine, the turbine inlet temperature is mainly determined by exhaust energy, and affected by boost pressure, fuel injection mass (namely air flow rate), combustion phasing, cooling loss, and pump loss [264]. In this research, with HSM affecting the exhaust gas pressure pulsation and energy, pump loss and exhaust energy loss are the main factors to study the effect on turbine inlet temperature. One case is that if more pump loss occurs, the target engine torque will require more fuel to burn in the cylinder, thereby more fuel consumption and higher exhaust temperature. Another case is about turbine efficiency. For turbocharged engines, turbine is driven by exhaust gas energy (temperature and pressure). If the turbine is operating at higher efficiency, the turbine will require less exhaust gas energy to run the compressor to reach the target boot pressure, thereby the target engine load. Thus, the operating efficiency of the turbine is another factor that affects the inlet temperature of the turbine. Namely, inefficient turbine operation requires more exhaust energy to drive.

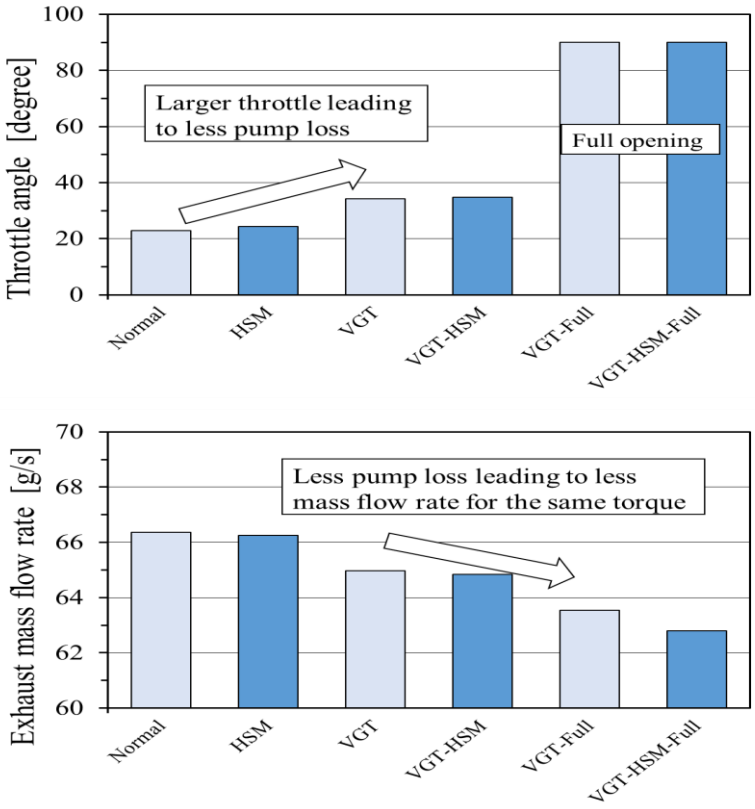

Figure 5-3. Throttle angle and exhaust mass flow rate at different conditions

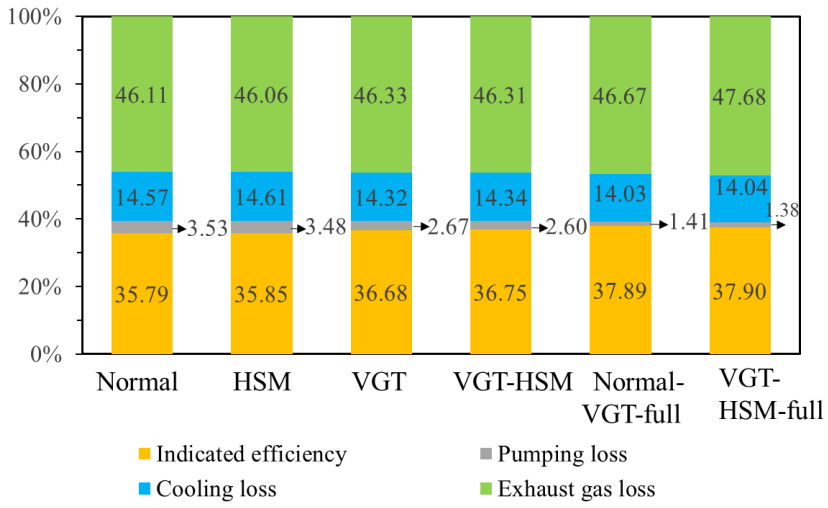

Figure 5-4. Engine heat balance at different conditions

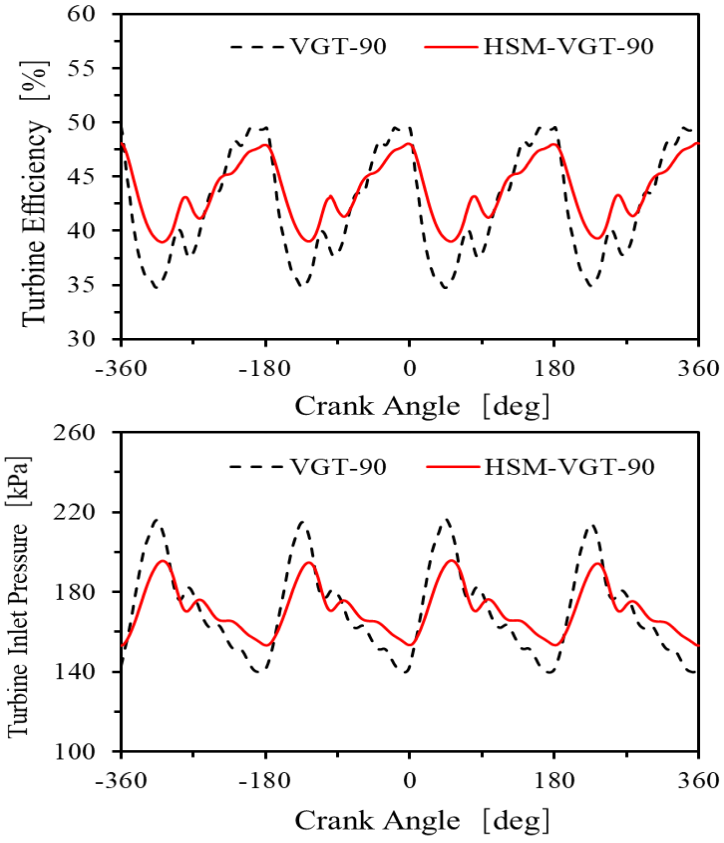

Figure 5-5. The effect of HSM on the turbine efficiency and turbine inlet pressure

The calculation results of throttle angle and exhaust mass flow rate are shown in Figure 5-3 for the engine conditions in Table 5-1. With HSM, it is obvious that throttle opening angle was increased compared to the throttle opening angle without HSM engine. This larger throttle opening angle by using porous material could decrease the pump loss. In addition, to change the vanes angles of VGT to reach the target engine torque with throttle full opening is another method to increase the throttle opening

angle. As a result, the increased throttle angle is 67 degree by using this method compared to that in the engine with fixed geometry turbine. A larger throttle angle led to less pump loss, resulting of lower fuel consumption [265]. Figure 5-4 also demonstrates the reduction in engine pump losses using HSM in the result of engine thermal balance analysis. The less pump loss means that it needs less fuel consumption to meet the target engine torque. In addition, Figure 8 also shows the pump loss decreasing from 3.5% to 0.4% by using VGT and HSM. Due to the same stoichiometric ratio ($\lambda = 1$) under these research conditions, the reduced exhaust mass flow shown in Figure 5-3 proved that the fuel flow rate (fuel injection mass) using HSM is lower compared to the cases without HSM. This resulted in a lower BSFC in engines using HSM, as shown in Figure 5-2. Another reason for fuel economy improvement is better turbine performance with HSM. The exhaust gas pulsation was reduced by adding HSM which was shown in Figure 5-5. After using HSM before the turbine, the turbine efficiency and exhaust pressure pulsation became smaller. It means that the HSM can weaken the exhaust gas pulsation, which results in better turbine performance and higher average turbine efficiency. This smaller pulsation resulted in an 8% increase in average turbine efficiency. This, in turn, led to a reduction in fuel consumption. The results in Figure 5-2 show that the BSFC was reduced by using VGT, HSM and throttle full opening methods compared to the normal fixed geometry turbocharged engine. The maximum reduction of BSFC happened when the engine combined with these three kinds of methods (VGT, HSM and throttle full opening), and the BSFC decreased by 11.7% compared to the fixed geometry turbine without HSM. In addition, HSM is effective to improve the fuel economy of both fixed-geometry and variable-geometry engines.

One reason of turbine inlet temperature reduction is fuel consumption reduction leading to lower exhaust temperature by using HSM. Another reason turbine inlet temperature reduction is that the addition of HSM parts inevitably increased the energy loss of the exhaust gas before the turbine by more heat exchange with the environment. However, this exhaust gas temperature reduction did not increase the fuel consumption, due to less pumping loss, and the improved turbine efficiency by smaller exhaust pulsation. These eventually led to the turbine inlet temperature decreasing and BSFC reduction by using HSM in the VGT engine. The lower turbine inlet temperature is important for the VGT application to the turbocharged gasoline engines, which can improve the high-temperature durability of VGT components. It provides a new method for the better application of VGT to the gasoline turbocharged engines. Another benefit is that, due to the given turbine safe operation limit, HSM can increase the peak power of the VGT engine by reducing the turbine inlet temperature. This will be discussed and explained below.

5.2.3 Effects of Porous Material on Peak Torque in VGT Engine

Due to the limitation of turbine operating temperature, it is difficult to run the engine under stoichiometric combustion within the full load range of the engine, especially under high engine load at different engine speed [266,267]. As a general method, rich- combustion (excess fuel in the mixture) has been used to reduce turbine inlet temperature and avoid turbine damage. In this study, HSM has been proved to be able to reduce the turbine inlet temperature in previous section. Under stoichiometric combustion conditions, exhaust temperature is restricted to protect the turbine at high engine load. However, turbine inlet temperature reduction caused by HSM may provide another selection to further increase the engine's maximum output (high power output) without worrying that excessive exhaust temperatures could damage the turbine. Namely, with HSM, there is no need to reduce the exhaust gas temperature by rich combustion at relatively high engine load. Therefore, by using HSM, the possibility of maintaining air-fuel ratio (AF) in a stoichiometric state over a wider engine load operating range was investigated.

It has been confirmed that turbine inlet temperature increased with engine load under stoichiometric state ($\lambda = 1$) [264]. In addition, boost pressure and exhaust mass flow rate increase with the engine load for a same engine speed. In this section, the effect of HSM on turbine inlet temperature was studied. First, as a comparison, the experimental data of the turbine inlet temperature and AF of the normal engine at an engine speed of 2000 RPM and 3200 RPM are shown in Figure 5-6. The turbine inlet temperature is restricted to 900 ℃, and the stoichiometric is 14.7. In Figure 5-6, the turbine inlet temperature increased with engine torque increasing. The maximum turbine inlet temperature is about 900 ℃ at the peak engine torque of the engine speed. However, the AF is changed to be lower than 14.7 at these engine loads. This means that fuel enrichment ($\lambda<1$) was applied to the engine operating conditions and led to deterioration of fuel economy inevitably. According to this characteristic, HSM was used in the engine to decrease the turbine inlet temperature, thereby increase engine peak power and improve fuel economy near peak power of the engine under $\lambda = 1$.

After HSM added before the turbine, exhaust gas flow first passed through the passage of the used porous material, and the exhaust gas could exchange heat with HSM. Then, exhaust gas flow went into the turbine and ran the vanes. To study the effect of porous material on the temperature of exhaust gas, the temperature of exhaust gas at the HSM inlet, the substrate of porous material, and the HSM outlet were investigated, as shown in Figure 11. Engine speed increased from 2000 RPM to 4000 RPM, and engine torque changed from 153 Nm to 229 Nm. The temperature of HSM_in and HSM_out are the exhaust gas temperature at the position of HSM inlet and HSM outlet, respectively. The temperature of HSM is the average temperature of the substrate temperature of porous material.

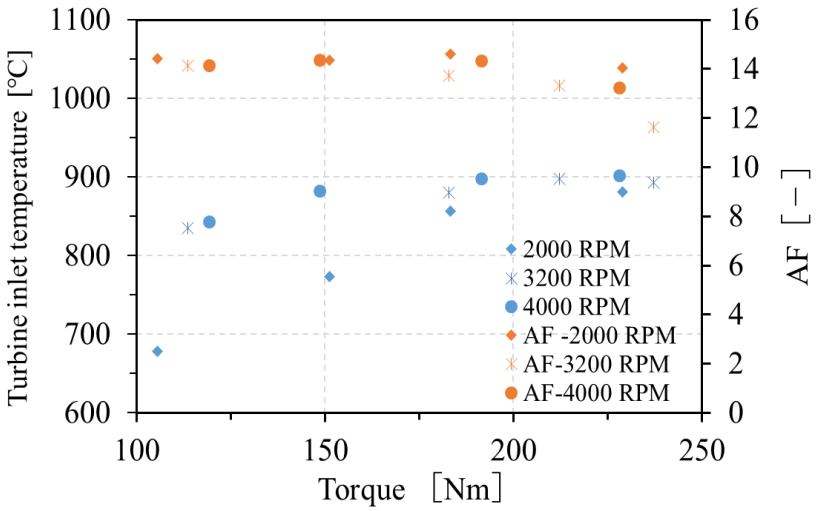

Figure 5-6. The effect of HSM on the turbine efficiency and turbine inlet pressure

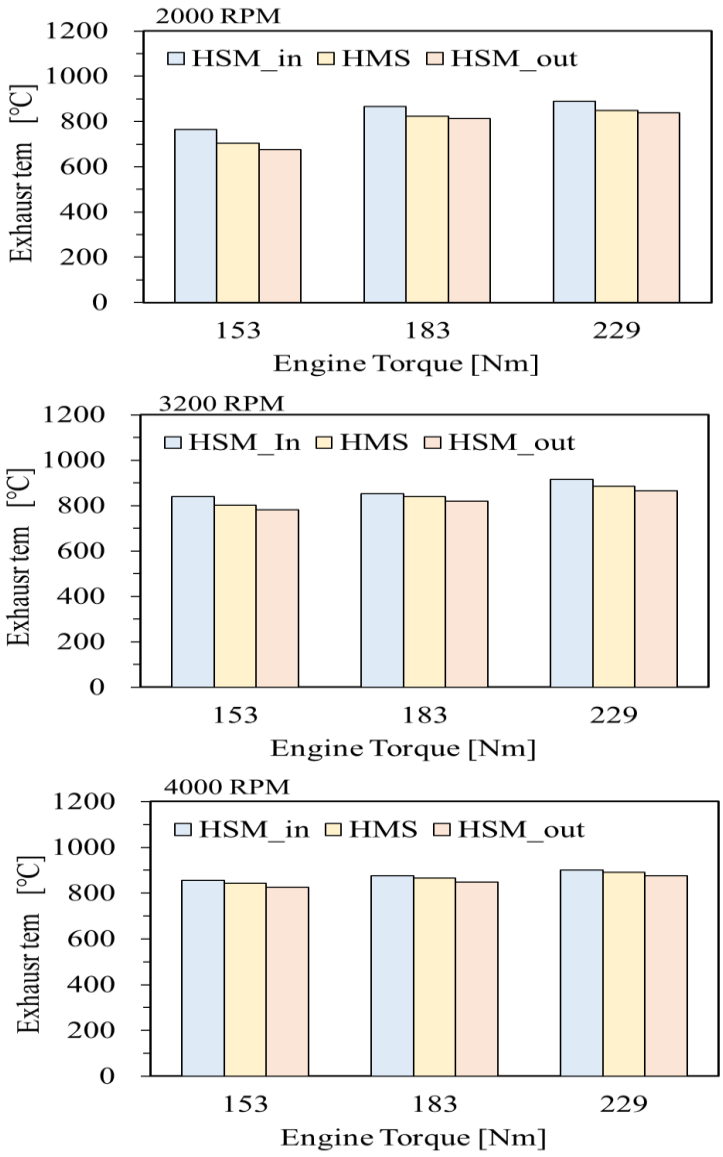

Figure 5-7. The effects of HSM on exhaust temperature of VGT engine

Figure 5-7 shows that the average temperature of HSM is lower than HSM_in, and higher than HSM_out. As a result, the added HSM has affected on exhaust gas temperature, namely a reduction of turbine inlet temperature. This is beneficial to applied VGT in gasoline turbocharged engine for temperature limit. This lower turbine inlet temperature facilitates the application of VGT to gasoline turbocharged engines due to temperature restriction of the material in VGT. In addition, the effects of HSM on turbine inlet temperature changed with engine speed and torque. The temperature reduction caused by HSM decreased with the increase of engine speed and torque. This resulted from different exhaust mass flow rate at different engine load and engine speed. It is obvious that different exhaust mass flow rate means different heat capacity of the exhaust gas [268]. These various heat capacities of exhaust gas at different engine conditions required different temperature reduction capabilities. However, in this research, the HSM sizes were kept the same which means that the heat capacity does not change with engine load, and it may induce different effects on the exhaust gas, namely the temperature drops could decrease with engine load increasing. The exhaust temperature drop is shown in Figure 5-8. The temperature drop (98℃) is the largest one at the engine speed of 2000 RPM engine speed and the torque of 153 Nm. In that the exhaust mass flow rate is the lowest at these conditions as shown in Figure 5-8. In addition, exhaust mass flow and temperature drop show opposite changes in these results. With the increase of engine load, exhaust mass flow rate also increased, however, turbine inlet temperature drops decreased. These confirmed that the fixed size HSM may has various effects on turbine inlet temperature. At high engine speed and load, these effects could change to be small. In general, for a same engine speed, the exhaust gas temperature increases with engine load, and a large exhaust mass flow rates is always along with high exhaust gas temperature [268]. Therefore, the energy of the exhaust gas increases with the engine load. However, for a fixed-size porous heat storage material, the heat capacity of HSM could not change with the increase of engine load which results in a relatively small effect on the temperature of the exhaust, which means that the exhaust temperature drop affected by HSM decreases as the load increases as shown in Figure 5-8.

c

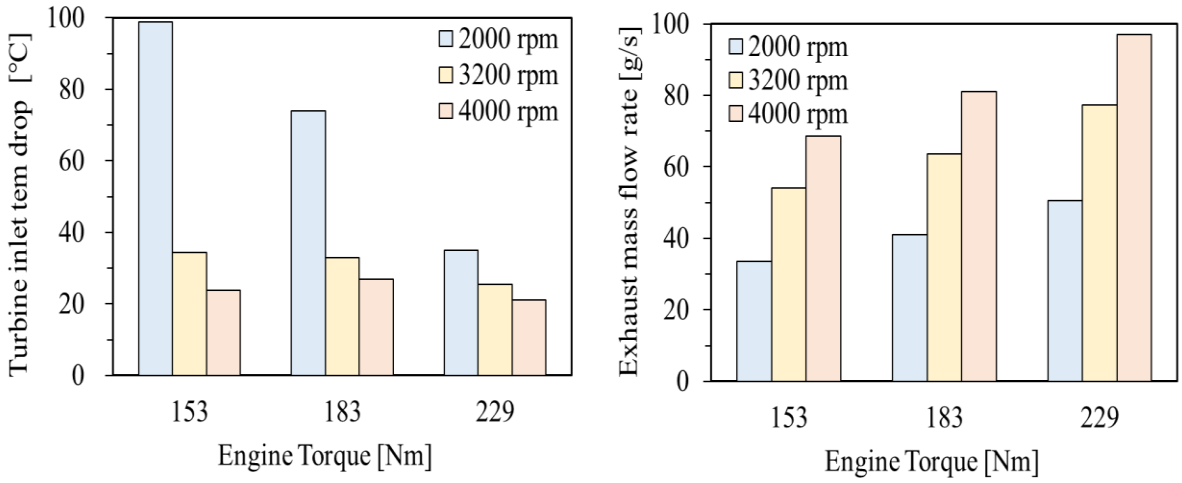

Figure 5-8. The effect of HSM on the turbine inlet temperature at different engine speed and torque

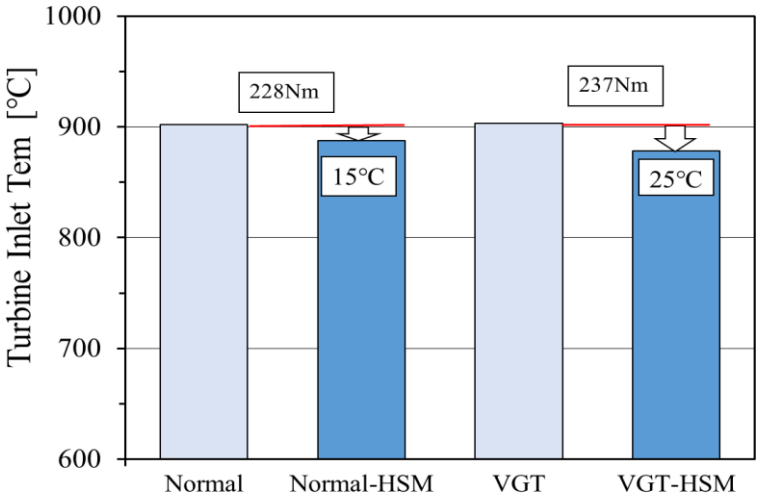

Figure 5-9. The effect of HSM on the turbine inlet temperature under stoichiometric combustion at 4000 RPM

More importantly, these turbine inlet temperature drop could also occur under fuel-rich combustion conditions. Due to the maximum turbine inlet temperature restriction leading to fuel-rich combustion, it is beneficial to expand the range of stoichiometric combustion and improve peak torque under stoichiometric operating conditions by using HSM. To evaluate and prove this effect, the peak torque of 4000 RPM with HSM was applied to investigate as shown in Figure 5-9. For normal engine, the peak torque was 228 Nm, and at this condition, turbine inlet temperature reached the temperature limit. However, the turbine inlet temperature is 15 ℃ lower with HSM compared to the turbine temperature of without HSM engine. As a result, this provides chance to further increase peak engine torque, namely the engine maximum output power. For VGT added engine, the peak torque was increased to 237 Nm compared to the torque of normal engine. This demonstrated the fact of power increase with VGT. At this condition, the adding of HSM on the VGT engine also decrease the turbine inlet temperature.

Compared with the turbine inlet temperature of ordinary VGT engine, HSM can reduce the turbine inlet temperature by 25° C as shown in Figure 5-9.

5.3 Summary

VGT has disadvantages of bad high-temperature durability to apply in gasoline engines. To improve the high temperature durability and the engine fuel economy of VGT gasoline engines. A kind of porous material (Si-SiC) was used as the heat storage medium added before the turbine. The effects of porous material on engine fuel consumption and turbine inlet temperature were investigated under different engine conditions. The main conclusions are as follows:

1) At steady engine condition (3200rpm,183Nm), the engine fuel consumption of the fixed geometry turbocharged engine was reduced by using HSM and VGT. Using HSM, the reduced pump loss, higher turbine efficiency due to weaken exhaust pulsation, a fuel consumption reduction about 1% was obtained in VGT engine.

2) The turbine inlet temperature achieved a drop by adding HSM before the turbine. The heat loss from HSM parts and reduced fuel consumption led to turbine inlet temperature decrease. These temperature drop decreased with engine speed and load for fixed size HSM. Using HSM to reduce turbine inlet temperature is beneficial to improve the high temperature durability of VGT in gasoline engines.

3) The stoichiometric combustion of engine is always restricted by the safe temperature limit of turbine operation. Under high engine load and speed, the stoichiometric combustion range could be expanded due to the reduced exhaust temperature. At the same time, using HSM also has potential to increase engine peak torque for lower exhaust temperature.

Chapter 6 Conclusions

This study pays attentions on the drawbacks of turbocharged engines application and the strict fuel consumption regulations, and the purpose is to investigate the application of the porous Si-SiC material to a turbocharged gasoline engine. The porous Si-SiC material added before the turbine can affect the exhaust gas pressure and temperature. As 4-cylinder engine has irreversible cyclic variation, including intake and exhaust process, combustion in the cylinder pulsation, turbocharging system operation. Pulsations of exhaust pressure and temperature lead to inconstant turbine operation, which leads to the changes in turbine efficiency. Pulsation is reduced by using porous Si-SiC material, and at the same time, exhaust gas energy is recovered by energy storage of porous Si-SiC material.

1）Model Development of Porous Material and Engine

Model development and application of the porous material and engine is helpful for the following studies. The structure characteristics of the used porous Si-SiC material were obtained by micro-structure analysis, including the calculation of the skeletal surface area and skeletal volume. To define and develop the model of the porous Si-SiC material, the physical parameters and thermal properties were studied, such as porosity, substrate surface area, substrate volume, thermal capacity, conductivity. In addition, the pressure loss model and heat transfer model were evaluated to simulate the exhaust gas pressure drops and temperature changes under different conditions.

To investigation the effects porous material of engine performance, a model of the engine was calibrated at different conditions, and BSFC results was typically tested with high accuracy. To study the fuel consumption under transient conditions, a WLTC driving cycle model was developed and validated. As a result, the engine model was combined with the developed porous material model which was used in the following study.

2） Effects of Porous Material on Engine Response of Turbocharged Gasoline

The verified HSM model was added to the turbocharged engine to investigate the effects on turbine and engine performance by simulation method. Results show that two factors are essential for the improvement of engine performance in which the turbine efficiency becomes better by decreasing pulsation amplitude with porous Si-SiC material. The turbine efficiency improved about 5% with HSM of lower engine speed (1200rpm, 125N.m) and BSFC decreases about 1% (2000rpm,183N-m) due to the reduced pulsation of turbine inlet exhaust gas. Furthermore, engine takes less time (reduced by about 0.8s with a 1s dwell time of 3200rpm) to reach target torque and intake pressure. This means a higher turbine response at load recovery condition because the high load exhaust gas thermal energy is stored and reused by heat storage medium Si-SiC. These results prove that it is feasible and beneficial to use

porous Si-SiC as a storage medium for exhaust gas energy recovery and improve engine response under load recovery conditions.

3）Effects of Porous Material on Fuel Economy of Turbocharged Gasoline

The porous Si-SiC material was used as heat storage medium, and the effects of porous Si-SiC material on engine fuel consumption was investigated under steady and transient conditions (WLTC driving cycle) by simulation. Under different steady engine conditions (engine speed from 1600 rpm to 4400 rpm), engine fuel consumption was investigated with porous material compared to the normal engine. It demonstrated that with porous Si-SiC material HSM, the engine indicate efficiency increased due to lower pumping loss resulting from increased turbine efficiency. This BSFC reduction changed with engine speed and load, and the higher BSFC reduction was at medium engine speed. Under transient engine condition in the WLTC driving cycle, calculation results showed fuel consumption reduction in all the four vehicle speed regions of the WLTC driving cycle. The largest effect of fuel consumption improvement happened at medium speed of WLTC driving cycle by about 6.6%. This is due to higher turbine efficiency, PMEP reduction, exhaust energy storage and reusing with HSM under transient engine conditions. As a result, the porous Si-SiC material can be applied to the turbocharged gasoline engine and improve the fuel economy of the turbocharged engine.

4） Effects of Porous Material on Variable Geometry Turbocharged Engine Performance

VGT has disadvantages of bad high-temperature durability to apply in gasoline engines. To improve the high temperature durability and the engine fuel economy of VGT gasoline engines. Porous Si-SiC material was used as the heat storage medium added before the turbine. The effects of porous material on engine fuel consumption and turbine inlet temperature were investigated under different engine conditions. The main conclusions are as follows: At steady engine condition (3200rpm,183Nm), the engine fuel consumption of the fixed geometry turbocharged engine was reduced by using both porous Si-SiC material and VGT. Using porous Si-SiC material, the reduced pump loss, higher turbine efficiency due to weaken exhaust pulsation, a fuel consumption reduction about 1% was obtained in VGT engine. The turbine inlet temperature achieved a drop by adding HSM before the turbine. The heat loss from porous Si-SiC material parts and reduced fuel consumption led to turbine inlet temperature decrease. These temperature drop decreased with engine speed and load for fixed size porous Si-SiC material. Using porous Si-SiC material to reduce turbine inlet temperature is beneficial to improve the high temperature durability of VGT in gasoline engine. The stoichiometric combustion of engine is always restricted by the safe temperature limit of turbine operation. Under high engine load and speed, the stoichiometric combustion range could be expanded due to the reduced exhaust temperature. At the same time, using porous Si-SiC material also has potential to increase engine peak torque for lower exhaust temperature.

References

1. European Union. Worldwide Emission Standards and Related Regulations - Passenger Cars / Light and Medium Duty Vehicles. Cont Futur Motion 2019:210 pages.
2. Wang J, Wu Q, Liu J, et al. Vehicle emission and atmospheric pollution in China: problems, progress, and prospects. PeerJ. 2019;7:e6932. Published 2019 May 16. doi:10.7717/peerj.6932
3. Yang Z, Bandivadekar A. Light-duty vehicle greenhouse gas and fuel economy standards[J]. ICCT report, 2017.
4. Outlook I E A G E V. to Electric Mobility[J]. IEA: Paris, France, 2019.
5. Du J, Ouyang M. Review of electric vehicle technologies progress and development prospect in China[C]//2013 World Electric Vehicle Symposium and Exhibition (EVS27). IEEE, 2013: 1-8.
6. Cheng K W E. Recent development on electric vehicles[C]//2009 3rd International Conference on Power Electronics Systems and Applications (PESA). IEEE, 2009: 1-
7. Kumar A R. Focus on Expansion of Hydrogen and Electric Fleets for Passenger and Freight Transport in United Kingdom[D]. College of Physical Sciences, School of Engineering University of Aberdeen, King's College, 2016.
8. Yang Z, Ge Y, Thomas D, et al. Real driving particle number (PN) emissions from China-6 compliant PFI and GDI hybrid electrical vehicles[J]. Atmospheric environment, 2019, 199: 70-79.
9. Duarte G O, Varella R A, Gonçalves G A, et al. Effect of battery state of charge on fuel use and pollutant emissions of a full hybrid electric light duty vehicle[J]. Journal of Power Sources, 2014, 246: 377-386.
10. Huang Y, Surawski N C, Organ B, et al. Fuel consumption and emissions performance under real driving: Comparison between hybrid and conventional vehicles[J]. Science of The Total Environment, 2019, 659: 275-282.
11. An Y, Jaasim M, Raman V, et al. Homogeneous charge compression ignition (HCCI) and partially premixed combustion (PPC) in compression ignition engine with low octane gasoline[J]. Energy, 2018, 158: 181-191.
12. Bendu H, Murugan S. Homogeneous charge compression ignition (HCCI) combustion: Mixture preparation and control strategies in diesel engines[J]. Renewable and Sustainable Energy Reviews, 2014, 38: 732-746.
13. Yasuo MORIYOSHI TK. Recent Progress in HCCI Combustion for a Practical Usage as a Gasoline Engine. J Automot Saf Energy 2012;3:105 — 115. doi:10.3969/j.issn.1674-8484.2012.02.002.
14. Park C, Kim S, Kim H, et al. Stratified lean combustion characteristics of a spray-guided combustion system in a gasoline direct injection engine[J]. Energy, 2012, 41(1): 401-407.

15. M. Bunce, et al., The Effects of Turbulent Jet Characteristics on Engine Performance Using a Pre-Chamber Combustor, SAE Technical Paper, 2014
16. F.A. Rodrigues Filho, et al.E25 stratified torch ignition engine performance, CO2 emission and combustion analysis Energy Convers. Manage., 115 (2016), pp. 299-307
17. Tanoue, K., Kuboyama, T., Moriyoshi, Y., Hotta, E. et al., "Extension of Lean and Diluted Combustion Stability Limits by Using Repetitive Pulse Discharges," SAE Technical Paper 2010-01-0173, 2010, https://doi.org/10.4271/2010-01-0173.
18. Zhao F, Lai M C, Harrington D L. Automotive spark-ignited direct-injection gasoline engines[J]. Progress in energy and combustion science, 1999, 25(5): 437-562.
19. SN PLUS & LSPI – What You Need to Know, https://www.tyreeoil.com/news/sn-plus-amp-lspi-what-you-need-to-know
20. Shuai S, Ma X, Li Y, et al. Recent progress in automotive gasoline direct injection engine technology[J]. Automotive Innovation, 2018, 1(2): 95-113.
21. Mitroglou N, Nouri J M, Yan Y, et al. Spray structure generated by multi-hole injectors for gasoline direct-injection engines[R]. SAE Technical Paper, 2007.
22. Leng X, Jin Y, He Z, et al. Numerical study of the internal flow and initial mixing of diesel injector nozzles with V-type intersecting holes[J]. Fuel, 2017, 197: 31-41.
23. Leng X, Jin Y, He Z, et al. Effects of V-type intersecting hole on the internal and near field flow dynamics of pressure atomizer nozzles[J]. International Journal of Thermal Sciences, 2018, 130: 183-191.
24. Tang Y, Deng W, Liu B, et al. The new ChangAn inline 4-cylinder 1.6 L gasoline naturally aspirated GDI engine[R]. SAE Technical Paper, 2018.
25. Shiraishi T. A Study of Low Temperature Plasma-Assisted Gasoline HCCI Combustion[J]. SAE International Journal of Engines, 2019, 12(1): 101-114.
26. Moriyoshi Y, Kuboyama T, Tanoue K. Combustion Enhancement in a Gas Engine Using Low Temperature Plasma [R]. SAE Technical Paper, 2020.
27. Adamovich I, Baalrud S D, Bogaerts A, et al. The 2017 Plasma Roadmap: Low temperature plasma science and technology[J]. Journal of Physics D: Applied Physics, 2017, 50(32): 323001.
28. Bae C, Kim J. Alternative fuels for internal combustion engines[J]. Proceedings of the Combustion Institute, 2017, 36(3): 3389-3413.
29. Agarwal A K. Biofuels (alcohols and biodiesel) applications as fuels for internal combustion engines[J]. Progress in energy and combustion science, 2007, 33(3): 233-271.
30. Gong C, Li Z, Yi L and Liu F. Comparative study on combustion and emissions between methanol port-injection engine and methanol direct-injection engine with H2-enriched port-injection under lean-burn conditions. Energy Conversion and Management. 2019; 200: 112096.

31. Verhelst S, Turner J W G, Sileghem L, et al. Methanol as a fuel for internal combustion engines[J]. Progress in Energy and Combustion Science, 2019, 70: 43-88.
32. Shapur talks about the downsides of the downsizing trend on engines for India.Is downsizing dead? https://www.autocarindia.com/auto-blogs/is-downsizing-dead-410640
33. Patil C, Varade S, Wadkar S. A review of engine downsizing and its effects[J]. International Journal of Current Engineering and Technology, 2017, 7(7): 319-324.
34. Clenci A C, Descombes G, Podevin P, et al. Some aspects concerning the combination of downsizing with turbocharging, variable compression ratio, and variable intake valve lift[J]. Proceedings of the Institution of Mechanical Engineers, Part D: Journal of Automobile Engineering, 2007, 221(10): 1287-1294.
35. Isenstadt A, German J, Dorobantu M, et al. Downsized, boosted gasoline engines[J]. The international council on clean transportation, 2016.
36. Wirth M, Mayerhofer U, Piock W F, et al. Turbocharging the DI gasoline engine[J]. SAE transactions, 2000: 146-155.
37. Shahed SM, Bauer K-H. Parametric Studies of the Impact of Turbocharging on Gasoline Engine Downsizing. SAE Int J Engines 2009;2:1347–58. doi:10.4271/2009-01-1472.
38. Bandel W, Fraidl G K, Kapus P E, et al. The turbocharged GDI engine: boosted synergies for high fuel economy plus ultra-low emission[R]. SAE Technical Paper, 2006.
39. D. Petitjean, L. Bernardini, C. Middlemass, and S. M. Shahed, Advanced Gasoline Engine Turbocharging Technology for Fuel Economy Improvements, no. 724, 2004.
40. Lumsden G, OudeNijeweme D, Fraser N, Blaxill H. Development of a Turbocharged Direct Injection Downsizing Demonstrator Engine. SAE Int J Engines 2009;2:1420–32. doi:10.4271/2009-01-1503.
41. Variable Valve Timing (VVT), https://www.austincc.edu/wkibbe/vvt.htm
42. Shigeo OKUI,Tsutomu KISHI,Naohiro ISHIKAWA, Development of 3-stage i-VTEC VCM Engine for CIVIC Hybrid. Honda R&D technical review, 2006, 18(2): 44-51.
43. Toyota Variable Valve Timing.VVT-iW.https://toyota-club.net/files/faq/16-01-01_faq_vvt_iw_eng.htm.
44. Lou Z, Zhu G. Review of Advancement in Variable Valve Actuation of Internal Combustion Engines[J]. Applied Sciences, 2020, 10(4): 1216.
45. Mitsubishi Innovative Valve timing Electronic Control system,https://www.mitsubishimotors.com/en/innovation/technology/library/mivec.html.
46. Wei H, Zhu T, Shu G, et al. Gasoline engine exhaust gas recirculation–a review[J]. Applied energy, 2012, 99: 534-544.

47. Hoepke B, Jannsen S, Kasseris E, et al. EGR effects on boosted SI engine operation and knock integral correlation[J]. SAE International Journal of Engines, 2012, 5(2): 547-559.
48. Hu E, Huang Z, Liu B, et al. Experimental study on combustion characteristics of a spark-ignition engine fueled with natural gas–hydrogen blends combining with EGR[J]. International journal of hydrogen energy, 2009, 34(2): 1035-1044.
49. Ibrahim A, Bari S. Optimization of a natural gas SI engine employing EGR strategy using a two-zone combustion model[J]. Fuel, 2008, 87(10-11): 1824-1834.
50. Nande A M, Szwaja S, Naber J. Impact of EGR on combustion processes in a hydrogen fuelled SI engine[R]. SAE Technical Paper, 2008.
51. Zhao L, Wang D. Combined Effects of a Biobutanol/Ethanol–Gasoline (E10) Blend and Exhaust Gas Recirculation on Performance and Pollutant Emissions[J]. ACS omega, 2020.
52. Stone R. Introduction to internal combustion engines[M]. London: Macmillan, 1999.
53. Rose A T J M, Akehurst S, Brace C J. Modelling the performance of a continuously variable supercharger drive system[J]. Proceedings of the Institution of Mechanical Engineers, Part D: Journal of Automobile Engineering, 2011, 225(10): 1399-1414.
54. Lysholm AJR. A new rotary compressor. Proc IMechE 1943: 150: 11–16.
55. Lysholm supercharger https://grabcad.com/library/lysholm-supercharger.
56. How Does a Supercharger Work and Its Functions. https://carsintrend.com/what-does-a-supercharger-work.
57. Takabe S, Hatamura K, Kanesaka H, et al. Development of the high performance Lysholm compressor for automotive use[R]. SAE Technical Paper, 1994.
58. Hu B, Tang H, Akehurst S, et al. Modelling the Performance of the Torotrak V-Charge Variable Drive Supercharger System on a 1.0 L GTDI-Preliminary Simulation Results[R]. SAE Technical Paper, 2015.
59. Turner J W G, Popplewell A, Marshall D J, et al. SuperGen on ultraboost: variable-speed centrifugal supercharging as an enabling technology for extreme engine downsizing[J]. SAE International Journal of Engines, 2015, 8(4): 1602-1615.
60. Turner, J., Popplewell, A., Patel, R., Johnson, T. et al., “Ultra Boost for Economy: Extending the Limits of Extreme Engine Downsizing,” SAE Int. J. Engines 7(1):387-417, 2014, doi:10.4271/2014-01-1185.
61. Terdich N, Martinez-Botas R. Experimental efficiency characterization of an electrically assisted turbocharger[R]. SAE Technical Paper, 2013.
62. Flohr A, Gödeke H, Kech J, et al. Electrically Assisted Turbocharging for Optimized Performance[J]. MTZ industrial, 2018, 8(2): 24-31.

63. Gödeke H, Löffler R. Electrification of standard TCs and its impact on the ICE Cross-Charger—turbo by wire[C]//10th MTZ Conference Ladungswechsel im Verbrennungsmotor, Stuttgart. 2017.
64. Katrasnik T, Rodman S, Trenc F, et al. Improvement of the dynamic characteristic of an automotive engine by a turbocharger assisted by an electric motor[J]. J. Eng. Gas Turbines Power, 2003, 125(2): 590-595.
65. Scaffidi C, De Caro S, Foti S, et al. Electrically Assisted Internal Combustion Engines: A Comparative Analysis[J]. International journal of automotive technology, 2018, 19(6): 1091-1101.
66. Ibaraki S, Yamashita Y, Sumida K, et al. Development of the hybrid turbo, an electrically assisted turbocharger[J]. Mitsubishi Heavy Industries Technical Review, 2006, 43(3): 1-5.
67. Balis C, Middlemass C, Shahed S M. Design & development of e-turbo for SUV and light truck applications[R]. Garrett Engine Boosting Systems (US), 2003.
68. How turbocharging works. https://x-engineer.org/automotive-engineering/internal-combustion-engines/ice-components-systems/turbocharging-works.
69. Impeller vs. Turbine. https://www.askdifference.com/impeller-vs-turbine.
70. Generator.https://fadhilglory.wordpress.com/2018/04/22/makalah-pembangkit-listrik-tenaga-air-plta.
71. Turbine Engines. http://www.aviationchief.com/turbine-engines.html.
72. Rahnke C J. Axial Flow Automotive Turbocharger[C]//ASME 1985 International Gas Turbine Conference and Exhibit. American Society of Mechanical Engineers Digital Collection, 1985.
73. Pesiridis A, Ferrara A, Tuccillo R, et al. Conceptual design of an axial turbocharger turbine[C]//ASME Turbo Expo 2017: Turbomachinery Technical Conference and Exposition. American Society of Mechanical Engineers Digital Collection, 2017.
74. Pesiridis, A.; Saccomanno, A.; Tuccillo, R.; Capobianco, A. Conceptual Design of a Variable Geometry, AxialFlow Turbocharger Turbine. In Proceedings of the 13th International Conference on Engines & Vehicles,Napoli, Italy, 10–14 September 2017.
75. Nichols K E. How to select turbomachinery for your application[M]. Arvada Barber Nichols Eng. Company, 2015.
76. How a turbo works. https://iloveturbos.wordpress.com/about.
77. Nguyen-Schäfer H. Rotordynamics of automotive turbochargers[M]. Springer International Publishing, 2015.
78. Aungier, R. H. (2006). Turbine aerodynamics. ASME, New York.
79. Cumpsty, N. A. (2004). Compressor aerodynamics. Department of Engineering University of Cambridge.
80. Performance corrections for compressor maps. https://www.conceptsnrec.com/blog/performance-corrections-for-compressor-maps.

81. Turbo/supercharger maps. https://www.rbracing-rsr.com/turbotech.html.
82. Uddin N, Gravdahl J T. Bond graph modeling of centrifugal compression systems[J]. Simulation, 2015, 91(11): 998-1013.
83. Centrifugal Compressor Surge. https://www.enggcyclopedia.com/2012/01/centrifugal-compressor-surge/.
84. Compressor Choke or Stonewall. https://www.enggcyclopedia.com/2012/02/compressor-choke-stonewall/.
85. COMPRESSOR CHOKE.https://www.turbomachinerymag.com/compressor-choke/.
86. Zheng X, Lin Y, Kawakubo T, et al. Extension of Operating Range of a Centrifugal Compressor by Use of a Non-Axisymmetric Diffuser[J]. IHI Eng. Rev, 2018, 51: 43-56.
87. Korakianitis T, Sadoi T. Turbocharger-design effects on gasoline-engine performance[J]. J. Eng. Gas Turbines Power, 2005, 127(3): 525-530.
88. Moulin P, Grondin O. Control design for a second order dynamic system: Two-stage turbocharger[J]. IFAC Proceedings Volumes, 2013, 46(21): 470-476.
89. Lee B, Jung D, Assanis D, et al. Dual-stage turbocharger matching and boost control options[C]//ASME 2008 Internal Combustion Engine Division spring technical conference. American Society of Mechanical Engineers Digital Collection, 2008: 267-277.
90. Lumsden G, OudeNijeweme D, Fraser N, et al. Development of a turbocharged direct injection downsizing demonstrator engine[J]. SAE International Journal of Engines, 2009, 2(1): 1420-1432.
91. Galindo J, Serrano J R, Climent H, et al. Impact of two-stage turbocharging architectures on pumping losses of automotive engines based on an analytical model[J]. Energy Conversion and Management, 2010, 51(10): 1958-1969.
92. Shan P, Zhou Y, Zhu D. Mathematical model of two-stage turbocharging gasoline engine propeller propulsion system and analysis of its flying characteristic[J]. Journal of Engineering for Gas Turbines and Power, 2015, 137(5).
93. Albin T, Ritter D, Liberda N, et al. Two-stage turbocharged gasoline engines: Experimental validation of model-based control[J]. IFAC-PapersOnLine, 2015, 48(15): 124-131.
94. Albin T, Ritter D, Abel D, et al. Nonlinear MPC for a two-stage turbocharged gasoline engine airpath[C]//2015 54th IEEE Conference on Decision and Control (CDC). IEEE, 2015: 849-856.
95. Albin T, Ritter D, Liberda N, et al. In-vehicle realization of nonlinear MPC for gasoline two-stage turbocharging airpath control[J]. IEEE Transactions on Control Systems Technology, 2017, 26(5): 1606-1618.
96. Cantemir C G. Twin turbo strategy operation[R]. SAE Technical Paper, 2001.

97. Luttermann C, Mährle W. BMW High Precision Fuel Injectionin Conjunction with Twin-Turbo Technology: a Combination for Maximum Dynamic and High Fuel Efficiency[R]. SAE Technical Paper, 2007.
98. Schuetz M, Kemmler R, Doll G, et al. The new Mercedes-Benz 3.0-l V6 DI gasoline engine with twin turbo; Der neue 3, 0-L-V6-DI-Ottomotor mit Bi-Turbo von Mercedes-Benz[J]. 2013.
99. Schütz M, Doll G, Waltner A, et al. The new Mercedes-Benz 3.0-l V6 DI gasoline engine with twin turbo[J]. MTZ worldwide, 2013, 74(6): 18-24.
100. Turbocharging.https://www.autozine.org/technical_school/engine/Forced_Induction_3.htm.
101. Wang A, Zheng X. Design criterion for asymmetric twin-entry radial turbine for efficiency under steady and pulsating inlet conditions[J]. Proceedings of the Institution of Mechanical Engineers, Part D: Journal of Automobile Engineering, 2019, 233(8): 2246-2256.
102. Moustapha H, Zelesky MF, Baines NC, et al. Axial and radial turbines, vol. 2. White River Junction, VT: Concepts NREC, 2003.
103. Wijetunge R S, Hawley J G, Vaughan N D. An exhaust pressure control strategy for a diesel engine[J]. Proceedings of the Institution of Mechanical Engineers, Part D: Journal of Automobile Engineering, 2004, 218(4): 449-464.
104. Brinkert N, Sumser S, Schulz A, et al. Understanding the Twin Scroll Turbine: Flow Similarity[C]//ASME 2011 Turbo Expo: Turbine Technical Conference and Exposition. American Society of Mechanical Engineers Digital Collection, 2011: 2207-2218.
105. Zhu D, Zheng X. Asymmetric twin-scroll turbocharging in diesel engines for energy and emission improvement[J]. Energy, 2017, 141: 702-714.
106. https://x-engineer.org/automotive-engineering/internal-combustion-engines/ice-components-systems/turbocharging-works/.
107. Reitz R D, Ogawa H, Payri R, et al. IJER editorial: the future of the internal combustion engine[J]. 2020.
108. https://www.carthrottle.com/post/engineering-explained-the-pros-and-cons-of-turbochargers-vs-superchargers.
109. https://www.autotrainingcentre.com/blog/pros-and-cons-turbo-charged-engines.
110. Isenstadt, Aaron, et al. "Downsized, boosted gasoline engines." The international council on clean transportation (2016).
111. Chen, Tao, et al. "Turbocharger Design for a 1.8 Liter Turbocharged Gasoline Engine Using an Integrated Method." ASME Turbo Expo 2009: Power for Land, Sea, and Air. American Society of Mechanical Engineers Digital Collection, 2009.
112. Kunanoppadon, Jarut. "Thermal efficiency of a combined turbocharger set with gasoline engine." Am. J. Eng. Applied Sci 3 (2010): 342-349.

113. Reddy, S. Sunil Kumar, Dr V. Pandurangadu, and SP Akbar Hussain. "Effect of Turbo charging On Volumetric Efficiency in an Insulated Di Diesel Engine For Improved Performance." International Journal of Modern Engineering Research (IJMER)3.2 (2013): 674-677.
114. Boretti, Alberto. "Towards 40% efficiency with BMEP exceeding 30 bar in directly injected, turbocharged, spark ignition ethanol engines." Energy conversion and management 57 (2012): 154-166.
115. A. Cairns, H. Blaxill, Exhaust Gas Recirculation for Improved Part and Full Load Fuel Economy in a Turbocharged Gasoline Engine Reprinted From : SI Combustion and Direct Injection SI Engine Technology, Sae, no. 724, 2013.
116. LAKE, T.; STOKES, Turbocharging Concepts for Downsized DI Gasoline Engines, 12th Aachen Colloquium, Aachen, Germany, 2003.
117. H. Nguyen-Schäfer, Rotordynamics of Automotive Turbochargers, 2015.
118. Deligant, Michaël, et al. "Surge detection on an automotive turbocharger during transient phases." IOP Conference Series: Materials Science and Engineering. Vol. 252. No. 1. IOP Publishing, 2017.
119. Semlitsch, Bernhard, and Mihai Mihăescu. "Flow phenomena leading to surge in a centrifugal compressor." Energy 103 (2016): 572-587.
120. Guillou, E., et al. "Surge characteristics in a ported shroud compressor using PIV measurements and large eddy simulation." 9th International Conference on Turbochargers and Turbocharging, 19 May 2010 through 20 May 2010, Westminster, London, UK. 2010.
121. Elkamel, Chiheb, et al. "Experimental study of the surge behaviour of a centrifugal compressor." 2011.
122. Hellstrom, Fredrik, et al. Stall development in a ported shroud compressor using piv measurements and large eddy simulation. No. 2010-01-0184. SAE Technical Paper, 2010.
123. Wang X, Ge Y, Yu L, Feng X 2013 Effects of altitude on the thermal efficiency of a heavy-duty diesel engine Energy 59 543.
124. Galindo J, Tiseira A, Navarro R, Tari D, Meano C.M. 2017 Effect of the inlet geometry on performance, surge margin and noise emission of an automotive turbocharger compressor Applied Thermal Engineering 110 875.
125. Zhen, Xudong, et al. "The engine knock analysis–An overview." Applied Energy 92 (2012): 628-636.
126. Yue, Zongyu, et al. "Prediction of Cyclic Variability and Knock-Limited Spark Advance (KLSA) in Spark-Ignition (SI) Engine." ASME 2018 Internal Combustion Engine Division Fall Technical Conference. American Society of Mechanical Engineers Digital Collection, 2018.

127. Qi, Yunliang, et al. "Effects of thermodynamic conditions on the end gas combustion mode associated with engine knock." Combustion and Flame 162.11 (2015): 4119-4128.
128. Chen, Yu, Yuesen Wang, and Robert Raine. "Correlation between cycle-by-cycle variation, burning rate, and knock: a statistical study from PFI and DISI engines." Fuel 206 (2017): 210-218.
129. Willand, Jürgen, et al. "Limits on downsizing in spark ignition engines due to pre-ignition." MTZ worldwide 70.5 (2009): 56-61.
130. Winklhofer, E., et al. TC GDI engines at very high power density—irregular combustion and thermal risk. No. 2009-24-0056. SAE Technical Paper, 2009.
131. Wang, Zhi, et al. Experimental study on pre-ignition and super-knock in gasoline engine combustion with carbon particle at elevated temperatures and pressures. No. 2015-01-0752. SAE Technical Paper, 2015.
132. Wang, Zhi, Hui Liu, and Rolf D. Reitz. "Knocking combustion in spark-ignition engines." Progress in Energy and Combustion Science 61 (2017): 78-112.
133. Amann, Manfred, Terrence Alger, and Darius Mehta. "The effect of EGR on low-speed pre-ignition in boosted SI engines." SAE International Journal of Engines 4.1 (2011): 235-245.
134. Wang, Zhi, et al. "Relationship between super-knock and pre-ignition." International Journal of Engine Research 16.2 (2015): 166-180.
135. Capobianco, M., and A. Gambarotta. "Variable geometry and waste-gated automotive turbochargers: measurements and comparison of turbine performance." (1992): 553-560.
136. IHI Corporation A Powerful Run with a Compact Engine, IHI Engineering Review Vol. 50, No. 2, 2017.
137. Ebisu M, Danmoto Y, Akiyama Y, Arimizu H and Sakamoto K. Development of variable geometry turbocharger contributes to improvement of gasoline engine fuel economy. Mitsubishi Heavy Ind Tech Rev 2016; 53: 30–36.
138. Srinivasa Rao K, Gopinadh Chowdary P and Jamuna Rani G. Performance and emission characteristics of a turbocharged SI engine using petrol-ethanol fuel. Int J Mech Prod Eng Res Dev 2019; 9: 463–470.
139. Vishnu Varthan R and Senthil Kumar D. Emission characteristics of turbocharged single cylinder diesel engine. Indian J Sci Technol 2016; 9: 93158.
140. Enisu M, Terakawa Y and Ibaraki S. Mitsubishi turbochargerfor lower pollution cars. Mitsubishi Heavy Ind Tech Rev 2004; 41: 1–3.
141. Chen, Longfei, Richard Stone, and Dave Richardson. "Effect of the valve timing and the coolant temperature on particulate emissions from a gasoline direct-injection engine fuelled with gasoline and with a gasoline–ethanol blend." Proceedings of the Institution of Mechanical Engineers, Part D: Journal of Automobile Engineering 226.10 (2012): 1419-1430.

142. Kirwan, John E., et al. "3-cylinder turbocharged gasoline direct injection: a high value solution for low CO2 and NOx emissions." SAE International Journal of Engines 3.1 (2010): 355-371.
143. Hoepke, Bjoern, et al. "EGR effects on boosted SI engine operation and knock integral correlation." SAE International Journal of Engines 5.2 (2012): 547-559.
144. Lapuerta, Magín, et al. "High-pressure versus low-pressure exhaust gas recirculation in a Euro 6 diesel engine with lean-NOx trap: effectiveness to reduce NOx emissions." International Journal of Engine Research 20.1 (2019): 155-163.
145. Inaba, Kazuki, et al. "Thermal efficiency improvement with super-charging and cooled exhaust gas recirculation in semi-premixed diesel combustion with a twin peak shaped heat release." International Journal of Engine Research 20.1 (2019): 80-91.
146. Fu, Jianqin, et al. "A comparative study on various turbocharging approaches based on IC engine exhaust gas energy recovery." Applied energy 113 (2014): 248-257.
147. Y. Zhang, S. Zheng, Evaluation of paraffin infiltrated in various porous silica matrices as shape-stabilized phase change materials for thermal energy storage, Energy Convers. Manag., vol. 171, no. March, pp. 361–370, 2018.
148. K. Vafai, Convective flow and heat transfer in variable-porosity media, vol. 147, 1984.
149. S. Du, Y. He, International Journal of Heat and Mass Transfer Optimization method for the porous volumetric solar receiver coupling genetic algorithm and heat transfer analysis, Int. J. Heat Mass Transf., vol. 122, pp. 383–390, 2018.
150. W. Stoffiibertragung, Wdrme-und Stoffiibertragung Flow Model for Velocity Distribution in Fixed Porous Beds Under Isothermal Conditions, vol. 12, pp. 105–111, 1979.
151. K. Vafai and C. L. Tien, Boundary and inertia effects on flow and heat transfer in porous media,vol. 24, pp. 195–203, 1981.
152. T. Liu, J. Ding, Porous two-dimensional materials for energy applications : Innovations and challenges, Mater. Today Energy, vol. 6, pp. 79–95, 2017.
153. Y. Li, B. Guo, Characterization and thermal performance of nitrate mixture/SiC ceramic honeycomb composite phase change materials for thermal energy storage, Appl. Therm. Eng., vol. 81, pp. 193–197, 2015.
154. A. Ghahremannezhad and K. Vafai, International Journal of Heat and Mass Transfer Thermal and hydraulic performance enhancement of microchannel heat sinks utilizing porous substrates, Int. J. Heat Mass Transf., vol. 122, pp. 1313–1326, 2018.
155. B. Alazmi and K. Vafai, Analysis of fluid fow and heat transfer interfacial conditions between a porous medium and a fluid layer, vol. 44, 2001.
156. R. Thiyagaraja, Analysis of flow and heat transfer at the interface region of a porous medium, vol. 30, no. 7, pp. 1391–1405, 1987.

157. W.D. Kingery, H.K. Bowen, Introduction to Ceramics, Wiley, New York (1976), pp. 636.
158. Y. Zhou, K. Hirao, Thermal conductivity of silicon carbide densified with rare-earth oxide additives,J. Eur. Ceram. Soc., vol. 24, no. 2, pp. 265–270, 2004.
159. I. H. Song, M. J. Pa, Microstructure and permeability property of si bonded porous SiC with variations in the carbon content, J. Korean Ceram. Soc., vol. 47, no. 6, pp. 546–552, 2010.
160. I.-H. Song, J.-H. Ha, "Effects of silicon particle size on microstructure and permeability of silicon-bonded SiC ceramics, J. Ceram. Soc. Japan, vol. 120, no. 1405, pp. 370–374, 2012.
161. Y. Li, B. Guo, G. Huang, Characterization and thermal performance of nitrate mixture/SiC ceramic honeycomb composite phase change materials for thermal energy storage, Appl. Therm. Eng., vol. 81, pp. 193–197, 2015.
162. J. Fu, J. Liu, A new approach for exhaust energy recovery of internal combustion engine: Steam turbocharging, Appl. Therm. Eng., vol. 52, no. 1, pp. 150–159, 2013.
163. D. Petitjean, L. Bernardini, Advanced Gasoline Engine Turbocharging Technology for Fuel Economy Improvements, no. 724, 2004.
164. E. G. Giakoumis, Review of Some Methods for Improving Transient Response in Automotive Diesel Engines through Various Turbocharging Configurations, Front. Mech. Eng., vol. 2, no. May, 2016.
165. J. H. Eom, Y. W. Kim, and S. Raju, Processing and properties of macroporous silicon carbide ceramics: A review, J. Asian Ceram. Soc., vol. 1, no. 3, pp. 220–242, 2013.
166. W.D. Kingery, H.K. Bowen and D.R. Uhlman, Introduction to Ceramics, Wiley, New York (1976), pp. 636.
167. Y. Zhou, K. Hirao, K. Watari, Y. Yamauchi, and S. Kanzaki, "Thermal conductivity of silicon carbide densified with rare-earth oxide additives," J. Eur. Ceram. Soc., vol. 24, no. 2, pp. 265–270, 2004.
168. Ohzawa Y, Nomura K, Sugiyama K. Relation between porosity and pore size or pressure drop of fibrous SiC filter prepared from carbonized cellulose-powder preforms 1998;255:33–8.
169. R. Article, M. A. Delavar, and M. Azimi, "I Using Porous Material for Heat Transfer Enhancement in Heat Exchangers: Review" vol. 6, no. 1, pp. 14–16, 2013.
170. ANDRONE C-F, RAO SB. Vehicle Simulation for Powertrain System Testing 2017.
171. Dong D, Moriyoshi Y, Kuboyama T, Shen F. Application of Porous Material as Heat Storage Medium to a Turbocharged Gasoline Engine 2019. JSAE 20199541 / SAE 2019-32-0541.
172. Dong, Dongsheng, Yasuo Moriyoshi, and Tatsuya Kuboyama. "Effect of porous material as heat storage medium on fuel consumption in a turbocharged gasoline engine." International Journal of Engine Research (2020): 1468087420910591.

173. Hierarchically Structured Porous Materials: From Nanoscience to Catalysis, Separation, Optics, Energy, and Life Science - Wiley Online Library. 2011.
174. Porous medium, https://en.wikipedia.org/wiki/Porous_medium.
175. J. H. Eom, Y. W. Kim, Processing and properties of macroporous silicon carbide ceramics: A review,J. Asian Ceram. Soc., vol. 1, no. 3, pp. 220–242, 2013.
176. 2016, GT-Suit, Flow Theory Manual.
177. M. A. Habib, Heat transfer characteristics of pulsated turbulent pipe flow, Heat and Mass Transfer, vol. 34, no. 5, pp. 413-421, 1999.
178. K. E. Pappacena, Thermal conductivity of porous silicon carbide derived from wood precursors,J. Am. Ceram. Soc., vol. 90, no. 9, pp. 2855–2862, 2007.
179. K. C. Mills and L. Courtney, physical Pro perties Thermo of Silicon j,vol. 40, pp. 30–38, 2000.
180. K. C. Mills and L. Courtney, physical Pro perties Thermo of Silicon j,vol. 40, pp. 30–38, 2000.
181. Turbocharger Assist with External Compressor. https://dieselnet.com/tech/air_turbo_assist_compressor.php.
182. Turbo vs. Non-Turbo: Putting Throttle Response to the Test. https://www.caranddriver.com/news/a15348405/turbo-vs-non-turbo-putting-throttle-response-to-the-test.
183. Morris, G., et al., 2010. “A New Engine Boosting Concept with Energy Recuperation for Micro/Mild Hybrid Applications”, 22nd International AVL Conference “Engine & Environment”, 9th – 10th September 2010, Graz, Austria,
184. Barman, Jyotirmoy, Kumar Patchappalam, and Himanshu Gambhir. Compressed Air in Engine Exhaust Manifold to Improve Engine Performance and Fuel Economy. No. 2019-26-0043. SAE Technical Paper, 2019.
185. Mutra, Rajasekhara Reddy, and J. Srinivas. "Comparative Studies on the Dynamic Performances of High Speed Turbocharger Rotor Supported on Oil-Free Bearings Versus Conventional Floating Ring Systems." Gas Turbine India Conference. Vol. 58516. American Society of Mechanical Engineers, 2017.
186. Heshmat, Hooshang, and James F. Walton. "On the Integration of Hot Foil Bearings Into Gas Turbine Engines: Theoretical Treatment." Turbo Expo: Power for Land, Sea, and Air. Vol. 58691. American Society of Mechanical Engineers, 2019.
187. Feneley, Adam J., Apostolos Pesiridis, and Amin Mahmoudzadeh Andwari. "Variable geometry turbocharger technologies for exhaust energy recovery and boosting-A Review." Renewable and sustainable energy reviews 71 (2017): 959-975.

188. Jiaqiang, E., et al. "Experimental investigation on performance and economy characteristics of a diesel engine with variable nozzle turbocharger and its application in urban bus." Energy Conversion and Management 193 (2019): 149-161.
189. Zhao, Ben, et al. "Variable nozzle turbocharger turbine performance improvement and shock wave alternation by distributing nozzle endwall clearances." Proceedings of the Institution of Mechanical Engineers, Part D: Journal of Automobile Engineering 233.8 (2019): 1971-1981.
190. Morand, Nicolas, et al. "Variable Nozzle Turbine Turbocharger for Gasoline" Miller" Engine." MTZ worldwide 78.1 (2017): 40-45.
191. Hu, Leon, et al. "Design and analysis of a novel split sliding variable nozzle for turbocharger turbine." ASME Turbo Expo 2017: Turbomachinery Technical Conference and Exposition. American Society of Mechanical Engineers Digital Collection, 2017.
192. Giakoumis, Evangelos G. "Review of some methods for improving transient response in automotive diesel engines through various turbocharging configurations." Frontiers in Mechanical Engineering 2 (2016): 4.
193. Kakaee, Amir-Hasan, and Mehdi Keshavarz. "Simultaneous dynamic optimization of valves timing and waste gate to improve the load step transient response of a turbocharged spark ignition engine." Journal of the Brazilian Society of Mechanical Sciences and Engineering 39.7 (2017): 2383-2394.
194. Sivaraman, Manoj, et al. "Design and Performance Analysis on E-Tronic Turbocharger to eliminate Turbo Lag." International Journal of Pure and Applied Mathematics 119.12 (2018): 15687-15700.
195. Tripathi, Sanskar, et al. "Despite the Turbo-Lag, Turbochargers are preferred to Superchargers by the Manufacturers." 2019 International Conference on Automation, Computational and Technology Management (ICACTM). IEEE, 2019.
196. Kocsis L, Optimizing the Responsiveness of a Turbocharged Ice Through a New Design of the Exhaust Line
197. Newton PJ. An Experimental and Computational Study of Pulsating Flow within a Double Entry Turbine with Different Nozzle Settings n.d.
198. V. Ravaglioli, N. Cavina, A. Cerofolini, E. Corti, D. Moro, and F. Ponti, Automotive turbochargers power estimation based on speed fluctuation analysis, Energy Procedia, vol. 82, pp. 103–110, 2015.
199. M. Capobianco and S. Marelli, Experimental analysis of unsteady flow performance in an automotive turbocharger turbine fitted with a waste-gate valve, Proc. Inst. Mech. Eng. Part D J. Automob. Eng., vol. 225, no. 8, pp. 1087–1097, 2011.

200. M. Capobianco and S. Marelli, Experimental analysis of unsteady flow performance in an automotive turbocharger turbine fitted with a waste-gate valve, Proc. Inst. Mech. Eng. Part D J. Automob. Eng., vol. 225, no. 8, pp. 1087–1097, 2011.
201. Marelli, S. and Capobianco, M. Measurement of instantaneous fluid dynamic parameters in automotive turbocharging circuit. In Proceedings of the Ninth International Conference on Engines for automobiles, 2009, SAE paper 2009-24-0124.
202. Capobianco M, Marelli S. Experimental analysis of unsteady flow performance in an automotive turbocharger turbine fitted with a waste-gate valve. Proc Inst Mech Eng Part D J Automob Eng.
203. Costall AW. A one-dimensional study of unsteady wave propagation in turbocharger turbines 2007:1–358.
204. Szymko S, Martinez-Botas RF, Pullen KR. Experimental evalation of turbocharger turbine performance under pulsating flow conditions. ASME Turbo Expo 2005 Power Land, Sea, Air.
205. 2016, GT-Suit, Flow Theory Manual.
206. Gong C, Li Z, Yi L and Liu F. Comparative study on combustion and emissions between methanol port injection engine and methanol direct-injection engine with H2-enriched port-injection under lean-burn conditions. Energ Convers Manag 2019; 200: 112096.
207. Meng X, Tian H, Long W, Zhou Y, Bi M, Tian J, et al. Experimental study of using additive in the pilot fuel on the performance and emission trade-offs in the diesel/CNG (methane emulated) dual-fuel combustion mode.Appl Therm Eng 2019; 157: 113718.
208. Meng X, Tian H, Zhou Y, Tian J, Long W and Bi M.Comparative study of pilot fuel property and intake air boost on combustion and performance in the CNG dual fuel engine. Fuel 2019; 256: 116003.
209. Leng X, Jin Y, He Z, Long W and Nishida K. Numerical study of the internal flow and initial mixing of diesel injector nozzles with V-type intersecting holes. Fuel 2017; 197: 31–41.
210. Leng X, Jin Y, He Z, Wang Q, Li M and Long W.Effects of V-type intersecting hole on the internal and near field flow dynamics of pressure atomizer nozzles. Int J Therm Sci 2018; 130: 183–191.
211. Isenstadt A, German J, Dorobantu M, Boggs D and Watson T. Downsized, boosted gasoline engines. Int Coun Clean Transp 2016; 2016: 1–23.
212. Petitjean D, Bernardini L, Middlemass C and Shahed SM. Advanced gasoline engine turbocharging technology for fuel economy improvements. SAE paper 2004-01- 0988, 2004.
213. Shahed SM and Bauer K-H. Parametric studies of the impact of turbocharging on gasoline engine downsizing.SAE Int J Engines 2009; 2: 1347–1358.
214. Lumsden G, OudeNijeweme D, Fraser N and Blaxill H.Development of a turbocharged direct injection downsizing demonstrator engine. SAE Int J Engines 2009; 2:1420–1432.

215. IHI Corporation A Powerful Run with a Compact Engine, IHI Engineering Review Vol. 50, No. 2, 2017.

216. Ebisu M, Danmoto Y, Akiyama Y, Arimizu H and Sakamoto K. Development of variable geometry turbocharger contributes to improvement of gasoline engine fuel economy.

217. Srinivasa Rao K, Gopinadh Chowdary P and Jamuna Rani G. Performance and emission characteristics of a turbocharged SI engine using petrol-ethanol fuel. Int J Mech Prod Eng Res Dev 2019; 9: 463–470.

218. Vishnu Varthan R and Senthil Kumar D. Emission characteristics of turbocharged single cylinder diesel engine. Indian J Sci Technol 2016; 9: 93158.

219. Enisu M, Terakawa Y and Ibaraki S. Mitsubishi turbocharger for lower pollution cars. Mitsubishi Heavy Ind Tech Rev 2004; 41: 1–3.

220. Chen L, Stone R and Richardson D. Effect of the valve timing and the coolant temperature on particulate emissions from a gasoline direct-injection engine fuelled with gasoline and with a gasoline-ethanol blend. Proc IMechE, Part D: J Automob Eng 2012; 226: 1419–1430.

221. Kirwan JE, Shost M, Roth G and Zizelman J. 3-cylinder turbocharged gasoline direct injection: a high value solution for low CO2 and NOx emissions. SAE Int J Engines 2010; 3: 355–371.

222. Hoepke B, Jannsen S, Kasseris E and Cheng WK. EGR effects on boosted SI engine operation and knock integral correlation. SAE Int J Engines 2012; 5(2): 547–559.

223. Lapuerta M, Ramos Fernandez-Rodrıguez A D and Gonzalez-GarcıaI. High-pressure versus low-pressure exhaust gas recirculation in a Euro 6 diesel engine with lean-NOx trap: effectiveness to reduce NOx emissions. Int J EngRes 2019; 20(1): 155–163.

224. Inaba K, Ojima Y, Masuko Y, Kobashi Y, Shibata Gand Ogawa H. Thermal efficiency improvement with super-charging and cooled exhaust gas recirculation in semi-premixed diesel combustion with a twin peak shaped heat release. Int J Eng Res 2019; 20(1): 80–91.

225. Fu J, Liu J, Wang Y, Deng B, Yang Y, Feng R, et al. A comparative study on various turbocharging approaches based on IC engine exhaust gas energy recovery. Appl Energy 2014; 113: 248–257.

226. Eom JH, Kim YW and Raju S. Processing and properties of macroporous silicon carbide ceramics: a review. J Asian Ceram Soc 2013; 1(3): 220–242.

227. Kingery WD, Bowen HK and Uhlman DR. Introduction to ceramics. New York: John Wiley & Sons, 1976, pp.6–36.

228. Zhou Y, Hirao K, Watari K, Yamauchi Y and KanzakiS. Thermal conductivity of silicon carbide densified with rare-earth oxide additives. J Eur Ceram Soc 2004; 24(2):265–270.

229. Ohzawa Y, Nomura K and Sugiyama K. Relation between porosity and pore size or pressure drop of fibrous SiC filter prepared from carbonized cellulosepowder performs. Mater Sci Eng 1998; 255: 33–38.

230. Delavar MA and Azimi MS. I using porous material for heat transfer enhancement in heat exchangers: review. JEng Sci technol Rev 2013; 6(1): 14–16.

231. Androne C-F and Rao SB. Vehicle simulation for powertrain system testing, 2017, https://odr.chalmers.se/handle/20.500.12380/254886

232. Vagnoni G, Eisenbarth M, Andert J, Sammito G, SchaubJ, Reke M, et al. Smart rule-based diesel engine control strategies by means of predictive driving information. Int J Eng Res 2019; 20(10): 1047–1058.

233. Luja´n JM, Climent H, Ruiz S and Moratal A. Influence of ambient temperature on diesel engine raw pollutants and fuel consumption in different driving cycles. Int J Eng Res 2019; 20(8–9): 877–888.

234. Andert J, Xia F, Klein S, Guse D, Savelsberg R, Tharmakulasingam R, et al. Road-to-rig-to-desktop: virtual development using real-time engine modelling and powertrain co-simulation. Int J Eng Res 2019; 20(7): 686–695.

235. Chiong MS, Abas MA, Tan FX, Rajoo S, Martinez-Botas R, Fujita Y, et al. Steady-state, transient and WLTC drive-cycle experimental performance comparison between single-scroll and twin-scroll turbocharger turbine. SAE technical paper 2019-01-0327.

236. Dong D, Moriyoshi Y, Kuboyama T and Shen F. Application of porous material as heat storage medium to a turbocharged gasoline engine. SAE technical paper 2019-32-0541, 2019.Dong et al.

237. Kaiadi M, Tunestal P and Johansson B. Reducing throttle losses using variable geometry turbine (VGT) in a heavy-duty spark-ignited natural gas engine. SAE technical paper, 2011-01-2022, 11.

238. Muller M. Volumetric efficiency and pumping torque estimation and compressor recirculation control of turbocharged engines. SAE Int J Engines 2009; 2: 344–356.

239. Olmeda P, Martı´n J, Arnau FJ and Artham S. Analysis of the energy balance during world harmonized light vehicles test cycle in warmed and cold conditions using a virtual engine. Int J Eng Res. Epub ahead of print 3 October 2019. DOI: 10.1177/1468087419878593.

240. Ito N, Ohta T, Kono R, Arikawa S, Matsumoto T. Development of a 4-cylinder gasoline engine with a variable flow turbo-charger. SAE Tech Pap 2007.

241. Arnold S, Groskreutz M, Shahed SM, Slupski K. Advanced variable geometry turbocharger for diesel engine applications. SAE Tech Pap 2002.

242. Tang H, Pennycott A, Akehurst S, Brace CJ. A review of the application of variable geometry turbines to the downsized gasoline engine. Int J Engine Res 2015;16:810–25.

243. Shimizu K, Sato W, Enomoto H and Yashiro M. Torque control of a small gasoline engine with a variable nozzle turbine turbocharger. SAE technical paper 2009-32-0169, 2009.
244. Andersen J, Karlsson E, Gawell A. Variable turbine geometry on SI engines. SAE Tech Pap 2006;2006:776–90.
245. Application of Variable Geometry Turbine on Gasoline Engines and the Optimisation of Transient Behaviours 2019.
246. Sauerstein R, Dabrowski R, Becker M, Christmann R. The Dual-Volute-VTG from BorgWarner – 2009.
247. Simon V, Oberholz G, Mayer M. Exhaust gas temperature 1050 ° C An engineering challenge. BorgWarner TurboSystems Acad 2000:1–12.
248. Gabriel H, Jacob S, Munkel U, Rodenhauser H and Schmalzl HP. The turbocharger with variable turbine geometry for gasoline engines. MTZ Worldwide 2007; 68(2): 96–103.
249. Europe I. IHI Corporation A Powerful Run with a Compact Engine 2012:12–3.
250. Industries MH. A Variable Geometry (VG) Turbocharger for Passenger Cars to Meet European Union Emission Regulations 2014;49:17–26.
251. Tetsui, T., 2002, "Development of a TiAl Turbocharger for Passenger Ve- hicles,"
252. Kenji, I., Keijiro, H., and Tomomi, S., 2006, "Development of HERCUNITE-S NSHR-A5N for High Performance Gasoline Engines," Hitachi Rev., 22, pp. 51–56.
253. Cairns A, Fraser N and Blaxill H. Pre versus post compressor supply of cooled EGR for full load fuel economy in turbocharged gasoline engines. SAE technical paper 2008-01-0425, 2008.
254. Ayala, F., Gerty, M., and Heywood, J., 2006, "Effects of Combustion Phasing, Relative Air Fuel Ratio, Compression Ratio, and Load on SI Engine Efficiency," SAE Paper No. 2006-01-0229.
255. Karnik AY, Shelby MH. Effect of Exhaust Gas Temperature Limits on the Peak Power Performance of a Turbocharged Gasoline Engine 2017;132:1–7. doi:10.1115/1.4000856.
256. Ishihara H, Adachi K, Kono S. Development of VFT part 2. SAE Tech Pap 2002.
257. Wallace FJ, Howard D and Roberts EW. Variable geometry turbocharging – optimization and control under steady state conditions. In: 3rd international conference on turbocharging and turbochargers, London, 6–8 May 1986. London, UK: Institution of Mechanical Engineers.
258. Lundstrom RR and Gall JM. A comparison of transient vehicle performance using a fixed geometry, wastegated turbocharger and a variable geometry turbocharger. SAE technical paper 860104, 1986. DOI: 10.4271/860104.
259. Uchida H. Transient performance prediction for turbo- charging systems incorporating variable-geometry turbochargers. R&D Rev Toyota CRDL 2006; 41(3): 22–28.
260. Feneley AJ, Pesiridis A, Andwari AM. Variable Geometry Turbocharger Technologies for Exhaust Energy Recovery and Boosting-A Review. Renew Sustain Energy Rev 2017;71:959–75.

261. Kawaguchi J. SAE TECHNICAL Development of VFT (Variable Flow Turbocharger) 2018.
262. Shettigar VO. Materials Selection for Variable Geometry Turbine Nozzle for Gasoline Engine Application. GT2014-27119 2016:1–11.
263. Industries MH. Development of Compact and High-performance turbocharger for 10 5 0 ° C Exhaust Gas 2010;45:1–5.
264. Karnik AY, Shelby MH. Effect of Exhaust Gas Temperature Limits on the Peak Power Performance of a Turbocharged Gasoline Engine 2017;132:1–7. doi:10.1115/1.4000856.
265. Kaiadi M, Tunestal P, Johansson B. Reducing Throttle Losses Using Variable Geometry Turbine (VGT) in a Heavy-Duty Spark-Ignited Natural Gas Engine. SAE Tech Pap Ser 2011;1.
266. Duchaussoy Y, Lefebvre A, Bonetto R. Dilution interest on turbocharged SI engine combustion. SAE Tech Pap 2003. doi:10.4271/2003-01-0629.
267. Szybist JP, Wagnon SW, Splitter D, Pitz WJ, Mehl M. The Reduced Effectiveness of EGR to Mitigate Knock at High Loads in Boosted SI Engines. SAE Int J Engines 2017;10. doi:10.4271/2017-24-0061.
268. Roberto B. Thermodynamic Analysis of a Turboprop Engine with Intercooling and Heat Recovery 2011;54:44–50.
269. Shibata, Mitsuhiro, et al. New 1.0 L I3 turbocharged gasoline direct injection engine. No. 2017-01-1029. SAE Technical Paper, 2017.
270. Simulation of improvement effect of mode running fuel efficiency brought by new technology in gasoline vehicles. Ueno Master Thesis, Chiba University.
271. Carberry B, Grasi G, Guerin S, Jayat F, Konieczny R. Pre-turbocharger catalyst - Fast catalyst light-off evaluation. SAE Tech Pap 2005. doi:10.4271/2005-01-2142.

List of publications

1. Dong, D., Moriyoshi, Y., Kuboyama, T., Shen, F., Hasegawa, N. (2020). Application of porous material as heat storage medium to a turbocharged gasoline engine (No. 2019-32-0541). SAE Technical Paper.
2. Dong, Dongsheng, Yasuo Moriyoshi, and Tatsuya Kuboyama. "Effect of porous material as heat storage medium on fuel consumption in a turbocharged gasoline engine." International Journal of Engine Research (2020): 1468087420910591.

ACKNOWLEDGEMENT

First and foremost, I would like to sincerely express my deepest gratitude to my primary supervisor Professor Moriyoshi, who provided me constant support and many previous opportunities during my PhD. In my study of Chiba University, I have obtained motivation and enthusiasm about engine research due to the key role of Moriyoshi. I have also learnt a lot from Professor Moriyoshi not only academically but also in everyday life.

In addition, a similar gratitude is for my secondary supervisor Associate Professor Kuboyama, who taught me a lot and give me many opinions about my research. Professor Yamada, Professor Morikawa and Associate Professor Kaneko also taught me a lot and gave me a lot of help in my everyday research project. They have a lot of practical experience to help me solve many questions and problem.

I would like to thank Specially Appointed Professor Chen, Dr student Shen, Researcher Hasegawa, Ishita,Kumar, Nagamura, Kim who help me a lot and taught me a lot of engine research and everyday life experiences. Dr student Li, Dr student Chen, Zhong, Wang, and Master student Koyano,Sala,Takizawa,Misono,Tan etc. also help me a lot during my PhD. I want to thank a master graduate (Mr. Ueno) who help me a lot about my the WLTC model. Special thanks to Master student Koyano who helped me a lot about experiment. I also want to thank my friends in Chiba University, Dr Qi,Chen,Yang,Wu,Zhao. Thanks to their friendly help and company.

I would like to thank Chiba University and Center for Power Research for Next- Generation Mobility to support my research. It is very grateful for Chiba University to accept me as Doctor course student. Special thanks to CSC for supporting my everyday life in Japan by giving scholarship. Therefore, I was able to come Japan for my PhD course.

Finally, I want to thank my family. There is so much I want to say but so little that can be expressed. They support me all the way regardless of gains and losses. I am proud as a member of my family.